

**Seismic Performance Assessment of RC Buildings
Case of: “Bekir Paşa” High School**

Aydin Gharagozloo

Submitted to the
Institute of Graduate Studies and Research
in partial fulfillment of the requirements for the Degree of

Master of Science
in
Civil Engineering

Eastern Mediterranean University
September 2011
Gazimağusa, North Cyprus

Approval of the Institute of Graduate Studies and Research

Prof. Dr. Elvan Yılmaz
Director

I certify that this thesis satisfies the requirements as a thesis for the degree of Master of Science in Civil Engineering.

Asst. Prof. Dr. Mürüde Çelikağ
Chair, Department of Civil Engineering

We certify that we have read this thesis and that in our opinion it is fully adequate in scope and quality as a thesis for the degree of Master of Science in Civil Engineering.

Assoc. Prof. Dr. Özgür Eren
Co-Supervisor

Asst. Prof. Dr. Serhan Şensoy
Supervisor

Examining Committee

1. Assoc. Prof. Dr. Özgür Eren

2. Asst. Prof. Dr. Erdiñç Soyer

3. Asst. Prof. Dr. Giray Özay

4. Asst. Prof. Dr. Mürüde Çelikağ

5. Asst. Prof. Dr. Serhan Şensoy

ABSTRACT

Early reinforced concrete structures present undetermined resistance to earthquakes. This situation is particularly unacceptable in the case of essential facilities such as school structures. For those countries which are located in the earthquake region determination of the building condition and deciding on possible strengthening methods is a necessity. Determining the performance of a building and classifying its safety level for a presumed earthquake will help to limit the damages during an earthquake.

In this thesis determination of possible weaknesses of one of the old school buildings in Cyprus, Iskele (Bekir Paşa High School) is taken as a case study. All the buildings located on this site are low rise reinforced concrete frame structures that have been constructed before 1974 and are currently being used, except one building that has been constructed during 1980's. In order to achieve seismic performance of buildings, first step is identifying the structural system geometry and material properties utilizing destructive and non-destructive testing, this allows engineer to create a model of structure representing the existing structural member's section properties.

Applying nonlinear static and dynamic analysis on created models will help engineer to find out the capacity of structure subjected to lateral loadings representing earthquake ground motions and behavior of structure subjected to actual recorded earthquake data scaled to design response spectrum. Nonlinear static pushover analysis and nonlinear

dynamic time history analysis are employed in this study to find capacity and behavior of buildings.

Framework of this work is to assess the performance of structures in event of an earthquake. Proposed methodology is applied on all buildings of Bekir Paşa High School in order to assess their existing performance subjected to seismic hazard. Performance level of structures is assessed according to specifications of FEMA356 and Lang's procedure is utilized to classify their damage grades, finally obtained results are compared and weak points of structures are highlighted. Methodology studied in this thesis can be used to assess reinforced concrete frame structures designed according to Turkish earthquake code 2007 for future studies.

Keywords: assessment, earthquake, performance, safety, analysis.

ÖZ

Eski betonarme yapıların depreme karşı dayanıklı olup olmadıkları belli değil ve bu durum okul binaları söz konusu olduğunda çok tehlike arz etmektedir. Deprem kuşağında olan ülkelerde bu tür yapıların durumunun ve olası güçlendirme metodlarının belirlenmesi bir gerekliliktir. Önceden yapıların performans düzeylerinin belirlenmesi ve olası depremlere karşı dayanımlarına göre sınıflandırılmaları depremlerde ileri düzeyde hasarlar oluşmasını önleyecektir.

Bu tezde, Kuzey Kıbrıs Türk Cumhuriyeti İskele kazasında bulunan Bekirpaşa Lisesi binaları incelenmiş ve olası zayıflıkları ortaya çıkarılmıştır. Binalar az katlı olup sadece bir blok hariç tümü 1974 yılı öncesinde tamamlanmış binalardır. Yapı modellerini oluşturabilmek amacıyla yapıların geometrik ve malzeme özellikleri tahribatlı ve tahribatsız deney yöntemleri ile belirlenmiştir.

Doğrusal olmayan statik ve dinamik analiz yöntemleri hazırlanan modellere uygulanmış ve yapıların deprem kapasiteleri ve davranışları ortaya çıkarılmıştır. Bu amaçla, doğrusal olmayan modeller bölgede geçerli (uygulanan) tasarım kodlarında belirlenen tasarım spektrumuna göre ölçeklendirilmiş gerçek deprem kayıtları kullanılarak zaman tanım alanında analiz edilmiştir.

Bu alıřmanın erevesi yapıların deprem performanslarının belirlenmesi ile sınırlıdır. Yukarıda belirtilen her iki metod ile Bekirpařa Lisesi yapıları analiz edilmiř ve blgenin deprem tehlikesi dikkate alındıėında yapıların performansları belirlenmiřtir. Performans seviyeleri FEMA 356 ve Lang methodu kullanılarak belirlenmiř ve her iki metod ile elde edilen sonular karřılařtırılarak yapıların zayıf oldukları noktalar belirlenmiřtir. Bu tezde uygulanan metodoloji benzer diėer betonarme yapılara da ileriki alıřmalarda uygulanabilmektedir.

To my Family

ACKNOWLEDGEMENT

First and foremost I offer my sincerest gratitude to my supervisor, Dr. Serhan Şensoy, and co-supervisor, Dr. Özgür Eren whom have supported me throughout my thesis with their patience and knowledge whilst allowing me the room to work in my own way, their guidance and support from the initial to the final level enabled me to develop an understanding of the subject.

Besides, I would like to thank the Department of Civil Engineering for providing a good environment and facilities to complete this study, and special thanks to Mr. Ogün Kiliç the laboratory engineer for helping and trusting me with laboratory equipment.

My special thanks go to Tuğba Tunç, for being next to me with her endless motivation and love. I am also grateful to Sarvenaz Pakravan for her support during this work.

Finally, yet most importantly, I would like to express my heartfelt thanks and appreciations to my beloved parents and brother for their blessings and support throughout my studies.

TABLE OF CONTENTS

ABSTRACT	iii
ÖZ	v
DEDICATION	vii
ACKNOWLEDGEMENT	viii
LIST OF TABLES	xiii
LIST OF FIGURES	xvi
1 INTRODUCTION	1
1.1 Importance of Seismic Performance Assessment	1
1.2 Defining the problem	3
1.3 Aim of study.....	5
1.4 Overview of chapters	6
2 METHODS OF SEISMIC ASSESSMENT	7
2.1 Introduction.....	7
2.1 Nonlinear Static Analysis.....	7
2.1.1 Idealizing force-displacement curve	9
2.1.2 Target displacement	10
2.3 Structural performance limit states (FEMA356).....	12
2.2 Damage prediction	14
2.3 Non linear Dynamic Analysis	18

3 NONLINEAR TIME HISTORY ANALYSIS	19
3.1 Nonlinear Time-History analysis	19
3.2 Specification of design acceleration spectrum	20
3.3 Selecting ground motion accelerations	23
3.3.1 Scaling Time series	24
4 METHODOLOGY.....	28
4.1 Geometry of buildings	28
4.1.1 Block A	29
4.1.2 Block B1	31
4.1.3 Block B2	32
4.1.4 Block C	34
4.1.5 Block D	36
4.2 Specification of building characteristics	37
4.2.1 Non-Destructive testing	37
4.2.2 Destructive testing.....	40
4.3 Modeling the buildings	44
4.3.1 Structural members section properties	45
4.3.2 Loads acting on structure	47
4.4 Pushover analysis	47
4.4.1 Nonlinear static pushover analysis steps	49

4.5 Non-Linear Time-History analysis	50
4.5.1 Nonlinear time history analysis steps.....	52
5 RESULTS AND DISCUSSION	53
5.1 Results obtained from pushover analysis	53
5.1.1 Capacity curves	53
5.1.2 Performance level limit states	59
5.1.3 Damage prediction	69
5.2 Time-History analysis	75
5.2.1 Block A	77
5.2.2 Block B1	81
5.2.3 Block B2	85
5.2.4 Block C	89
5.2.5 Block D	93
6 CONCLUSIONS.....	98
6.1 Summary of works done	98
6.2 Low rise RC frame structures	99
6.3 Concluding findings for buildings	100
6.3.1 Block A	101
6.3.2 Block B1	103
6.3.3 Block B2	105

6.3.4 Block C	108
6.3.5 Block D	110
6.4 Conclusions.....	112
REFERENCES.....	114
APPENDICES	116
Appendix A: FEMA356 parameters to calculate target displacement.....	117
Appendix B: Rebound hammer readings from columns of buildings.....	120
Appendix C: Time history functions of selected earthquakes	121
Appendix D: Calculation of actual compressive strength of concrete core samples	124

LIST OF TABLES

Table 2.1: Classification of damage grades for RC structures (Lang, 2002).....	17
Table 3.1: Effective ground acceleration coefficient (Aydinoglu, 2007).	21
Table 3.2: Building Importance factor (Aydinoglu, 2007).	21
Table 3.3: Spectrum characteristic periods (Aydinoglu, 2007).	21
Table 3.4: Calculated MSE & SF for selected 20 ground motion records and earthquake specifications.....	27
Table 4.1: Block A beam section properties	45
Table 4.2: Block A column section properties.....	45
Table 4.3: Block B1 beam section properties	45
Table 4.4: Block B1 column section properties	45
Table 4.5: Block B2 beam section properties	46
Table 4.6: Block B2 column section properties	46
Table 4.7: Block C beam section properties	46
Table 4.8: Block C column section properties	46
Table 4.9: Block D beam section properties	46
Table 4.10: Block D column section properties.....	46
Table 5.1: Pushover steps – Block A	60
Table 5.2: Limit states – Block A	61
Table 5.3: Pushover steps – Block B1	62
Table 5.4: Limit states – Block B1	63

Table 5.5: Pushover steps – Block B2	64
Table 5.6: Limit states – Block B2	65
Table 5.7: Pushover steps – Block C	66
Table 5.8: Limit states – Block C	67
Table 5.9: Pushover steps – Block D	68
Table 5.10: Limit states – Block D	69
Table 5.11: Damage grade limits of Block A	70
Table 5.12: Damage grade limits of Block B1	71
Table 5.13: Damage grade limits of Block B2.....	72
Table 5.14: Damage grade limits of Block C.....	73
Table 5.15: Damage grade limits of Block D	74
Table 5.16: Maximum spectral displacement & corresponding spectral acceleration – block A.....	77
Table 5.17: Maximum spectral displacement & corresponding spectral acceleration – block B1	81
Table 5.18: Maximum spectral displacement & corresponding spectral acceleration – block B2	85
Table 5.19: Maximum spectral displacement & corresponding spectral acceleration – block C	89
Table 5.20: Maximum spectral displacement & corresponding spectral acceleration – block D.....	93
Table 6.1: Seismic performance of buildings	101
Table A.1: FEMA356 parameters for 3D model – Block A.....	117

Table A.2: FEMA356 parameters for frame model Block A..... 117

Table A.3: FEMA356 parameters for 3D model - Block B1 117

Table A.4: FEMA356 parameters for frame model – Block B1..... 117

Table A.5: FEMA356 parameters for 3D model – Block B2 118

Table A.6: FEMA356 parameters for frame model – Block B2..... 118

Table A.7: FEMA356 parameters for 3D model – Block C 118

Table A.8: FEMA356 parameters for frame model – Block C..... 118

Table A.9: FEMA356 parameters for 3D model – Block D..... 119

Table A.10: FEMA356 parameters for 3D model – Block D..... 119

Table B.1: Rebound hammer readings – Block A 120

Table B.2: Rebound hammer readings – Block B1..... 120

Table B.3: Rebound hammer readings – Block B2..... 120

Table B.4: Rebound hammer readings – Block C..... 120

Table B.5: Rebound hammer readings – Block D 120

LIST OF FIGURES

Figure 1.1: Map showing the principal tectonic elements of the northeastern Mediterranean region (from U.S. Geological Survey Circular 1193, 1999, as modified from Barka, 1992).	1
Figure 1.2: PGA contours having a 10% probability of being exceeded in any 50-year interval (Algermissen and Rogers, 2004).	2
Figure 1.3: Left: Satellite image of site, Right: Map of site	5
Figure 2.1: Capacity curve of a regular framed structure for adaptive pushover analysis (Elnashai and Di Sarno, 2008).	9
Figure 2.2: Idealized Force-Displacement curve (ASCE, 2000)	10
Figure 2.3: Component or element acceptance criteria defined by FEMA356 (ASCE, 2000).	13
Figure 2.4: Typical Moment resisting plastic hinge of reinforced concrete elements	14
Figure 2.5: Force-Displacement Relation for linear elastic and elastic-plastic behaviors	16
Figure 2.6: Typical Vulnerability function for R/C building (Lang, 2002).	16
Figure 3.1: Design spectral acceleration coefficients-Time period spectrum.....	23
Figure 3.2: Spectral acceleration-Time period spectrum calculated for seismic zone 2.	23
Figure 3.3: Target response spectrum and geometric mean of Earthquake records selected from database (PEER, 2010).....	26
Figure 4.1: Showing expandable staff; measuring height of column.....	28

Figure 4.2: Typical ground floor plan – Block A	29
Figure 4.3: Typical storey plan – Block A	29
Figure 4.4: Frame elevation – Block A.....	30
Figure 4.5: Front view of Block A	30
Figure 4.6: Left: Typical ground floor plan block B1 – Right: Storey plan block B1	31
Figure 4.7: Frame elevation – Block B1	31
Figure 4.8: Side view of Block B1	31
Figure 4.9: Typical ground floor plan – Block B2.....	32
Figure 4.10: Typical storey plan – Block B2	32
Figure 4.11: Frame elevation – Block B2.....	32
Figure 4.12: Front view of Block B2	33
Figure 4.13: Typical ground floor – Block C.....	34
Figure 4.14: Typical storey plan – Block C	34
Figure 4.15: Frame elevation – Block C	35
Figure 4.16: Front view of block C.....	35
Figure 4.17: Typical ground floor – Block D	36
Figure 4.18: Frame elevation – Block D.....	36
Figure 4.19: Front view of block D.....	36
Figure 4.20: Rebound Hammer (Bungey, 2006).....	38
Figure 4.21: Ferro scan device	39
Figure 4.22: Typical scan of reinforcement bar from a column	40
Figure 4.23: Concrete core drilling machine – taking carrot from a column.....	41
Figure 4.24: showing drilled area after taking the sample from column	41

Figure 4.25: Showing capped concrete core sample	42
Figure 5.1: Capacity curve for 3D model pushover analysis of Block A	55
Figure 5.2: Capacity curve for frame model pushover analysis of Block A.....	55
Figure 5.3: Capacity curve for 3D model pushover analysis of Block B1	56
Figure 5.4: Capacity curve for frame model pushover analysis of Block B1	56
Figure 5.5: Capacity curve for 3D model pushover analysis of Block B2	57
Figure 5.6: Capacity curve for Frame model pushover analysis of Block B2	57
Figure 5.7: Capacity curve for 3D model pushover analysis of Block C	58
Figure 5.8: Capacity curve for frame model pushover analysis of Block C	58
Figure 5.9: Capacity curve for 3D model pushover analysis of Block D	59
Figure 5.10: Capacity curve for frame model pushover analysis of Block D.....	59
Figure 5.11: Structure performance limit states of frame model – Block A.....	62
Figure 5.12: Structure performance limit states of frame model – Block B1	64
Figure 5.13: Structure performance limit states of frame model – Block B2.....	66
Figure 5.14: Structure performance limit states of frame model – Block C	67
Figure 5.15: Structure performance limit states of frame model – Block D.....	69
Figure 5.16: Damage grades of Block A.....	71
Figure 5.17: Damage grades of Block B1	72
Figure 5.18: Damage grades of Block B2.....	73
Figure 5.19: Damage grades of Block C.....	74
Figure 5.20: Damage grades of Block D.....	75
Figure 5.21: S_a - S_d showing group of time histories causing elastic behavior for block A	78

Figure 5.22: S_a-S_d showing group of time histories causing IO performance level for block A	78
Figure 5.23: S_a-S_d showing group of time histories causing LS performance level for block A	79
Figure 5.24: S_a-S_d showing group of time histories causing collapse performance level for block A	79
Figure 5.25: Probability of structure performing in different levels – block A	80
Figure 5.26: S_a-S_d showing group of time histories causing elastic behavior for block B1	82
Figure 5.27: S_a-S_d showing group of time histories causing IO performance level for block B1	82
Figure 5.28: S_a-S_d showing group of time histories causing LS performance level for block B1	83
Figure 5.29: S_a-S_d showing group of time histories causing collapse performance level for block B1	83
Figure 5.30: Probability of structure performing in different levels – block B1	84
Figure 5.31: S_a-S_d showing group of time histories causing elastic behavior for block B2	86
Figure 5.32: S_a-S_d showing group of time histories causing IO performance level for block B2	86
Figure 5.33: S_a-S_d showing group of time histories causing LS performance level for block B2	87

Figure 5.34: S_a-S_d showing group of time histories causing collapse performance level for block B2 87

Figure 5.35: Probability of structure performing in different levels – block B2 88

Figure 5.36: S_a-S_d showing group of time histories causing elastic behavior for block C 90

Figure 5.37: S_a-S_d showing group of time histories causing IO performance level for block C 90

Figure 5.38: S_a-S_d showing group of time histories causing LS performance level for block C 91

Figure 5.39: S_a-S_d showing group of time histories causing collapse performance level for block C 91

Figure 5.40: Probability of structure performing in different levels – block C 92

Figure 5.41: S_a-S_d showing group of time histories causing elastic behavior for block D 94

Figure 5.42: S_a-S_d showing group of Time Histories causing IO performance level for block D 94

Figure 5.43: S_a-S_d showing group of time histories causing LS performance level for block D 95

Figure 5.44: S_a-S_d showing group of time histories causing collapse performance level for block D 95

Figure 5.45: Probability of structure performing in different levels – block D 96

Figure 6.2: Critical frame – Block A 101

Figure 6.1: Deformed shape and generation of plastic hinges on 3D model of block A
..... 102

Figure 6.3: Deformed shape and generation of plastic hinges on 3D model of block B1
..... 104

Figure 6.4: Critical frame – Block B1..... 104

Figure 6.5: Deformed shape and generation of plastic hinges on 3D model of block B2
..... 106

Figure 6.6: Critical frame – Block B2..... 107

Figure 6.8: critical frame – Block C 108

Figure 6.7: Deformed shape and generation of plastic hinges on 3D model of block C
..... 109

Figure 6.10: Critical frame – Block D 111

Figure 6.9: Deformed shape and generation of plastic hinges on 3D model of block D
..... 111

Chapter 1

1 INTRODUCTION

1.1 Importance of Seismic Performance Assessment

Cyprus is located in between the Eurasian and African plates, many destructive earthquakes that have made damages and life loss were experienced throughout the island's history, Earthquakes like; year 1222 with Magnitude 6.8, year 1577 with Magnitude 6.7, year 1785 with Magnitude 7.1, year 1940 with Magnitude 6.7, and year 1996 with Magnitude 6.7 (Cagnan and Tanircan, 2009). Figure 1.1 shows the location of Cyprus between Eurasian and African plates where Cyprus Arc is passing through north part of the island.

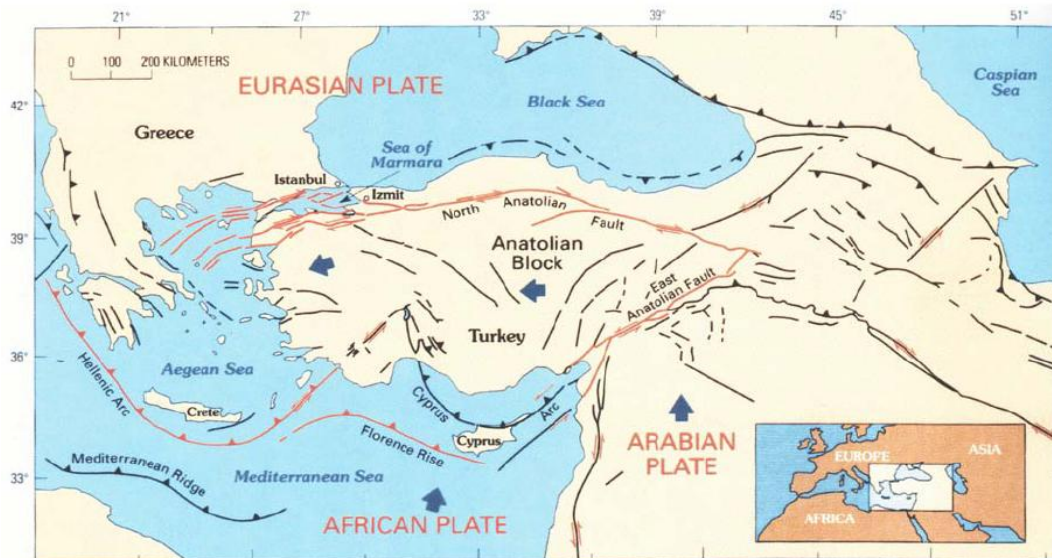


Figure 1.1: Map showing the principal tectonic elements of the northeastern Mediterranean region (from U.S. Geological Survey Circular 1193, 1999, as modified from Barka, 1992).

Figure 1.2 is showing map of contour lines presenting Peak Ground Accelerations (PGA) for Cyprus with 10% probability of being exceeded in 50 years that will be used later on to assess the buildings vulnerability based on ground acceleration to assess possible behavior of buildings according to PGA contour lines of Cyprus, Iskele area.

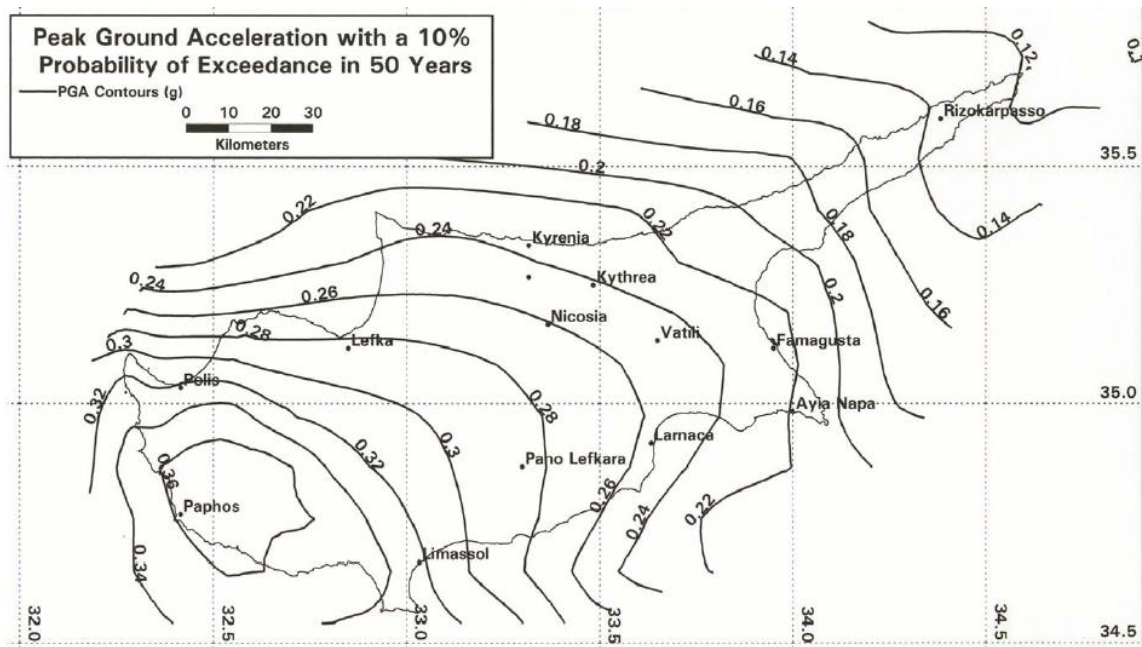


Figure 1.2: PGA contours having a 10% probability of being exceeded in any 50-year interval (Algermissen and Rogers, 2004).

It has to be taken into consideration that Cyprus has many reinforced concrete structures aging over 20 or 30 years. Climate characteristics has affect on the durability of these buildings causing a slight decrease in strength of concrete and corrosion of the reinforcement bars and this will lead to loss in stability comparing to the design expectations. At the same time early generation of design codes were based on linear elastic behavior of structure, therefore an assessment shall be carried out to find out the present properties of existing buildings and their response in an event of earthquake. Buildings which are used as schools, hospitals or any other type that is used by public is in priority. Performance assessment of buildings shows the weak points of structure and

the possible damages to the structure in case of any possible ground trembling, this assessment will allow engineer to design and strengthen the critical weak members of structure that brings it to expected behavior and to prevent possible collapse of structure in event of an earthquake.

1.2 Defining the problem

An assessment was requested for the buildings of a school located in North Cyprus, city of Iskele named “Bekir Paşa High School”. This school site is consisting of five buildings constructed before 1974. Satellite image and street map of location is shown in Figure 1.3. One of the buildings referenced as block D had damages and was suspicious for the safety of students for using it as classrooms. This is the only building on site that has been constructed during 1980’s. Cracks observed on primary members of building D and amount of corrosion observed from removed concrete cover on reinforcement bars was disturbing, hence building was forbidden to use. The other buildings are being used every day by staff and students. Request for assessment were sent to department of civil engineering and decision was made to study the existing buildings of “Bekir Paşa High School” to evaluate the conditions of structures and decide whether it has to be repaired or strengthened, or in some cases demolish and reconstruct the structure. Seismic performance assessment of the buildings is the research topic of this thesis.

During visual investigation of site cracks were spotted on beams and columns of buildings. Reinforcement bars of block D were observed through the removal of concrete column. All buildings are low rise reinforced concrete frame structures with irregularities in plan. Cantilever beams are supporting the balconies which might show a

weak performance during an earthquake and cannot hold the slabs. Columns are continuous to the roof and between each two columns there is a masonry partial height wall which restrains portion of column from moving, therefore development of short columns. Since the effective height over which a short column can freely bend is small, it offers more resistance to horizontal motion and thereby attracts a larger force as compared to the regular column (Murty, 1993). This will lead short columns to sustain more damage during an earthquake. Considering the age of buildings, corroded reinforcement and having short columns shows that these structures might be weak and experience heavy damages during an earthquake. Therefore existing properties of structural members shall be identified to be able to perform analysis to investigate the response of the buildings during lateral loading representing inertia forces of earthquake.

Buildings are chosen to be known by parameters A, B1, B2, C, D1 and D2 shown in Figure 1.3 to make it simple to recognize during the study. Block A and C are two storey structures used as classrooms. Block B is consisting of a two storey (B1) and a single storey (B2) separated from each other by an expansion joint. Block D1 and D2 are sharing same structural plans with an expansion joint in between; therefore one of the plans is studied as block D.

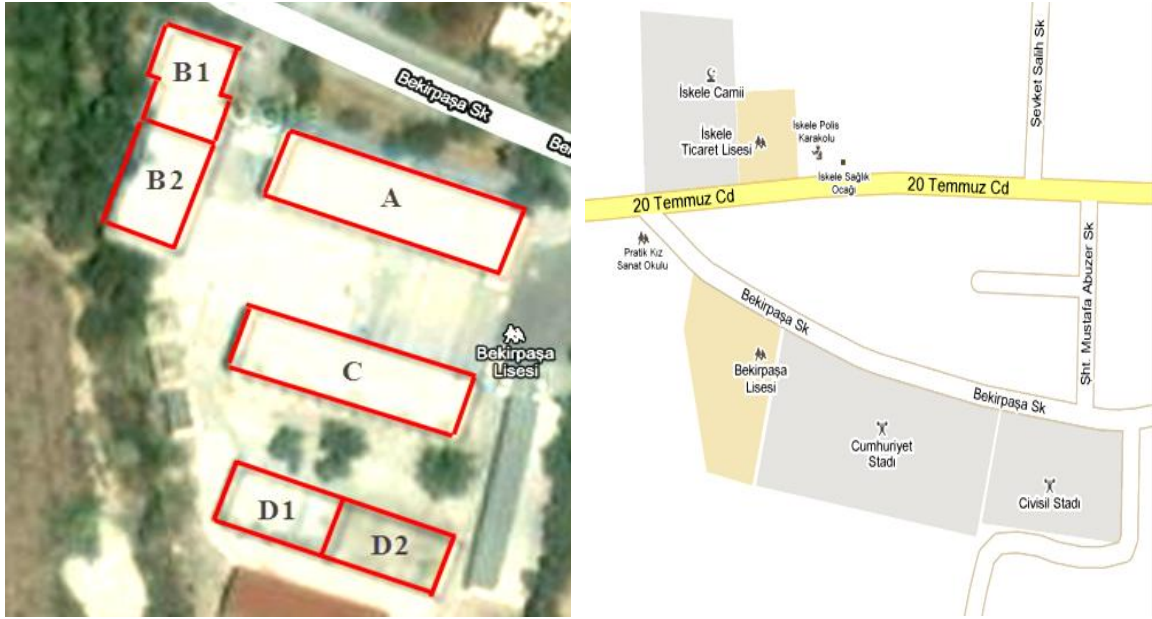


Figure 1.3: Left: Satellite image of site, Right: Map of site

1.3 Aim of study

As it is mentioned in Section 1.2, an assessment was required for the buildings of “Bekir Paşa High School” site buildings, In order to achieve the requirements; the following objectives were selected and studied;

- 1- Evaluating geometry of buildings
- 2- Evaluating member section properties of buildings
- 3- Modeling buildings using “CSI SAP2000”
- 4- Performing pushover analysis to find the capacity of structures subjected to increased horizontal forces and finding critical members of each structure.
- 5- Performing time-history analysis to find out the response of structures subjected to earthquake recorded ground accelerations.
- 6- Making engineering judgments according to obtained results and highlighting the weak points of structures.

1.4 Overview of chapters

Total of six chapters are in this thesis, where Chapter 1 gives a brief introduction to Cyprus seismicity and importance of assessment. Chapter 2 focuses on methods of seismic performance assessment; nonlinear static and dynamic analysis is explained including FEMA356 and Lang's procedure. Chapter 3 concentrates on nonlinear time-history analysis, selection of earthquake records and scaling the records to suitable design response spectra. Chapter 4 explains the methods and steps taken to assess the selected buildings of this study. Chapter 5 shows the results obtained from procedures taken in this study including discussion and comparison of achievements. Finally Chapter 6 concludes the study and highlights weaknesses of structures and future studies.

Chapter 2

2 METHODS OF SEISMIC ASSESSMENT

2.1 Introduction

Recent major destructive earthquakes (e.g. Northridge 1994, Kobe 1995, Kocaeli 1999) proved the fact that previously design codes as well as assessment procedures based on elastic methods were not effective enough to prevent destructive damages (Pinho, 2007). Many researchers believe that even old codes like 1975 Turkish code was very successful, however especially for reinforced concrete buildings wrong construction caused disaster. Furthermore newer versions of codes like 2007 Turkish code suggests inelastic methods may be very effective tool for assessment rather than design. Because of that it is required to perform more proper approaches considering structure's nonlinearity and its materials plastic behavior. Book of "Advanced Earthquake Engineering Analysis" (2007) suggests two analysis approaches for assessment of existing buildings seismic response, nonlinear static pushover analysis and nonlinear dynamic analysis known as time history. These two methods are known as the most accurate tools for seismic assessment for existing structures (Pinho, 2007).

2.1 Nonlinear Static Analysis

Nonlinear Static analysis (NSA) or pushover analysis is one of the assessment methods to verify the capacity of structure against lateral loading, in linear static analysis of structure only deformation of members due to dead and live loads acting on structure

can be obtained, but for assessing the behavior of structure nonlinear analysis needs to be performed. This will allow engineer to observe and identify the response of structure to increased lateral loading, generation of plastic hinges in members and yielding till complete failure of structure.

According to the book of “Fundamentals of Earthquake Engineering” (Elnashai and Di Sarno, 2008), in pushover analysis method forces are applied along the height of structure horizontally and structure is trying to resist this applied lateral loads, lateral loading will continue and increase along the height of structure and will stop when structure exceeds its resisting capacity. There are two types of pushover, one when the loading pattern is kept constant during the analysis called “conventional pushover”, the other one is known as “adaptive pushover” that load patterns will change with respect to mode shapes of structure in plastic range. Although static pushover analysis has some restrictions regarding number of stories and irregularities, in this study the method used conveniently and compared with the results of nonlinear time history analysis.

A typical capacity curve of a frame structure is shown in Figure 2.1, where increasing lateral loading is shown as base shear causing increase in total drift which is the ratio of top displacement of structure to its height. FEMA 356 suggests nonlinear static analysis procedure that is explained in this chapter. According to FEMA 356 (ASCE, 2000), once NSA is chosen to find out the response of structure to lateral loading that presents inertia forces of an earthquake, a model of building shall be created with respect to its existing structural characteristics. Control node should be selected to be able to record its displacement due to increasing loads. The obtained base shear force-displacement relationship shall be idealized and target displacement of structure must be calculated.

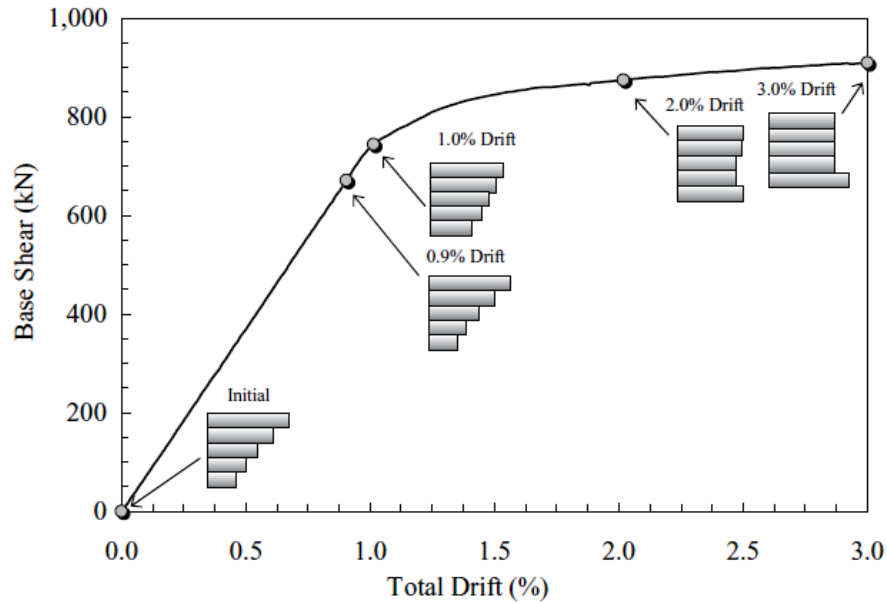


Figure 2.1: Capacity curve of a regular framed structure for adaptive pushover analysis (Elnashai and Di Sarno, 2008).

2.1.1 Idealizing force-displacement curve

In order to calculate the effective lateral stiffness K_e and effective yield strength V_y , the obtained force-displacement relationship curve from analysis shall be idealized to a bilinear relationship. The lines shall be constructed in a way that areas above and below the curve remain balanced (ASCE, 2000).

Figure 2.2 shows a typical idealized bilinear force-displacement curve defined by FEMA356 where K_i is the elastic lateral stiffness of building, K_e is the effective lateral stiffness of the building, α is the post yield slope, V_y is the effective yield strength and target displacement is shown as δ_t representing the performance point of building that shall be calculated and checked on capacity curve to find out buildings performance level at that displacement.

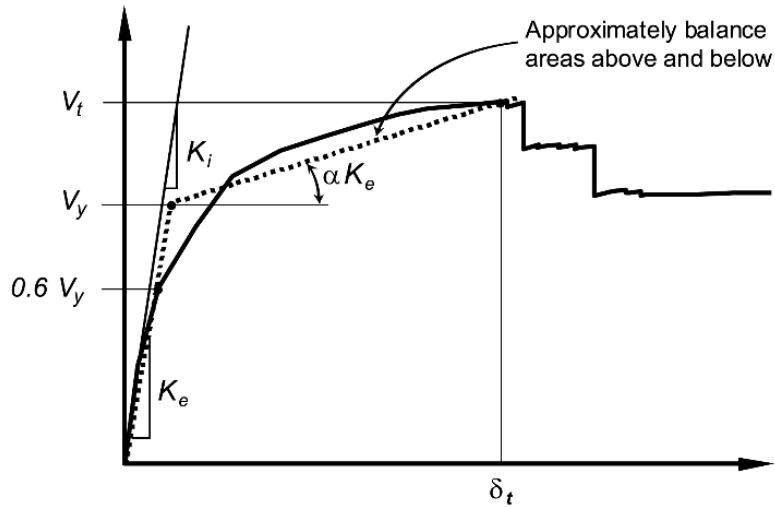


Figure 2.2: Idealized Force-Displacement curve (ASCE, 2000)

2.1.2 Target displacement

When nonlinear pushover analysis is selected for seismic performance assessment of building, increasing load distributed among height of structure will push structure to reach a target displacement. There are two popular methods generally used to calculate target displacement, FEMA356 coefficient method (ASCE, 2000) and ATC40 capacity spectrum (Goel et. all., 2011), coefficient method is selected to be used in this study.

The target displacement of structure δ_t , shall be calculated from equation given in FEMA356 document (ASCE, 2000):

$$\delta_t = C_0 C_1 C_2 C_3 S_a \frac{T_e^2}{4\pi^2} g \quad (\text{eq. 2.1})$$

Where response spectrum acceleration S_a , gravity acceleration g , and T_e is the effective fundamental period of building.

$$T_e = T_i \sqrt{\frac{K_i}{K_e}} \quad (\text{eq. 2.2})$$

K_i And K_e are elastic and effective stiffness of building respectively, calculated from idealization of capacity curve obtained from pushover analysis.

Coefficients are defined by FEMA356 document (ASCE, 2000) as follow:

C_0 , Modification factor to relate spectral displacement of an equivalent SDOF system to the roof displacement of the building MDOF system

C_1 , Modification factor to relate expected maximum inelastic displacements to displacements calculated for linear elastic response:

$$C_1 = \begin{cases} 1 & T_e \geq T_S \\ 1 + \frac{(R-1)T_e}{T_S} & T_e < T_S \\ 1.5 & T_e < 0.1 \text{ Sec} \end{cases} \quad (\text{eq. 2.3})$$

Where T_S is the characteristic period of the response spectrum and R is the strength ratio.

C_2 Is Modification factor to represent the effect of pinched hysteretic shape, stiffness degradation and strength deterioration on maximum displacement response, C_3 is modification factor to represent increased displacement.

$$C_3 = \begin{cases} 1 & \alpha \geq 0 \\ 1 + \frac{\alpha(R-1)^{3/2}}{T_e} & \alpha < 0 \end{cases} \quad (\text{eq. 2.4})$$

$$R = \frac{S_a}{V_y/W} C_m \quad (\text{eq. 2.5})$$

Where; V_y is the yielding strength of structure obtained from capacity curve, W is weight and C_m accounts for effective modal mass factor for fundamental mode of structure.

2.3 Structural performance limit states (FEMA356)

Performance limit states specified in FEMA356 (ASCE, 2000) classifies the limit states in three discrete performance levels; Immediate Occupancy (IO), Life Safety (LS) and Collapse prevention (CP).

IO level is the damage range of structure after subjecting to earthquake ground motions where structure stays safe to be occupied. In this case very slight structural damages are observed that can be repaired. Structural members almost keep their stiffness and strength compare to before resisting earthquake loads.

LS level is described as the damage range after earthquake loading where resisting frames of structure have major damages but still has a small resistance to prevent collapse. There is a risk of injury because of falling waste separated from members. Structural repair can be done but might not be very economical comparing to reconstruction.

CP is a state after event of earthquake where structure is on edge to collapse partially or completely. Large displacement of structural member can be observed and resisting frames have lost their pre loading strength and stiffness where still needs to carry self weights. There is huge possibility of injury or life loss because of falling objects. Repair is not a good solution since any aftershock can result in collapse of system.

General acceptance criteria for deformation or deformation ratios for primary members (P) and secondary members (S) corresponding to the target building performance level defined by FEMA356 is shown in Figure 2.3.

CSI SAP2000 analysis program has the ability to allow user to observe the changes in plastic hinge limit states in each step, Figure 2.4 shows general changes in performance limit states of a reinforced concrete element moment resisting plastic hinge. Increase in lateral loading cause structure to yield and post yield changes resistance is only provided by plastic hinges capacity according to specifications defined for member sections. Specifications of plastic hinges are account for member section moment carrying capacity calculated from identified member section characteristics explained in following chapters.

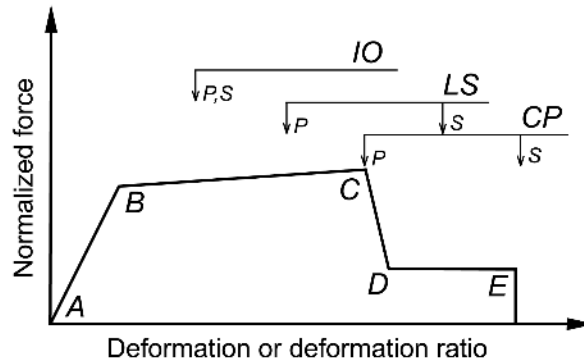


Figure 2.3: Component or element acceptance criteria defined by FEMA356 (ASCE, 2000).

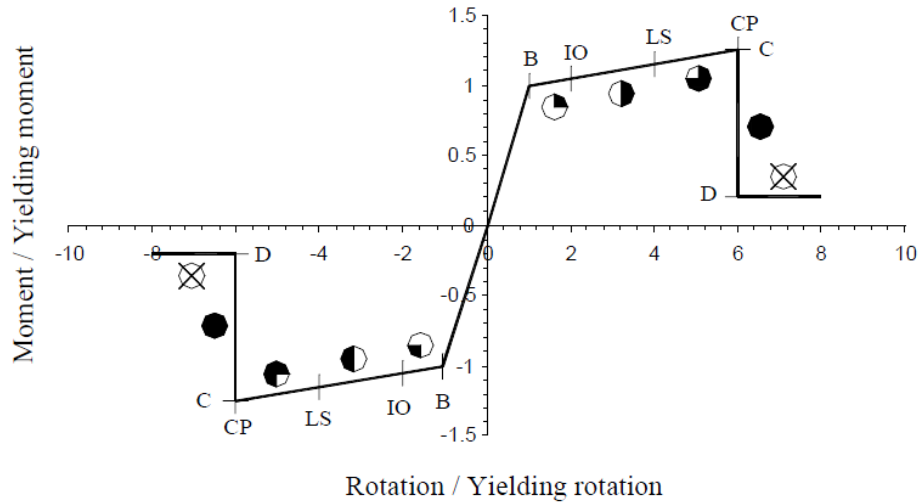


Figure 2.4: Typical Moment resisting plastic hinge of reinforced concrete elements

2.2 Damage prediction

Study of “Seismic Vulnerability of existing buildings” (Lang, 2002), has a method to obtain the damage grades of structures and evaluating existing structure’s performance. Lang has studied the vulnerability of existing structures in Switzerland, city of Basel and has proposed a simple method to evaluate reinforced concrete buildings based on their engineering models (Lang, 2002), since there was no major destructive earthquake records available at the time. Cyprus has the same situation regarding historical records of destructive earthquake even though many of them are mentioned that had happened during its history. In order to observe the behavior of buildings selected in this study, Lang’s procedure is chosen as well as FEMA to be able to compare results and better investigation and evaluation of buildings.

The procedure is considering the pushover curve of structure and tries to construct the vulnerability function from displacement demand of structure and spectral displacement

in response to lateral loading presenting earthquake ground acceleration. Equation below shall be used to calculate the top displacement of structure;

$$\Delta_{top} = \frac{\Gamma \cdot \mu_D \cdot T_1^2 \cdot S_a}{R_y \cdot 4\pi^2} \quad (\text{eq. 2.6})$$

Where Γ is the modal participation factor, μ_D presents ductility demand, T_1 is the fundamental mode period of structure, S_a is spectral acceleration, R_y presents yield strength reduction factor.

$$\Gamma = \frac{\sum_1^n m_i \cdot \Phi_i}{\sum_1^n m_i \cdot (\Phi_i)^2} \quad (\text{eq. 2.7})$$

Where m is representing the mass of each storey of structure and Φ_i is the normalized fundamental mode shape displacement of each storey.

Fundamental period of structure can be read from structural analysis results and then corresponding spectral acceleration with respect to design response spectra with accordance to code limits and local site conditions, explained in chapter 3. Calculating fundamental frequency of structure will find the spectral displacement.

$$\omega = \frac{2\pi}{T} \quad (\text{eq. 2.8}) \quad \Delta_D = \mu_D \cdot \Delta_y \quad (\text{eq. 2.12})$$

$$S_d = \frac{S_a}{\omega^2} \quad (\text{eq. 2.9}) \quad V_0 = K_E \cdot \Delta_0 \quad (\text{eq. 2.13})$$

$$\Delta_0 = \Gamma \cdot S_d \quad (\text{eq. 2.10}) \quad R_y = \frac{V_0}{V_y} \quad (\text{eq. 2.14})$$

$$\mu_D = \frac{\Delta_y}{\Delta_0} \quad (\text{eq. 2.11})$$

Where, V_0 is the required base shear by the system to remain elastic, V_y is the force at yield (for bi-linear systems) or the shear capacity of the building (for elastic-plastic systems), Δ_y is the top displacement at the first yield (for bi-linear systems), Δ_0 is the required top displacement by the system to remain elastic shown in Figure 2.5. Top displacement is shown on a general vulnerability function of RC building with specified damage grades in Figure 2.6.

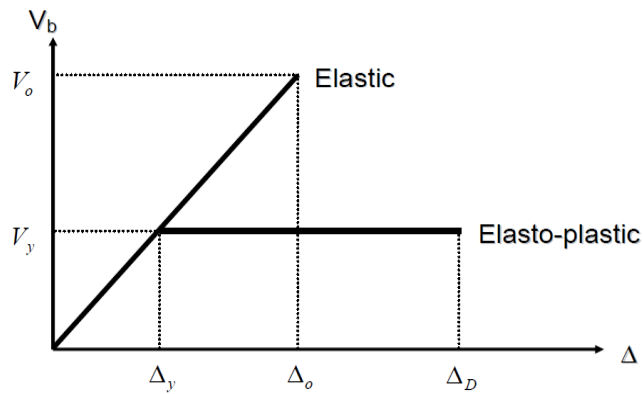


Figure 2.5: Force-Displacement Relation for linear elastic and elastic-plastic behaviors

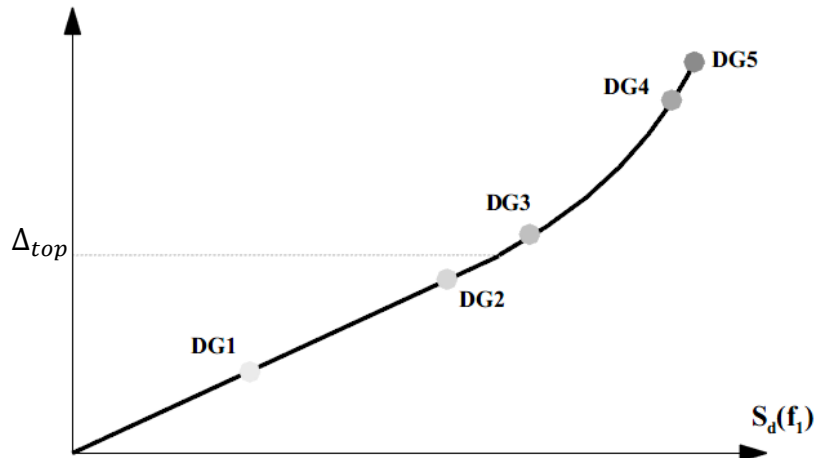







Figure 2.6: Typical Vulnerability function for R/C building (Lang, 2002).

Table 2.1: Classification of damage grades for RC structures (Lang, 2002).

Damage Grade	Simulation	EMS 98	Identification (Start of Damage Grade)
Grade 1		<i>Negligible to slight damage (no structural damage, slight non-structural damage)</i> Fine cracks in plaster over frame elements or in walls at base. Fine cracks in partitions and infills.	After cracking. Onset of tensile strength of members.
Grade 2		<i>Moderate damage (slight structural damage, moderate non-structural damage)</i> Cracks in columns and beams of frames and in structural walls. Cracks in partition and infill walls; fall of brittle cladding and plaster. Falling mortar from the joints of wall panels.	First plastic section. Reduction starts in structural stiffness.
Grade 3		<i>Substantial to heavy damage (moderate structural damage, heavy non-structural damage)</i> Cracks in columns and beam column joints of frames at the base and at joints of coupled walls. Spalling of concrete cover, buckling of reinforced rods. Large cracks in partition and infill walls, failure of wall-panels.	Final plastic section before individual section failure. Building stiffness tends to zero.
Grade 4		<i>Very heavy damage (heavy structural damage, very heavy non-structural damage)</i> Large cracks in structural elements with compression failure of concrete and fracture of rebars; bond failure of beam-reinforced bars; tilting of columns. Collapse of a few columns or a single upper floor.	First individual section failure. Start of reduction in base shear.
Grade 5		<i>Destruction (very heavy structural damage)</i> Collapse of ground floor or parts of the building.	Final individual section failure. Loss of lateral stability. Buckling of some columns.

Observing the change in damage stages of building allows engineer to interpret the capacity of structure to resist damage grades with corresponding shear force causing it, hence can estimate the loss of building in case of earthquake. Classification of damage grades proposed by Lang (2002) is shown in Table 2.1.

2.3 Non linear Dynamic Analysis

Nonlinear Dynamic Analysis (NDA) or nonlinear time history analysis is another tool for assessment of existing structures, this method can be very much time consuming depending on size of structure and output time-steps requested for assessment.

Usually the earthquake records are selected and normalized to show an exponential increase of ground motion and used in nonlinear dynamic analysis known as incremental dynamic analysis, but time history analysis is presenting actual ground motions simulating the earthquake scaled to design response spectra that building were designed with will be applied to the structure and response will be recorded. After application of time series the peak displacement due to ground acceleration can be identified, the displacement caused by the peak ground acceleration of selected and scaled earthquakes can also be identified to investigate the deformation caused from it.

Time history analysis only shows the response of structure as displacement function, so the only output will be displacements caused to control node during time period of simulated earthquake. Combining capacity of structure considering displacement function and deformations obtained from nonlinear time history analysis can give the engineer an idea of possible scenarios that might happen to structure due to selected simulated earthquakes. For the purpose of this study 20 earthquake records are selected and applied to each structure to be able to find out more accurate seismic response of structures. Process of time history analysis, selecting and scaling of earthquake record to adequate design response spectrum is explained in chapter 3.

Chapter 3

3 NONLINEAR TIME HISTORY ANALYSIS

3.1 Nonlinear Time-History analysis

Nonlinear Time-History analysis also known as Nonlinear Dynamic analysis is a powerful method to identify the response of structure to ground motion accelerations. The book of “Advanced Earthquake Engineering Analysis” states that “It is widely recognized that nonlinear time-history analysis constitutes the most accurate way for simulating response of structures subjected to strong levels of seismic excitation” (Pinho, 2007).

This method of analysis shows the displacement of structural members subjected to selected acceleration series applied to structure. In this study critical frame of each structure has been selected and ground motion accelerations were applied to study the behavior of each frame in terms of displacement to find out the possibility of each frame to be in different performance limit states. For the purpose of this study structure models were created using computer program “CSI SAP2000 14.0 Advanced”. In order to select the Earthquake records to apply for analysis three steps shall be taken; First step is to specify the design response spectrum, second step is to search for Earthquake records according to Earthquake design spectrum and site characteristics and final step is to upload and create load case to apply the selected time series to the structure and investigate the response of it subjected to applied acceleration load.

3.2 Specification of design acceleration spectrum

Existing reinforced concrete buildings located in TRNC are designed and constructed according to 1975 Turkish Earthquake design code. However, 1998 and then 2007 Turkish Earthquake codes (Aydinoglu, 2007) have been used effectively to design earthquake resistant reinforced concrete buildings. The “Part III – Earthquake disaster prevention” of 2007 Earthquake code defines the spectral acceleration coefficients and design acceleration spectrum.

Spectral acceleration coefficient normalized by the acceleration of gravity (g) is specified by (Aydinoglu, 2007).

$$A(T) = A_0 I S(T) \quad (\text{eq. 3.1})$$

A_0 Is the effective ground motion coefficient that is classified according to seismic zones in Table 3.1.

I Is the Importance factor of the buildings which are specified according to types of buildings in Table 3.2.

$S(T)$ Is the spectrum coefficient that can be calculated; according to structure’s natural period and local site conditions specified in Table 3.3.

$$S(T) = \frac{1+1.5 T}{T_A} \quad (0 \leq T \leq T_A) \quad (\text{eq. 3.2})$$

$$S(T) = 2.5 \quad (T_A < T \leq T_B) \quad (\text{eq. 3.3})$$

$$S(T) = 2.5 \left(\frac{T_B}{T}\right)^{0.8} \quad (T \geq T_B) \quad (\text{eq. 3.3})$$

Table 3.1: Effective ground acceleration coefficient (Aydinoglu, 2007).

<i>Seismic Zone</i>	<i>A_o</i>
1	0.40
2	0.30
3	0.20
4	0.10

Table 3.2: Building Importance factor (Aydinoglu, 2007).

<i>Purpose of Occupancy or Type of Building</i>	<i>Importance Factor (I)</i>
<p><u>1. Buildings to be utilised after the earthquake and buildings containing hazardous materials</u></p> <p>a) Buildings required to be utilised immediately after the earthquake (Hospitals, dispensaries, health wards, fire fighting buildings and facilities, PTT and other telecommunication facilities, transportation stations and terminals, power generation and distribution facilities; governorate, county and municipality administration buildings, first aid and emergency planning stations)</p> <p>b) Buildings containing or storing toxic, explosive and flammable materials, etc.</p>	1.5
<p><u>2. Intensively and long-term occupied buildings and buildings preserving valuable goods</u></p> <p>a) Schools, other educational buildings and facilities, dormitories and hostels, military barracks, prisons, etc.</p> <p>b) Museums</p>	1.4
<p><u>3. Intensively but short-term occupied buildings</u></p> <p>Sport facilities, cinema, theatre and concert halls, etc.</p>	1.2
<p><u>4. Other buildings</u></p> <p>Buildings other than above defined buildings. (Residential and office Buildings, hotels, building-like industrial structures, etc.)</p>	1.0

Table 3.3: Spectrum characteristic periods (Aydinoglu, 2007).

<i>Local Site Class acc. to Table 12.2</i>	<i>T_A (second)</i>	<i>T_B (second)</i>
Z1	0.10	0.30
Z2	0.15	0.40
Z3	0.15	0.60
Z4	0.20	0.90

Turkish Earthquake design code has specified a limit for acceleration spectrum that “spectral acceleration coefficients corresponding to so obtained acceleration spectrum

ordinates shall in no case be less than those determined by equation 3.2” as $S(T)$, (Aydinoglu, 2007).

Local site class is specified as $Z4$ ($T_A=0.2$, $T_B=0.9$) for site of “Bekir Paşa High School” according previous experiments and investigations of Cyprus (Cagnan and Tanircan, 2009). The buildings of site fit the 2nd category for importance factor for school and other educational facilities according to Turkish earthquake code and read as 1.4.

Studies done on seismicity of Cyprus shows that the island is located on seismic zone 2 (Cagnan and Tanircan, 2009) with effective ground acceleration coefficient specified as 0.3 from Turkish earthquake code (Aydinoglu, 2007). There is no official seismic hazard assessment to north Cyprus but previous studies (Cagnan and Tanircan, 2009) shows that there are no records of major destructive earthquakes happened in history of Cyprus, but studies show that most of destructive earthquake were within range of 6 to 7 magnitude, zero to 40 km distance from epicentre and zero to 40 km depth to the surface. These specifications are used as search criteria to find the best matching earthquake time series for Cyprus with respect to design response spectrum calculated for building according to local site conditions.

Spectral acceleration coefficients has been calculated based on local site class specification for $Z4$, seismic zone 2 (Cagnan and Tanircan, 2009), building importance factor for schools and applicable distinctive periods specified for time period of ten seconds and result is plotted as Spectral coefficient versus time period shown in Figure 3.1 and calculated Spectral acceleration versus time periods shown in Figure 3.2.

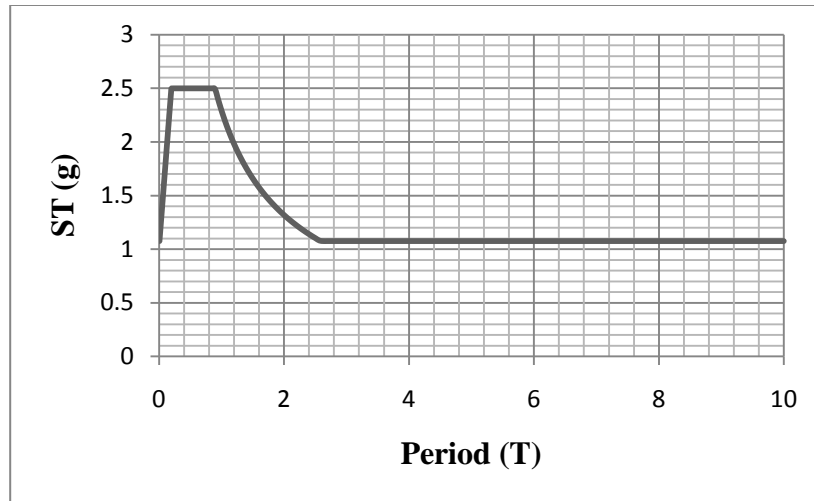


Figure 3.1: Design spectral acceleration coefficients-Time period spectrum

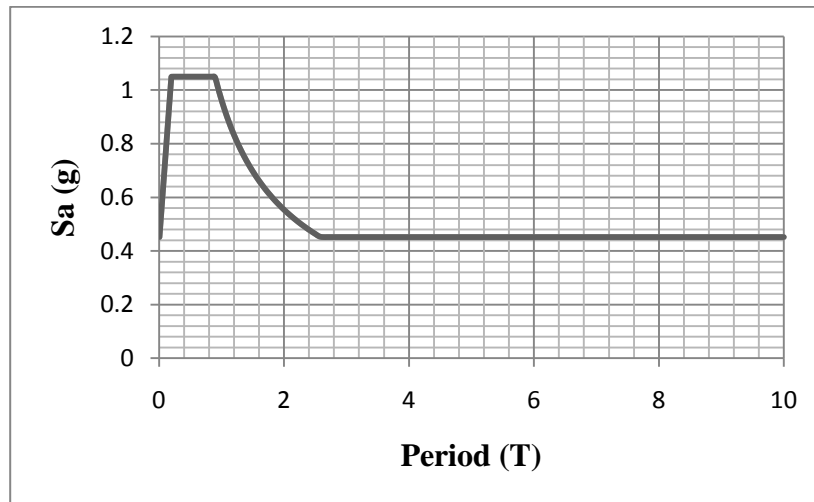


Figure 3.2: Spectral acceleration-Time period spectrum calculated for seismic zone 2

3.3 Selecting ground motion accelerations

Pacific earthquake engineering research center (PEER) of university of Berkley, California, has database of previous earthquake's records data. It also has a web application to search and scale the selected ground accelerations (PEER, 2010). In this study PEER ground motion acceleration database web application has been used to select time series and scaling them to specified design acceleration spectra.

PEER database has three steps process to form the acceleration data according to design response spectrum (PEER, 2010);

- 1- Specification of target design spectrum
- 2- Specification of limits for time series
- 3- Searching database, selecting and recording the acceleration data

In order to develop the target design spectrum, user defined spectrum option has been used which allows the user to upload the calculated design response spectrum according to Earthquake code to the web application. This tool will plot the user defined target design response spectrum that shall be calculated according to Turkish earthquake code (Aydinoglu, 2007) and from there user is able to go to next step and define the limits for search criteria.

3.3.1 Scaling Time series

PEER ground motion database web application uses mean squared error (MSE) of variation among the record's spectral acceleration and the user defined target spectrum to find the best match within the period of interest. MSE is calculated using logarithms of spectral acceleration and period, from there this web application searches the database according to the user defined specifications and then sorts the records in an increasing order of MSE with the records having the lowest MSE to match the target spectrum. This tool also provides linear scaling of time series to bring the closest match to the target spectrum (PEER, 2010).

3.3.1.1 Calculation of mean squared error (MSE)

MSE among the response spectrum of the record and defined target spectrum is calculated base on variation in natural logarithm of spectral accelerations. Time period between 0.01 to 10 second is divided into 301 points including the end points. Mean squared error is calculated using following equation (PEER, 2010);

$$MSE = \frac{\sum_i w(T_i) \{ \ln[SA_{target}(T_i)] - \ln[f SA_{record}(T_i)] \}^2}{\sum_i w(T_i)} \quad (\text{eq. 3.4})$$

Parameter $w(T_i)$ is defined as weight function which let user to assign comparative weights to any points of period range; this function should be taken $w(T_i) = 1$, unless user likes highlight a match above an expansive period variation.

Parameter “ f ” is defined as the linear scale factor which will be applied to response spectrum of record, application of this scale factor is for minimization MSE to give the best equivalent spectral shape for response spectrum of records with respect to defined target spectrum. Scale factor is calculated using following equation (PEER, 2010);

$$\ln f = \frac{\sum_i w(T_i) \ln \left(\frac{SA_{target}(T_i)}{SA_{record}(T_i)} \right)}{\sum_i w(T_i)} \quad (\text{eq. 3.5})$$

After calculation of MSE and minimizing it using the calculated scale factor time series records has been selected considering the best matching horizontal components, these are normal and parallel horizontal components where the geometric mean of accelerations is given in following equation (PEER, 2010);

$$SA_{GM} = \sqrt{SA_{FN} \cdot SA_{FP}} \quad (\text{eq. 3.6})$$

3.3.1.2 Specification of search criteria

User is able to specify different limits to find the suitable records for study; these may consist of: type of faulting which is selected as Strike-Slip, distance ranged which is selected as 0 to 40 km to epicenter, duration range which is assumed to be 10 seconds, depth of earthquake which is selected to be from 0 to 40 km to the surface and Earthquake magnitude that is limited up to 7 Richter for the purpose of this study, however after scaling the time series the magnitude will not be affecting the results since the accelerations are scaled to the defined design response spectrum respectively.

Total of 20 Earthquake records were searched, scaled and recorded to be used for this study, Figure 3.3 shows the geometric mean and specified target spectrum plotted by PEER ground motion database web application, and these records are shown in Appendix C.

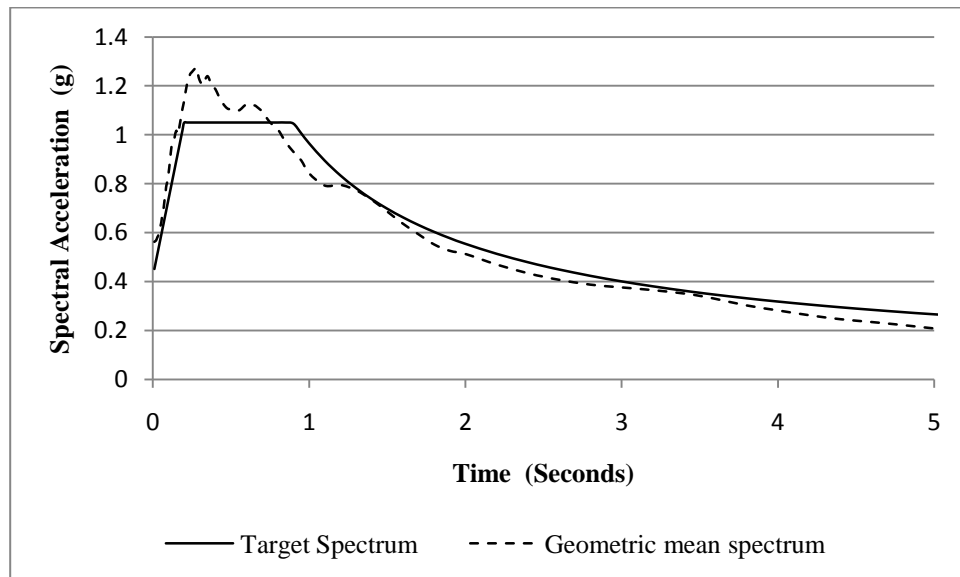


Figure 3.3: Target response spectrum and geometric mean of Earthquake records selected from database (PEER, 2010)

Table 3.4: Calculated MSE & SF for selected 20 ground motion records and earthquake specifications

Name	MSE	Scale F	Event	Year	Magnitude	Mechanism	PGA (g)
TH1	0.3140	10.8413	Park field	1966	6.19	Strike-Slip	0.6470
TH2	0.0687	2.6382	Imperial Valley-06	1979	6.53	Strike-Slip	0.4741
TH3	0.0703	6.6741	Imperial Valley-06	1979	6.53	Strike-Slip	0.5122
TH4	0.1677	4.7040	Victoria- Mexico	1980	6.33	Strike-Slip	0.4950
TH5	0.0869	2.7845	Westmorland	1981	5.90	Strike-Slip	0.4788
TH6	0.3016	16.8445	Morgan Hill	1984	6.19	Strike-Slip	0.5485
TH7	0.1464	2.6054	Superstition Hills-02	1987	6.54	Strike-Slip	0.5476
TH8	0.1332	2.5265	Superstition Hills-02	1987	6.54	Strike-Slip	0.5226
TH9	0.0671	5.2387	Landers	1992	7.28	Strike-Slip	0.7231
TH10	0.0837	2.7455	Landers	1992	7.28	Strike-Slip	0.6087
TH11	0.1118	6.7796	Kobe- Japan	1995	6.90	Strike-Slip	0.4981
TH12	0.0892	1.7984	Kocaeli- Turkey	1999	7.51	Strike-Slip	0.5080
TH13	0.0403	1.8289	Kocaeli- Turkey	1999	7.51	Strike-Slip	0.5098
TH14	0.2194	3.2088	Kocaeli- Turkey	1999	7.51	Strike-Slip	0.4887
TH15	0.0700	16.3662	Duzce- Turkey	1999	7.14	Strike-Slip	0.6735
TH16	0.2197	7.6520	Duzce- Turkey	1999	7.14	Strike-Slip	0.8761
TH17	0.4343	4.8329	Hector Mine	1999	7.13	Strike-Slip	0.6601
TH18	0.0523	1.6906	Denali- Alaska	2002	7.90	Strike-Slip	0.5539
TH19	0.0403	8.8293	Chi-Chi- Taiwan-04	1999	6.20	Strike-Slip	0.4964
TH20	0.0564	12.0436	Chi-Chi- Taiwan-04	1999	6.20	Strike-Slip	0.5495

Chapter 4

4 METHODOLOGY

4.1 Geometry of buildings

For the purpose of this study a complete survey had to be done to find out the geometry of building in order to be able to create their structural models. Chain surveying was chosen to find the measurements of structural members.

A tape meter was used to find length and width of building, distance between columns in length and width of building and dimensions of columns and beams. Also an expandable staff of 5 meters was used to find the height of columns, beams and thickness of slabs.



Figure 4.1: Showing expandable staff; measuring height of column

4.1.1 Block A

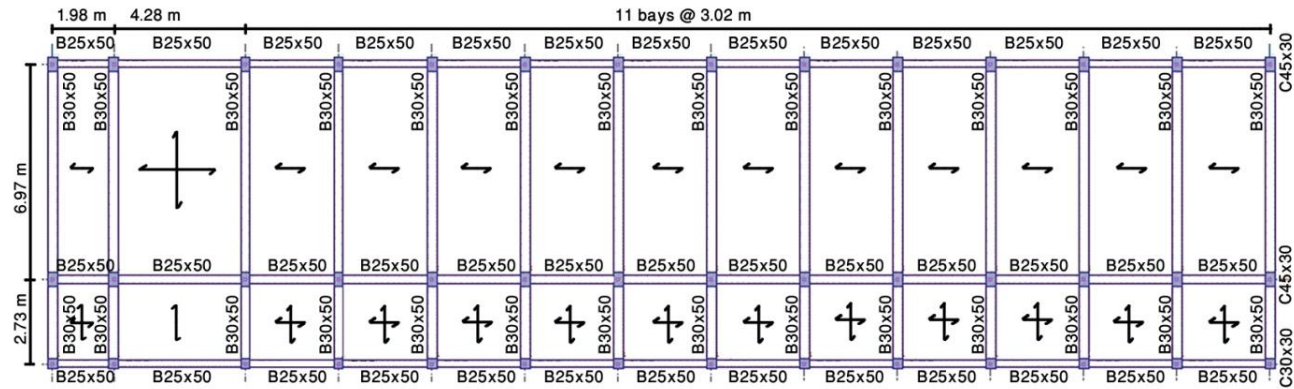


Figure 4.2: Typical ground floor plan – Block A

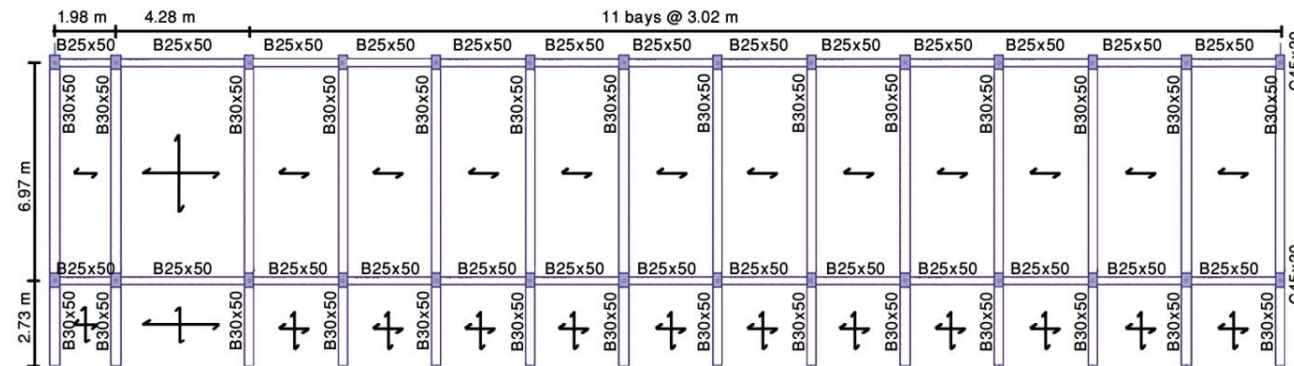


Figure 4.3: Typical storey plan – Block A

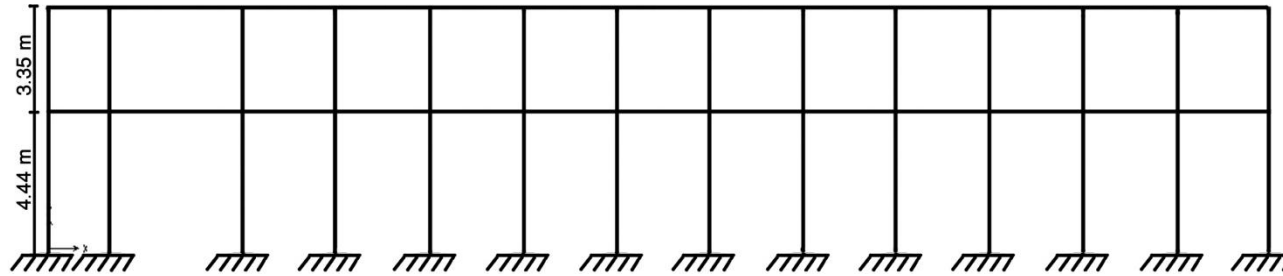


Figure 4.4: Frame elevation – Block A



Figure 4.5: Front view of Block A

4.1.2 Block B1

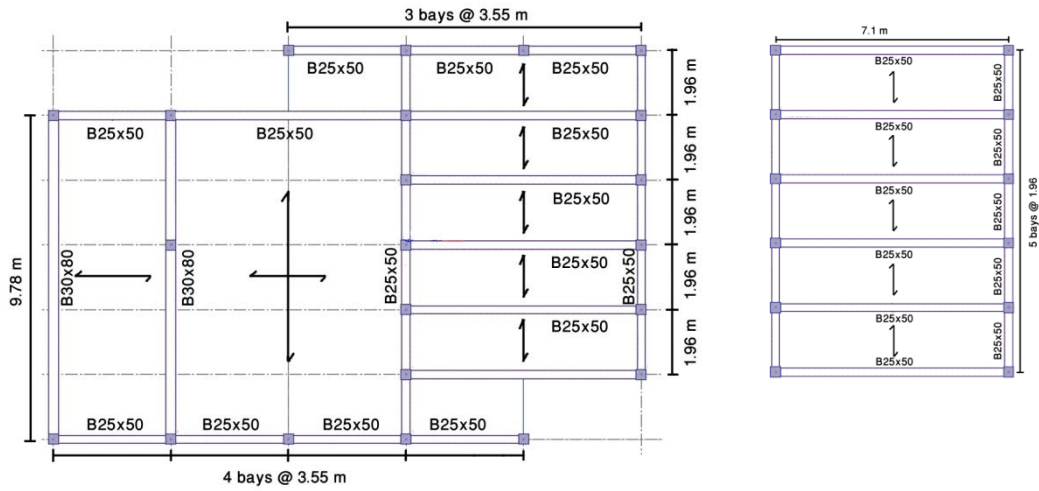


Figure 4.6: Left: Typical ground floor plan block B1 – Right: Storey plan block B1

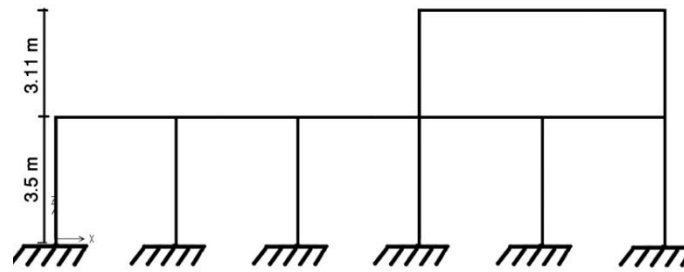


Figure 4.7: Frame elevation – Block B1



Figure 4.8: Side view of Block B1

4.1.3 Block B2

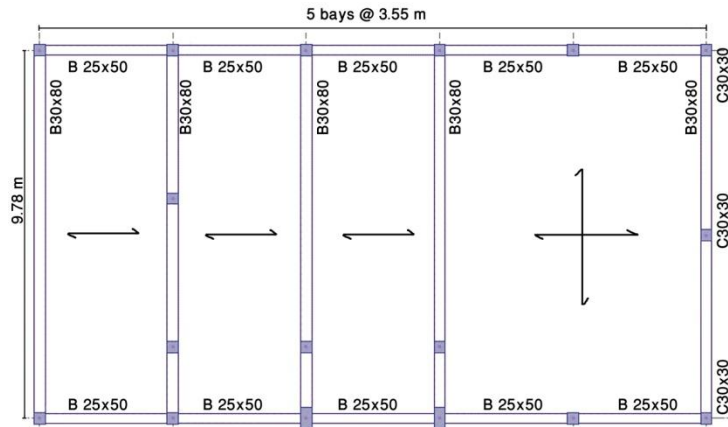


Figure 4.9: Typical ground floor plan – Block B2

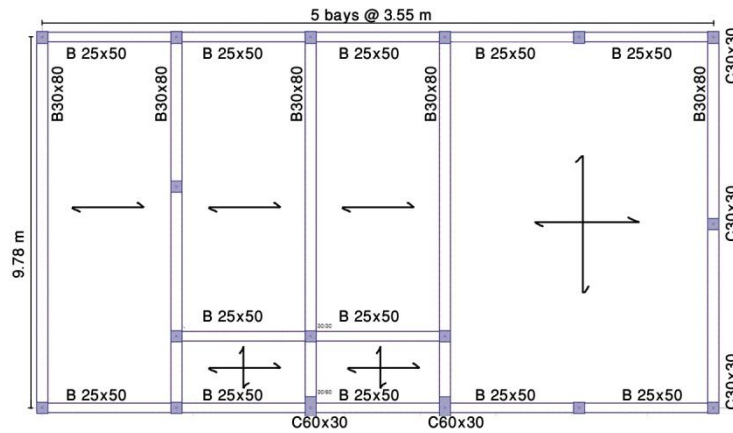


Figure 4.10: Typical storey plan – Block B2

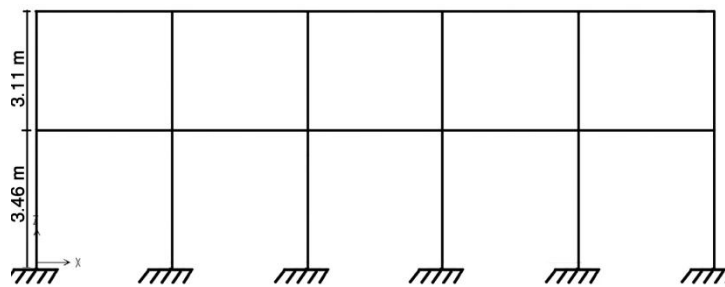


Figure 4.11: Frame elevation – Block B2



Figure 4.12: Front view of Block B2

4.1.4 Block C

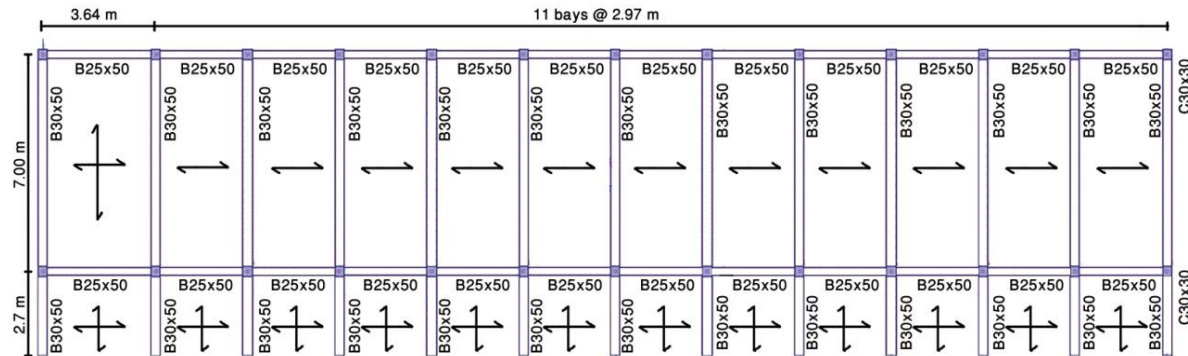


Figure 4.13: Typical ground floor – Block C

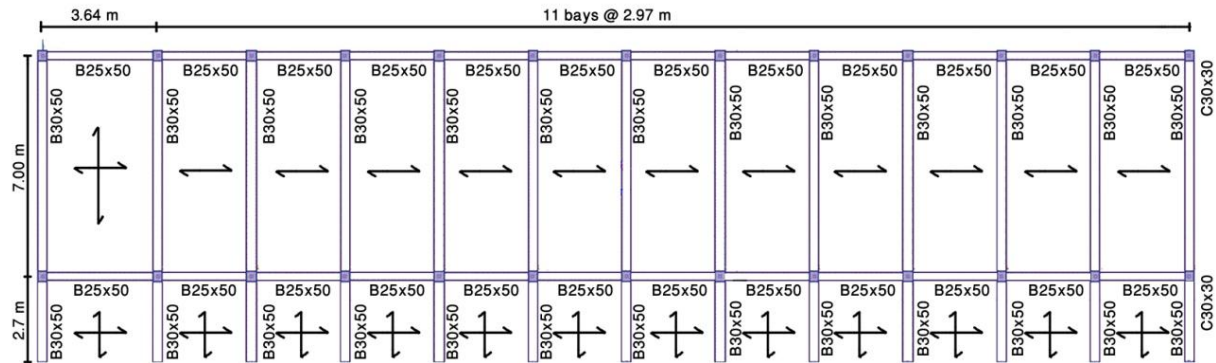


Figure 4.14: Typical storey plan – Block C

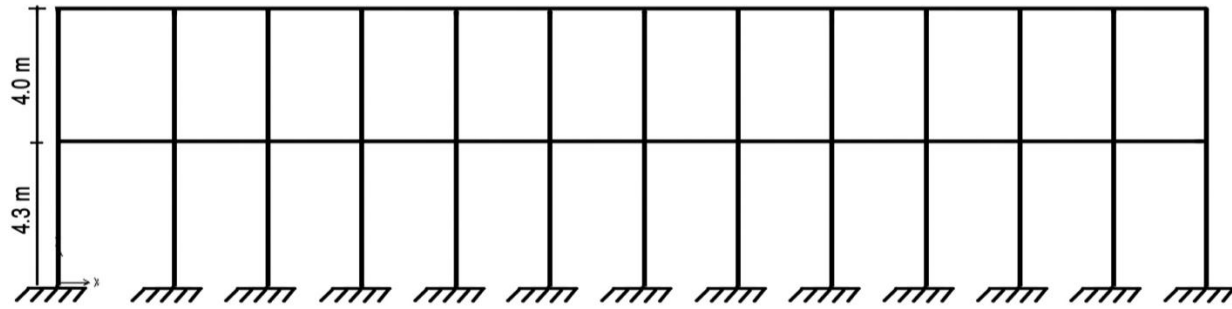


Figure 4.15: Frame elevation – Block C



Figure 4.16: Front view of block C

4.1.5 Block D

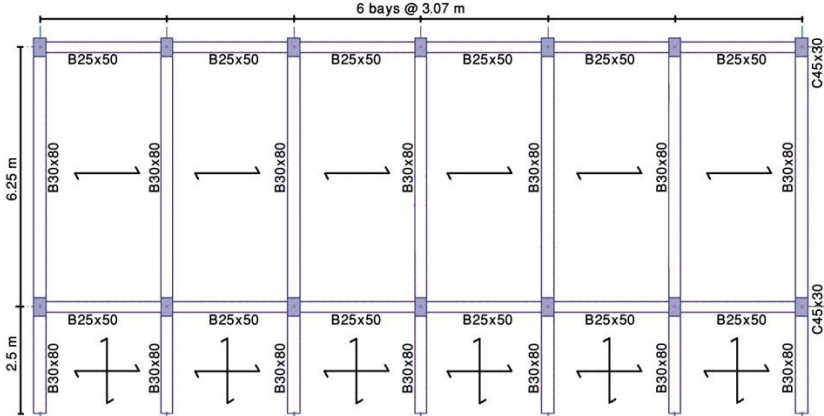


Figure 4.17: Typical ground floor – Block D

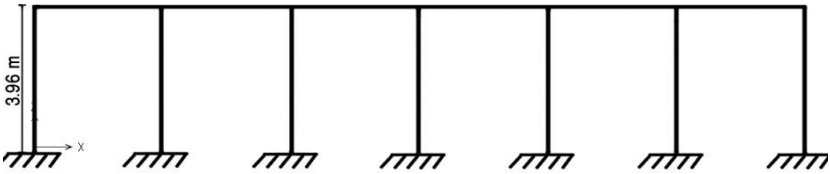


Figure 4.18: Frame elevation – Block D



Figure 4.19: Front view of block D

4.2 Specification of building characteristics

First step to assess a reinforced concrete building after having all the measurements on plan is to find the properties of existing materials of construction and identify the beam and column sections of the existing structure. Drawings were not available for existing buildings of Bekir Paşa high school site, therefore as-built plans had been produced shown in Section 4.1. Destructive and non-destructive tests were performed to identify the present section characteristics of the structure.

4.2.1 Non-Destructive testing

4.2.2.1 Rebound test

Rebound test also known as Schmidt Hammer test is a non destructive test which is sensitive to the surface hardness of concrete and is used to find the compressive strength of concrete. A typical rebound hammer is shown in Figure 4.20.

The plunger should be placed normal to the concrete surface and strongly pushed to cause hammer mass to make an impact on the surface through plunger, once the impact is made spring rebounds and rebound number will be shown on scaling window, at this point hammer needs to be locked and number should be recorded. Reading is sensitive to the variation of concrete surface. Several reading should be taken from the interest surface to decrease the error since this test is particularly sensitive to the aggregate particles close to the surface. ASTM C805 suggests taking at least ten readings from each test surface (Bungey, 2006).

In order to perform this on an existing reinforced concrete structure, a square surface shall be chosen on the structure member where there is no reinforcement is behind the

surface so steel will not affect the results. All coating and plasters should be removed from the selected area and surface must be sanded to become as smooth as possible, then rebound test will be applied as described above on different parts of surface.

In this study 30 percent of columns of each structure were selected to perform rebound test, columns were selected randomly from different parts of building to check the compressive strength of existing concrete in the members. Rebound hammer readings from columns of buildings are shown in Appendix B.

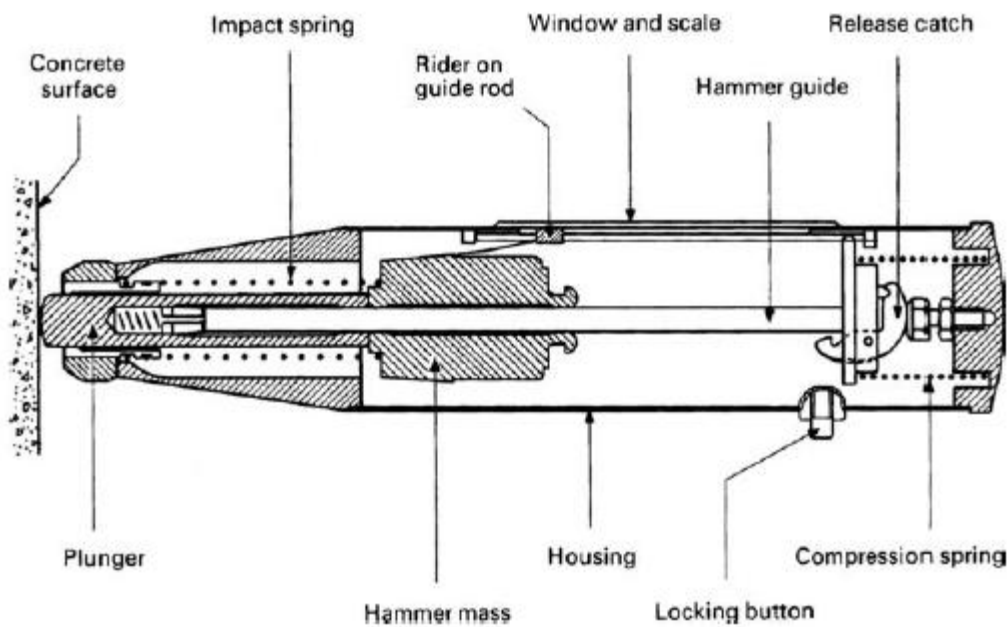


Figure 4.20: Rebound Hammer (Bungey, 2006)

4.2.2.2 Ferro scan test

Ferro scan test is very popular when it is required to identify the reinforcement bars and their location inside the structural member. Ferro scan device is basically consisting of a monitor and scanner, a 600 millimeters square board is also required.



Figure 4.21: Ferro scan device

The device is easy to use, after selection of the structural member to be scanned, 600 mm square board should be attached to the member and then device will be set to scan, the scanner is sensitive to any type of steel and metal so care must be taken while setting the scanner not to be facing any type of metal. Scanner is able to scan 15 mm width so 4 readings in horizontal direction and 4 in vertical direction should be scanned in order to cover the whole 600 mm square board where after covering the board area data will be saved in to the device and there after data can be uploaded to the software designed to analyze the depth of identified reinforcement bars and their distance from each other.

This equipment can read depth of 100 mm from surface so any points deeper than that cannot be analyzed, therefore while scanning the member user should check the result to see whether they are accurate or not, although the equipment has this disadvantage but still is the best way to detect the existing bars inside the structure member without removing the concrete cover.

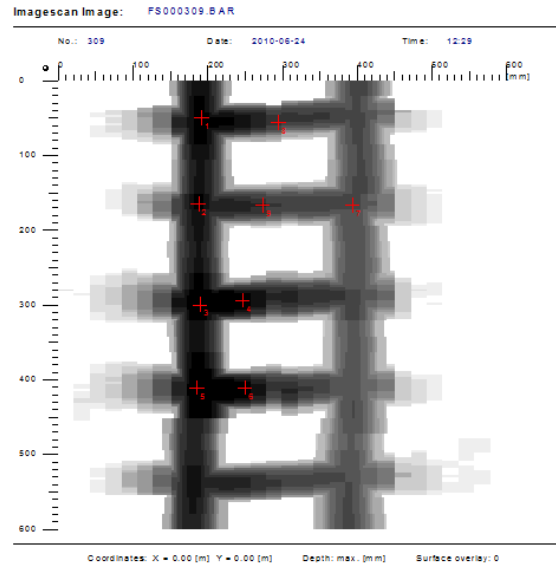


Figure 4.22: Typical scan of reinforcement bar from a column

For the purpose of this study readings were taken from columns and beams to detect the size and location of existing reinforcement bars of members so sections of these structure member could be identified for performing the analysis on the buildings.

4.2.2 Destructive testing

One of the most popular destructive tests for reinforced concrete buildings is core drilling also known as carrot taking from structural members. Concrete core drilling machine shown in Figure 4.23 was used to take samples from columns of building.

This machine is consisting of a stand that can be fixed to the ground, water pipe to pour water while drilling for cooling down the drill and the drill which has to be set on the stand to be able to drill horizontally through the member. Before setting the equipment for drilling reinforcement bars inside the member has be detected and marked on the member so while drilling only the concrete core will be taken from the member. The drill is able to take 100 mm diameter concrete cylinder samples shown in Figure 4.25.



Figure 4.23: Concrete core drilling machine – taking carrot from a column



Figure 4.24: showing drilled area after taking the sample from column



Figure 4.25: Showing capped concrete core sample

Once concrete cores are taken, top and bottom of cylindrical samples needs to be cut and smoothed so the sample can sit balanced, then both top and bottom should be capped by Sulfur-Sand mixture and placed into water tank for 48 hours so they become fully saturated. Thereafter cylindrical samples should be taken out and with use of a fabric become saturated surface dried and ready for compressive strength test, this will result in identifying the minimum compressive strength of the concrete core samples from buildings.

4.2.2.1 Calculation of actual strength

After performing compression test on concrete cores the actual strength of samples should be estimated, for this study actual strength is calculated according to Concrete society technical report No. 11.

For cores drilled in horizontal direction (Concrete society, 1987):

$$\text{Estimated Actual Strength} = \frac{2.5}{1.5 + \frac{1}{\lambda}} \times \text{Core Strength} \quad (\text{eq. 4.1})$$

Where;

$$\lambda = \frac{\text{length}}{\text{diameter}} \text{ For concrete core} \quad (\text{eq. 4.2})$$

$$\text{Core strength} = \frac{\text{Fracture load}}{\text{Secion area}} \quad (\text{eq. 4.3})$$

While taking cores from structure members care must be taken not to cut any of the reinforcing bars so the core sample will be from concrete part of structure member, although bars are checked from scanning the steel bars but there is always a chance that accidentally a partial piece of steel bar is cut so will be a part of core sample that will affect the compression test results, to solve this effect a corrections needs to be carried on results.

According to (Concrete Society, 1987);

$$\text{Corrected Actual Strength} = SF * \text{Estimated Actual Strength}$$

$$\text{Scale Factor} = 1 + 1.5 \left(\frac{D_{bar} * d_{bar}}{D_{core} * L_{core}} \right) \quad (\text{eq. 4.4})$$

D_{bar} : Diameter of the bar inside the sample

d_{bar} : Distance of the bar to the closest end

D_{core} : Diameter of concrete core sample

L_{core} : Length of concrete core sample

In order to investigate the compressive strength of “Bekir Paşa school” building’s 10 percent of columns from each building were selected randomly from different parts of structure, samples were taken and tested for compressive strength as explained above and results were calculated and recorded to be used for creation of structure members existing sections. Results obtained for actual compressive strength of core samples taken from columns of buildings are shown in Appendix D.

4.3 Modeling the buildings

In order to find out the behavior of structure against seismic loads, existing section properties of structural members should be identified, in this study results obtained from survey explained above material properties and location of reinforcement bars sitting inside the structure members were defined in software to find the weight of structure member sections and their moment carrying capacity.

Structure frame consist of beams, columns and slabs were modeled in structural analysis program SAP2000 and identified existing section properties of members were defined, a linear static analysis were performed to check structure member weight loads. For performing structural analysis on building located on Bekir Paşa high school site computer program CSI SAP2000 14A was selected, this program gives user ability to define section properties of structural members. All sections were defined in CSI SAP Section designer feature that can also calculate Moment-Curvature relationship of a section and assign section properties in model while plastic hinges assigned from FEMA356 specifications for reinforced concrete columns and beams (ASCE, 2000), are generating during nonlinear analysis.

4.3.1 Structural members section properties

Based on collected data and engineering assumptions all structural member section properties were identified and are listed in tables below.

4.3.1.1 Block A

Table 4.1: Block A beam section properties

Section	Dim (cm)	Bottom	Top	Stirrups	(+) My	(+) Mp	(-) Mp	W (kN/m)
Beam	30x50	3 Φ 20	2 Φ 12	Φ 8 / 15	65.8	90.02	-	3.68
Beam Edge	30x50	2 Φ 20	3 Φ 20	Φ 8 / 15	51.58	60.02	90.1	3.68
Beam	25x50	3 Φ 16	2 Φ 12	Φ 8 / 25	44.35	58.8	-	3.07

(Cover 2.5 cm, $f_c=16$ MPa, $f_y=220$ MPa, moments in kN.m)

Table 4.2: Block A column section properties

Section	Dim (cm)	Major	Minor	Stirrups	(\pm) My	(\pm) Mp	W (kN/m)
Column	45x30	4 Φ 20	2 Φ 20	Φ 8 / 15	39.2	51.4	3.31
Column	30x30	4 Φ 20	2 Φ 20	Φ 8 / 15	39.2	50.8	2.21

(Cover 2 cm, $f_c=16$ MPa, $f_y=220$ MPa, moments in kN.m)

4.3.1.2 Block B1

Table 4.3: Block B1 beam section properties

Section	Dim (cm)	Bottom	Top	Stirrups	(+) My	(+) Mp	(-) Mp	W (kN/m)
Beam	30x80	3 Φ 20	2 Φ 12	Φ 8 / 20	123.8	155.6	-	5.88
Beam Edge	30x80	2 Φ 20	3 Φ 20	Φ 8 / 20	89.2	98.4	147.8	5.88
Beam	25x50	3 Φ 16	2 Φ 12	Φ 8 / 25	49.2	56.7	-	3.07

(Cover 2.5 cm, $f_c=25$ MPa, $f_y=220$ MPa, moments in kN.m)

Table 4.4: Block B1 column section properties

Section	Dim (cm)	Major	Minor	Stirrups	(\pm) My	(\pm) Mp	W (kN/m)
Column	30x30	4 Φ 16	-	Φ 8 / 15	18.8	24.01	2.21

(Cover 2.5 cm, $f_c=25$ MPa, $f_y=220$ MPa, moments in kN.m)

4.3.1.3 Block B2

Table 4.5: Block B2 beam section properties

Section	Dim (cm)	Bottom	Top	Stirrups	(+) My	(+) Mp	(-) Mp	W (kN/m)
Beam	30x80	3 Φ 20	2 Φ 12	Φ 8 / 20	123.8	155.61		5.88
Beam Edge	30x80	2 Φ 20	3 Φ 20	Φ 8 / 20	89.16	98.42	147.7	5.88
Beam	25x50	3 Φ 16	2 Φ 12	Φ 8 / 25	49.16	56.66		3.07

(Cover 2.5 cm, $f_c=16$ MPa, $f_y=220$ MPa, moments in kN.m)

Table 4.6: Block B2 column section properties

Section	Dim (cm)	Major	Minor	Stirrups	(\pm) My	(\pm) Mp	W (kN/m)
Column	30x30	4 Φ 16	-	Φ 8 / 15	18.9	22.21	2.21
Column	60x30	4 Φ 16	4 Φ 16	Φ 8 / 15	34.28	44.86	4.41

(Cover 2 cm, $f_c=16$ MPa, $f_y=220$ MPa, moments in kN.m)

4.3.1.4 Block C

Table 4.7: Block C beam section properties

Section	Dim (cm)	Bottom	Top	Stirrups	(+) My	(+) Mp	(-) Mp	W (kN/m)
Beam	30x50	3 Φ 20	2 Φ 12	Φ 8 / 20	68.66	90.22	-	3.68
Beam Edge	30x50	2 Φ 20	3 Φ 20	Φ 8 / 20	51.69	60.19	90.1	3.68
Beam	25x50	3 Φ 16	2 Φ 12	Φ 8 / 25	49.2	56.7	-	3.07

(Cover 2.5 cm, $f_c=16$ MPa, $f_y=220$ MPa, moments in kN.m)

Table 4.8: Block C column section properties

Section	Dim (cm)	Major	Minor	Stirrups	(\pm) My	(\pm) Mp	W (kN/m)
Column	30x30	4 Φ 16	-	Φ 8 / 20	16.79	22.2	2.21

(Cover 3 cm, $f_c=16$ MPa, $f_y=220$ MPa, moments in kN.m)

4.3.1.5 Block D

Table 4.9: Block D beam section properties

Section	Dim (cm)	Bottom	Top	Stirrups	(+) My	(+) Mp	(-) Mp	W (kN/m)
Beam	30x80	3 Φ 20	2 Φ 12	Φ 8 / 23	129.39	150.48	-	5.88
Beam Edge	30x80	2 Φ 20	3 Φ 20	Φ 8 / 23	92.51	99.75	147.8	5.88
Beam	25x50	3 Φ 16	2 Φ 12	Φ 8 / 25	49.49	60.02	-	3.07

(Cover 2.5 cm, $f_c=30$ MPa, $f_y=220$ MPa, moments in kN.m)

Table 4.10: Block D column section properties

Section	Dim (cm)	Major	Minor	Stirrups	(\pm) My	(\pm) Mp	W (kN/m)
Column	45x30	4 Φ 16	2 Φ 16	Φ 8 / 20	29.58	34.98	3.31

(Cover 3.8 cm, $f_c=30$ MPa, $f_y=220$ MPa, moments in kN.m)

4.3.2 Loads acting on structure

After defining the geometry of buildings in computer software and assigning member sections and hinges to each end of frame structure, loads acting on frames shall be defined. Self weight of member sections, self weight of slabs, assumed live load and additional dead load have been distributed uniformly along the frame lengths. Following assumptions have been defined for all buildings.

Additional dead load of 1.2 kN/m^2 acting in gravity direction is assumed for all the members. Live load of 1.5 kN/m^2 acting on roof and 3.5 kN/m^2 acting along the stories are assumed in gravity direction (Aydinoglu, 2007). Self weights of slabs were calculated by “IDE CAD structural” program for 15 cm thickness as 5.15 kN/m^2 were distributed along the beams acting in gravity direction.

Self weight of beams and columns sections are defined in section 4.3.1, for each member SAP2000 were set to consider mass source from the defined member section self weight and additional dead load and live loads acting along them.

4.4 Pushover analysis

Pushover or non-linear static analysis is a method of analysis that can identify displacement of any point on structure due to accelerating lateral loading that presents inertia forces of an earthquake. Nonlinear pushover analysis is being used by structural engineers as a standard tool to find out the response of structures to seismic loads (Chopra and Goel, 2003).

In order to perform push-over analysis buildings were modeled as a three dimensional frame structure in analysis computer program “SAP2000”. Calculated loads in section

4.3.2 applied as uniformly distributed gravity loads on members. Mass sources selected to be from members self weights and additional loads acting on them. Identified reinforced concrete sections and their material properties were defined and attached to the corresponding member.

“SAP2000” offers a powerful nonlinear static push over analysis option which tracks hinge information and helps to identify failure modes of structure. Plastic hinges were assigned at relative distance of both ends of all beams and columns (ASCE, 2000); properties of generated hinges shall be controlled to be appropriate to obtained section moment capacities. Frame hinges were selected from FEMA356 table 6.7 (Concrete Beams – Flexure) and table 6.8 (Concrete Columns – Flexure) in M3 degree of freedom.

The push-over load case should be defined for program, basic idea of push-over is to keep the vertical loads on structure constant and start increasing lateral loading to bring structure to different limit states. In this study push-over load case is defined as a nonlinear static analysis, starting applying load as acceleration in U_x and U_y direction to the structure continued from state at end of nonlinear case on dead and live loads. Load application should be displacement controlled to push to displace the control joint to a selected length which can be assumed by user, in this study it is defined for program to push till 300 mm top displacement for all structures. Analysis should be performed in multiple steps, this will allow engineer to observe behavior of frames during push. All the buildings for this study were modeled, analyzed and capacity curves are constructed that will be discussed in chapter 5.

Observing displacement and generation of plastic hinges and their change in limit states in structure allows engineer to find the critical frames. These frames shall be analyzed separately; comparison of results obtained from both analyses is explained chapter 5.

4.4.1 Nonlinear static pushover analysis steps

In order to perform nonlinear static pushover analysis following steps shall be taken;

- 1- Creating elements presenting beams and columns of structure's frames
- 2- Defining existing material properties of building
- 3- Creating columns and beams sections according to their existing properties
- 4- Assigning defined frame sections to beams and columns
- 5- Assigning additional gravity loads distributed on structure's frames
- 6- Assigning plastic hinges to both ends of each member from FEMA356 plastic hinge specifications for reinforced concrete beams and columns. After generation of plastic hinges the hinges properties have to be overwrite and checked to verify that the calculated behavior is appropriate for the model
- 7- Pushover load case shall be defined, analysis type is nonlinear, horizontal load shall be applied as acceleration with displacement control so program will push to displace to a user specified displacement limit
- 8- Control node shall be specified to be able to record the displacements due to increased load at each step
- 9- Vertical loads shall be kept constant and program starts to push after effect of gravity loads, lateral load patterns will change with respect to each mode shape of structure

10- Running analysis and using output data to construct the capacity curve and investigate the performance point of structure

4.5 Non-Linear Time-History analysis

Non linear time history analysis is generally acknowledged to be the most correct way of investigating the response of structures to earthquake loading (Pinho, 2007). SAP2000 has a feature for time history analysis that allows engineer to observe the behavior of structure to the corresponding ground accelerations. This method records the displacement of any point on structure caused by earthquake recorded acceleration data during the chosen time period. In order to obtain more accurate results the selected critical frame from each structure is subjected to 20 different ground accelerations that has been selected and scaled explained in chapter 3.

Frame model of structure according to specifications identified in this chapter is set to experience ground motion accelerations. Mass source of structure should be from the defined elements, scaled time history is defined for program, and steps to be recorded is chose to be 20 steps per second for duration of 10 seconds. Load shall be applied as acceleration in U_x direction using the defined time history function with scale factor of 9.80665 to convert g unit to meter per square second.

Critical frames of each structure in this study were subjected to 20 earthquake excitations and displacement of control joint was recorded. Interpreting the results for obtained acceleration-displacement relationship for each time series is difficult, hence same control joint from pushover analysis were chosen to be able to compare the displacement caused by ground acceleration with displacement caused from accelerating

lateral loading and calculated limit state capacity of structure with respect to displacement function.

Behavior of reinforced concrete structures in the event of seismic loading has always been an issue; unfortunately the best test is an actual earthquake to identify structure's behavior but simulating the structure and study on its response to earthquake loading can help engineer to find out the possible behavior of system and thereafter try to prevent it from collapse, hence risk assessment of existing buildings should be done according to calculated plastic hinge states and finding possible damages to the structure. A statistical approach needs to be performed in order to interpret the obtained displacement data from non linear time history analysis (Shinozuka et. all., 2001).

In order to find a probabilistic risk analysis on structures in this study, spectral displacement (S_d) of control joint is constructed with respect to spectral acceleration (S_a) causing it, there after structure limit states for yielding, Immediate Occupancy, Life Safety and Collapse prevention identified from non-linear static pushover analysis on the same frame for control joint were used to find all the points that are located within the limits. Frequencies of points located in each limit state were identified and percentages of being in each performance level were calculated respectively. Frequency percentages of structure being in each limit state were assumed to specify vulnerability of structure subjected to selected earthquakes. Plotting found vulnerability against top displacement of structure shows an exponential increase in vulnerability with increase in top displacement. Finally finding the acceleration needed to cause those top displacements and plotting it against the frequency percentage of points located in each limit state presenting vulnerability of structure allows engineer to observe and predict

the vulnerability percentage of structure subjected to ground acceleration. Constructed curves and discussion on results is explained in chapter 5.

4.5.1 Nonlinear time history analysis steps

In order to perform the nonlinear time history analysis first 5 steps for nonlinear pushover analysis shall be taken to create the model of building according to structure's existing properties, and then following steps will be taken;

- 1- Time history function shall be defined, the scaled ground motion acceleration will be uploaded as time history function
- 2- Modal load case shall be set to use Ritz vectors and load type as acceleration
- 3- Defining time history load case, using the defined time series function with load type of acceleration with scale factor of 9.81 to convert the g unit to meters
- 4- Number of output time steps and time step size shall be specified, the more output time will simply provide more details on output
- 5- Running analysis and using output data to investigate performance level of structure according to its maximum displacement and constructing probability of being in different performance level with respect to structure's top displacement.

Chapter 5

RESULTS AND DISCUSSION

5.1 Results obtained from pushover analysis

Nonlinear static pushover analysis has been performed on three dimensional models of buildings and the selected critical weak 2D frame of the structure as described in Section 4.4. Results obtained from performing analysis are discussed in sections below.

5.1.1 Capacity curves

According to output data of the program force-displacement relationships of structure and the selected critical frame are constructed. Capacity curve is describing the displacement of the control node due to the lateral forces acting along the height of building. Lateral forces were applied in two horizontal directions (U_x & U_y) for the three dimensional model of structure. Forces applied for frame model were in one direction (U_x) and the corresponding displacements in same direction were recorded.

Both capacity curves of 3D model and 2D frame model of buildings are shown for each building in following sections. In order to investigate the response of structure, critical points where the behavior of structure changes due to increasing lateral forces should be identified. For all idealized curves a linear increase in base shear causing displacement is observed up to a point where the slope of line changes. This point is representing the response of structure where stiffness and strength starts to decrease and structure yields.

Any points before that on the linear line are representing the resistance of structure to applied loading. Yielding point of each structure is shown for each capacity curve on figures explained in following sections.

After structure starts to yield, stiffness and strength continue to decrease because of continuous increase in horizontal forces. The program (SAP2000) has continued increasing loading up to a point where the first collapse is observed. This point is known as the collapse prevention point and is representing the capacity of structure and the maximum deformation that will cause structure to collapse. For different structures this point can show collapse of a single member or some members together, hence after collapse of any member some structures might not completely collapse and might keep little resistance capacity, no matter how small this resistance can be it has to be identified to be able to evaluate the complete behavior of building. SAP2000 has the ability to continue from the point of first collapse, at this point first plastic hinge is failed so it is not acting in system anymore, hence loading drops to zero and starts to increase again to reach the next plastic hinge or hinges collapse. Collapse point of each structure is shown for each capacity curve and response of each structure is discussed at that point in following sections.

According to Table 7.7 of Turkish Earthquake code 2007 (Aydinoglu, 2007), target displacement obtained for assessed building shall not exceed Immediate Occupancy performance level for ground motions with 10% probability of being exceeded in 50 years. For all buildings assessed in this study target displacement is obtained and discussed in following sections.

5.1.1.1 Block A

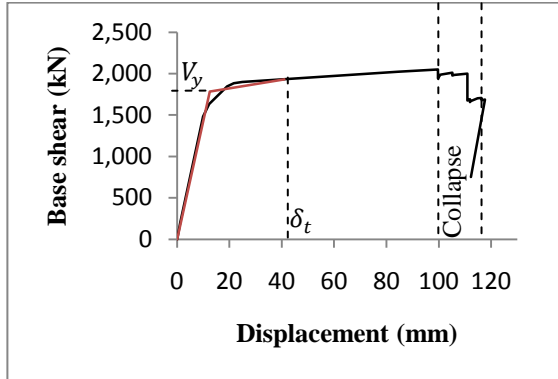


Figure 5.1: Capacity curve for 3D model pushover analysis of Block A

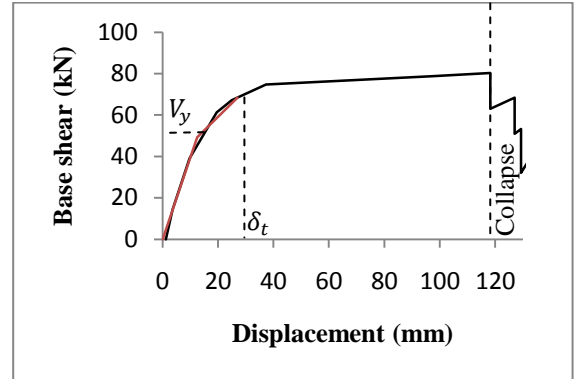


Figure 5.2: Capacity curve for frame model pushover analysis of Block A

Target displacement and the corresponding base shear force are calculated according to FEMA356 procedure explained in chapter 2 (ASCE, 2000). Capacity curve for 3D model of building is shown in Figure 5.1 where target displacement is calculated as $\delta_t = 41$ mm and base shear force causing this displacement is equal to 1932 kN. Capacity curve for frame model of building is shown in Figure 5.2 where target displacement is calculated as $\delta_t = 27$ mm and base shear force causing this displacement is equal to 68.5 kN. Looking at the obtained results it can be seen that in both capacity curve yielding will start when roof is displaced 12.5 mm. For 3D model first collapse happens at 100 mm but main collapse is at 118 mm roof displacement which is the same as displacement obtained for frame model at collapse stage. At this point structure cannot resist anymore loading and will be in mechanism.

5.1.1.2 Block B1

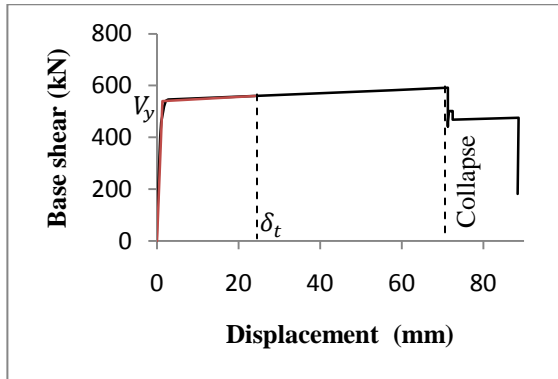


Figure 5.3: Capacity curve for 3D model pushover analysis of Block B1

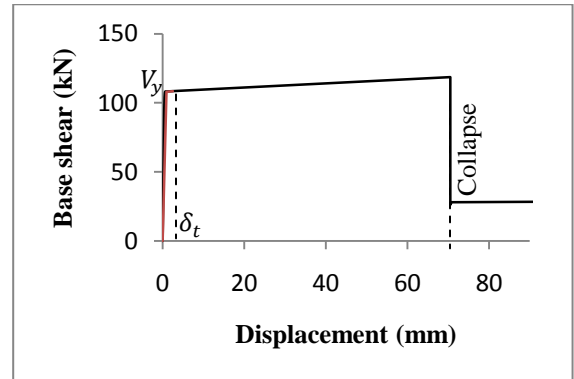


Figure 5.4: Capacity curve for frame model pushover analysis of Block B1

Capacity curve for 3D model of building is shown in Figure 5.3 where target displacement is calculated as $\delta_t = 24$ mm and base shear force causing this displacement is equal to 560 kN. Capacity curve for frame model of building is shown in Figure 5.4 where target displacement is calculated as $\delta_t = 2.6$ mm and base shear force causing this displacement is equal to 108.5 kN. Checking the idealized pushover curve for this block, it can be seen that 3D model starts to yield at displacement of 1.4 mm and frame model at 1 mm top displacement. Both pushover analysis results show same type of behavior for 3D and frame models of Block B1. Horizontal forces acting along the height of building causes structure to yield after 1 to 2 mm displacement of center of mass, this yielding will continue till top displacement of 70 to 71 mm where the collapse of some ground columns can be seen.

5.1.1.3 Block B2

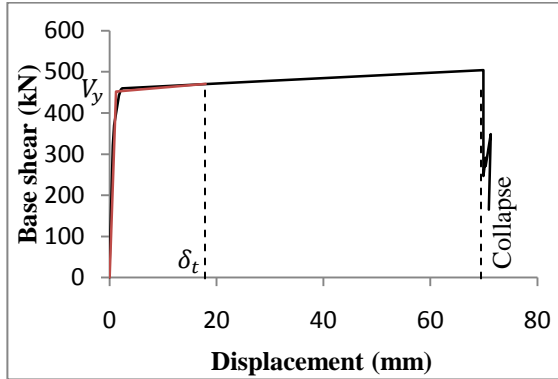


Figure 5.5: Capacity curve for 3D model pushover analysis of Block B2

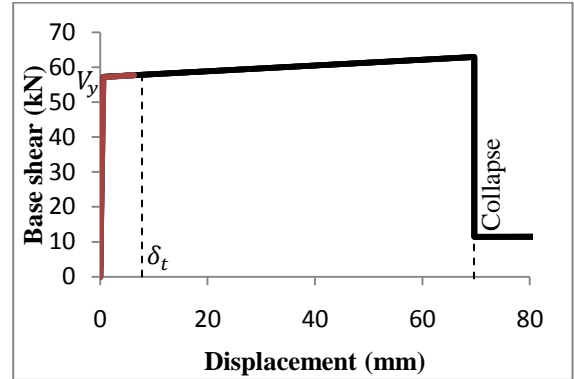


Figure 5.6: Capacity curve for Frame model pushover analysis of Block B2

Capacity curve for 3D model of building is shown in Figure 5.5 where target displacement is calculated as $\delta_t = 18$ mm and base shear force causing this displacement is equal to 470.35 kN. Capacity curve for frame model of building is shown in Figure 5.6 where target displacement is calculated as $\delta_t = 6.33$ mm and base shear force causing this displacement is equal to 58 kN.

Both pushover analysis results show same type of behavior for 3D and frame models of Block B2. Horizontal forces acting along the height of building causes structure to yield after 1 to 2 mm displacement of center of mass, this yielding will continue till top displacement of 70 to 71 mm where the collapse of some ground columns can be seen.

5.1.1.4 Block C

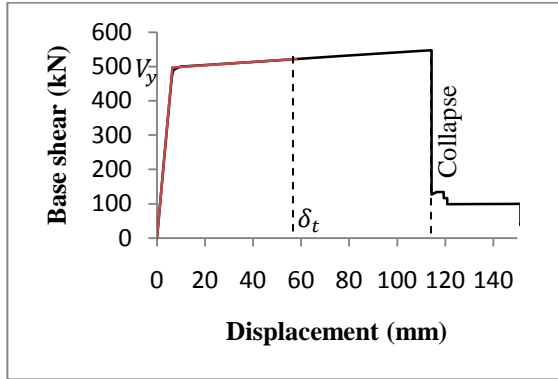


Figure 5.7: Capacity curve for 3D model pushover analysis of Block C

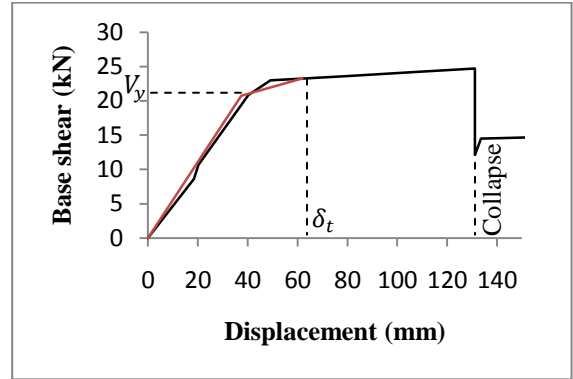


Figure 5.8: Capacity curve for frame model pushover analysis of Block C

Capacity curve for 3D model of building is shown in Figure 5.7 where target displacement is calculated as $\delta_t = 58$ mm and base shear force causing this displacement is equal to 521.72 kN. Capacity curve for frame model of building is shown in Figure 5.8 where target displacement is calculated as $\delta_t = 62$ mm and base shear force causing this displacement is equal to 23.3 kN.

Looking at the obtained results it can be seen that for 3D model collapse happens at 115 mm top displacement. Frame model at collapse stage has 131 mm top displacement. At this point structure cannot resist anymore loading and will be in mechanism.

5.1.1.5 Block D

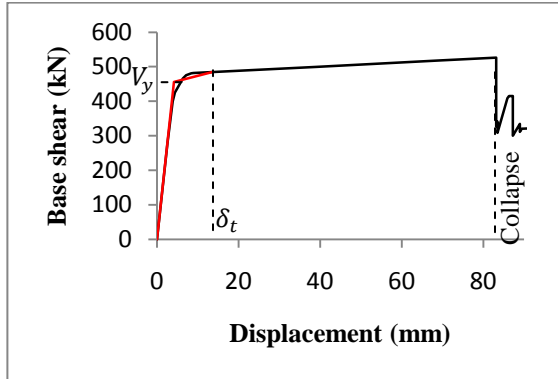


Figure 5.9: Capacity curve for 3D model pushover analysis of Block D

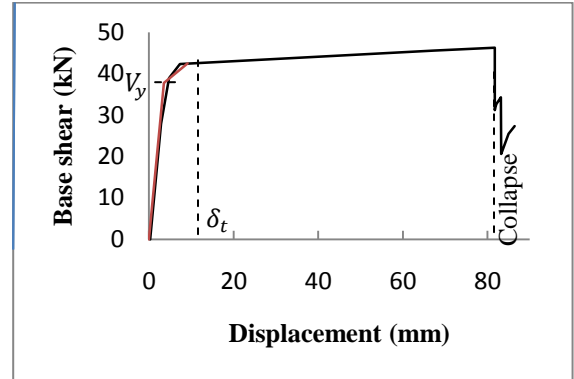


Figure 5.10: Capacity curve for frame model pushover analysis of Block D

Capacity curve for 3D model of building is shown in Figure 5.9 where target displacement is calculated as $\delta_t = 13.64$ mm and base shear force causing this displacement is equal to 484.64 kN. Capacity curve for frame model of building is shown in Figure 5.10 where target displacement is calculated as $\delta_t = 9.17$ mm and base shear force causing this displacement is equal to 42.44 kN.

Looking at the obtained results it can be seen that in both capacity curves yielding will start when roof is displaced 4 mm. For both models collapse happens at 80 to 83 mm top displacement. At this point structure cannot resist anymore loading and will be in mechanism.

5.1.2 Performance level limit states

According to member plastic hinge behavior during pushover analysis, results obtained for displacement function is listed in tables in following sections for each building, each displacement that causes a change in limit state of concrete hinges for control joint is identified. Target displacement obtained for each blocks frame model is the point that

structure go beyond the inelastic limit, in other words plastic hinges generated and structure start to resist the moments and changes its performance levels till collapse of frame. FEMA356 coefficient method parameters are shown in Appendix A.

Looking at the pushover steps taken for buildings, it can be observed that increasing horizontal loads increases the top displacement, this displacement can be defined as a ratio to height of building and observe the roof displacement with respect to height of building. Base shear is increased up to a point where the first plastic hinge or hinges is failed, that is the point where a decrease in base shear is seen but structure has lost its stiffness so smaller horizontal loads can result in more displacement of roof. Checking the generation of plastic hinges and their changes in performance level, the performance limit states of buildings are identified. Performance levels of buildings on their capacity curves are discussed in sections below for each building.

5.1.2.1 Block A

Table 5.1: Pushover steps – Block A

STEP	Base shear (kN)	Top displacement (mm)	Roof Drift %
1	14.29	3.62	0.05%
2	39.11	9.70	0.12%
3	61.37	19.55	0.25%
4	67.23	24.99	0.32%
5	74.73	37.36	0.48%
6	76.78	67.36	0.86%
7	78.82	97.36	1.25%
8	80.24	118.28	1.52%
9	62.96	118.28	1.52%
10	68.42	126.94	1.63%
11	51.02	126.94	1.63%
12	53.33	129.26	1.66%

Table 5.1 is showing the push over step taken for block A, obtained results show that structure starts to yield at 12.5 mm top displacement. Step 6 is where the ground columns plastic hinges change their states to immediate occupancy, according to FEMA356 (ASCE, 2000) at this level structure has damages that can be repaired and it is still safe to be used. Block A has 67.36 mm roof displacement at this level, columns hold this level up to next step where displacement is 97.36 mm and performance level changes to life safety. At this level major damages is expected and structure cannot be used anymore because it has high risk of injury. For block A exterior columns holding the balcony is in life safety and at step 8 will collapse, but the main building ground columns change their performance to life safety in step 8 and collapse at step 12 where displacement is 129.26 mm. Table 5.2 shows start and end of each performance level calculated for this structure. Figure 5.11 shows performance levels on structure's capacity curve.

Target displacement calculated from FEMA356 coefficient method is 27 mm; at this top displacement structure is in yielding stage with roof drift ratio of 0.35%. Plastic hinges are resisting moments but has not changed their limit states to immediate occupancy level yet. Therefore expected performance level is within the acceptance criteria specified by 2007 Turkish Earthquake code (Aydinoglu, 2007). Structure is expected to have very slight damages and will remain safe to use.

Table 5.2: Limit states – Block A

Limit state	Start (mm)	End (mm)
Yield	12.50	-
IO	12.50	67.36
LS	67.36	97.36
CP	97.36	118.30
Collapse	118.30	129.30

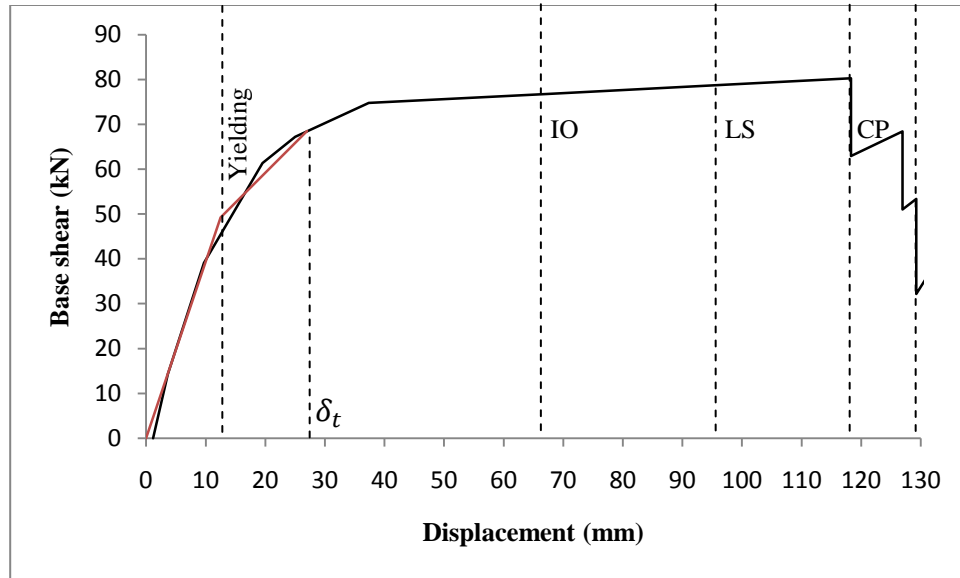


Figure 5.11: Structure performance limit states of frame model – Block A

5.1.2.2 Block B1

Table 5.3: Pushover steps – Block B1

STEP	Base shear (kN)	Top displacement (mm)	Roof Drift %
1	94.86	0.45	0.01%
2	104.06	0.50	0.01%
3	107.33	0.56	0.01%
4	108.18	0.64	0.01%
5	115.61	50.23	0.76%
6	118.63	70.55	1.07%
7	26.13	70.55	1.07%
8	28.09	70.75	1.07%
9	28.38	100.75	1.52%

Pushover analysis performed on block B1 shows that lateral loading representing ground motions will cause a very early yielding for building. Pushes over steps taken are shown in table 5.3. Existing building characteristics cannot behave elastic under affect of ground motions; it starts to yield at 1 mm top displacement and at step 5 performance level changes to immediate occupancy level. Top displacement at this point is 50 mm; within a 7 mm larger displacement due to increasing base shear, building will meet life

safety. Maximum displacement of roof that can stand ground motions is 71 mm where collapse of all ground columns will occur in frame model. For the 3D model structure can resist to displace 80 millimeters after partial collapse at 71 mm. Block B1 is partially 2 storey, columns of the single storey part of building is resisting the loads after collapse of 2 storey part. Frame model is taken out of 2 storey part of building to find out its performance during an earthquake. Displacement of control node to 71 mm will cause very heavy damage because of partial collapse of building so this point is considered as collapse prevention performance level. Table 5.4 shows start and end of each performance level calculated for this structure. Figure 5.12 shows performance levels on structure's capacity curve.

Target displacement calculated from FEMA356 coefficient method is 2.6 mm; at this top displacement structure is in yielding stage with roof drift ratio of 0.04%. Plastic hinges are resisting moments but has not changed their limit states to immediate occupancy level yet. Therefore expected performance level is within the acceptance criteria specified by 2007 Turkish Earthquake code (Aydinoglu, 2007). Structure is expected to have very slight damages and will remain safe to use.

Table 5.4: Limit states – Block B1

Limit state	Start (mm)	End (mm)
Yield	1.00	-
IO	1.00	50.00
LS	50.00	57.00
CP	57.00	71.00
Collapse	71.00	-

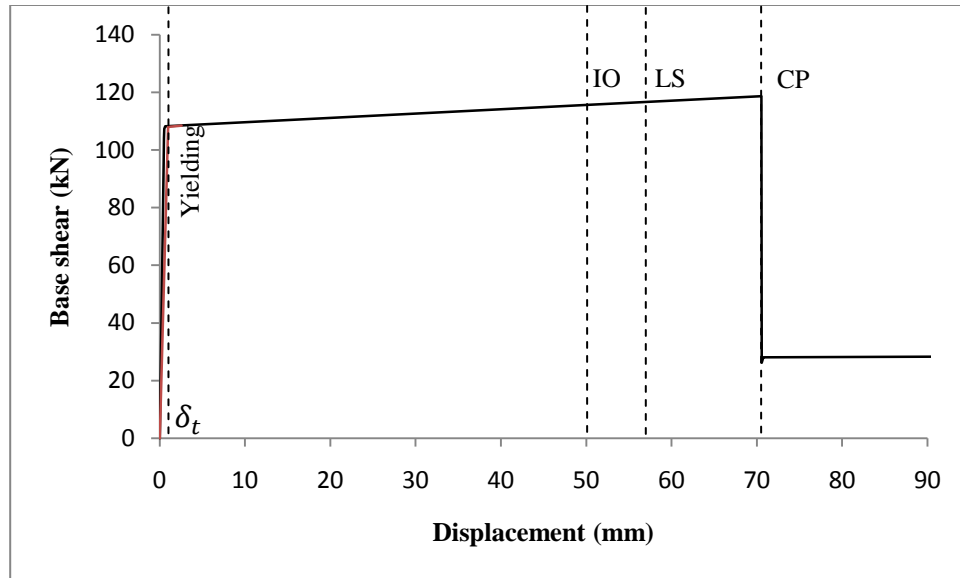


Figure 5.12: Structure performance limit states of frame model – Block B1

5.1.2.3 Block B2

Table 5.5: Pushover steps – Block B2

STEP	Base shear (kN)	Top displacement (mm)	Roof Drift %
0	0.00	0.00	0.00%
1	49.64	0.41	0.01%
2	53.99	0.46	0.01%
3	56.05	0.52	0.01%
4	57.22	0.64	0.01%
5	59.70	30.64	0.47%
6	62.18	60.64	0.92%
7	62.93	69.66	1.06%
8	11.44	69.67	1.06%
9	11.53	99.67	1.52%

Results obtained for block B2 shows an early yielding point, Push over steps taken are shown in Table 5.5; hence this building cannot remain its elastic properties for long time and very shortly starts to behave plastic. At step 5 building changes its performance level to immediate occupancy. This building has a small balcony where ground columns holding this balcony are the first to collapse. Hence after building changes to life safety stage at step 6, within 9 mm more displacement of control node balcony ground

columns will fail. Other ground columns of building holding the classrooms resist more to displace approximately 100 mm where the whole building will collapse. Table 5.6 shows start and end of each performance level calculated for this structure. Figure 5.13 shows performance levels on structure's capacity curve.

Target displacement calculated from FEMA356 coefficient method is 6.33 mm; at this top displacement structure is in yielding stage with roof drift ratio of 0.1%. Plastic hinges are resisting moments but has not changed their limit states to immediate occupancy level yet. Therefore expected performance level is within the acceptance criteria specified by 2007 Turkish Earthquake code (Aydinoglu, 2007). Structure is expected to have very slight damages and will remain safe to use.

Table 5.6: Limit states – Block B2

Limit state	Start (mm)	End (mm)
Yield	0.65	-
IO	0.65	30.70
LS	30.70	60.60
CP	60.60	71.00
Collapse	71.00	99.70

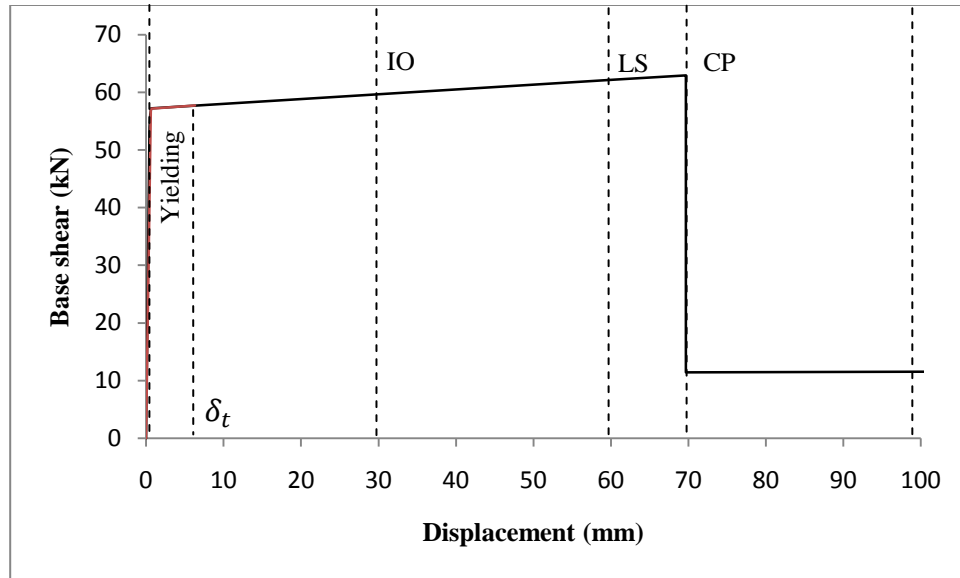


Figure 5.13: Structure performance limit states of frame model – Block B2

5.1.2.4 Block C

Table 5.7: Pushover steps – Block C

STEP	Base shear (kN)	Top displacement (mm)	Roof Drift %
1	8.63	18.48	0.22%
2	10.68	20.20	0.24%
3	20.83	40.31	0.49%
4	22.99	49.12	0.59%
5	23.61	79.12	0.95%
6	24.23	109.12	1.31%
7	24.69	131.17	1.58%
8	12.14	131.17	1.58%

Pushover analysis steps performed on block C are shown in Table 5.7. After 37.5 mm displacement of roof structure starts to yield and begin its plastic stage. From there till reaching 131.17 mm displacement that causes collapse of all ground floor columns, structure meets immediate occupancy level at 79.12 mm and changes performance level to life safety at 109.12 mm top displacement. This building shows good resistance to ground motions and has the highest capacity of buildings so far, but at the same time when the displacement reach 131.17 mm all ground floor columns will fail and structure completely collapse. For this building when roof drift ratio reaches 1%, becomes life

safety and resist until it reaches 1.5% drift ratio where it collapses. Table 5.8 shows start and end of each performance level calculated for this structure. Figure 5.14 shows performance levels on structure's capacity curve.

Target displacement calculated from FEMA356 coefficient method is 62 mm; at this top displacement structure is in yielding stage with roof drift ratio of 0.74%. Plastic hinges are resisting moments but has not changed their limit states to immediate occupancy level yet. Therefore expected performance level is within the acceptance criteria specified by 2007 Turkish Earthquake code (Aydinoglu, 2007). Structure is expected to have very slight damages and will remain safe to use.

Table 5.8: Limit states – Block C

Limit state	Start (mm)	End (mm)
Yield	37.50	-
IO	37.50	79.12
LS	79.12	109.12
CP	109.12	131.17
Collapse	131.17	-

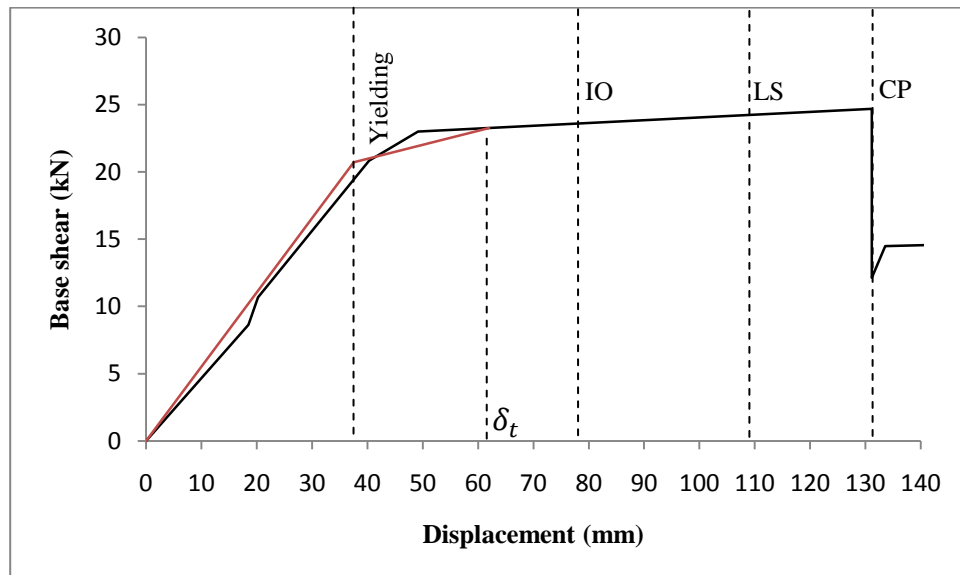


Figure 5.14: Structure performance limit states of frame model – Block C

5.1.2.5 Block D

Table 5.9: Pushover steps – Block D

STEP	Base shear (kN)	Top displacement (mm)	Roof Drift %
1	27.83	2.84	0.07%
2	38.89	4.76	0.12%
3	42.34	7.33	0.19%
4	43.93	37.33	0.94%
5	45.52	67.33	1.70%
6	46.29	81.76	2.06%
7	31.16	81.76	2.06%
8	31.96	81.88	2.07%
9	32.65	82.13	2.07%
10	34.27	83.22	2.10%

Push over steps taken for Block D is shown in Table 5.9, this building can last behaving elastic for a very short displacement of 3.5 mm, where structure starts to yield. Plastic sections generated in members of structure change their performance level to immediate occupancy after top displacement of 37.33 mm. Building will be in life safety stage after top displacement of 67.33 mm. pushing the structure further will cause collapse of all ground columns in one side of the building that will result in complete collapse of this single storey building. This block is immediate occupancy stage at the point where roof drift ratio reaches 1%, it will not collapse until this ratio becomes 2%. Table 5.10 shows start and end of each performance level calculated for this structure. Figure 5.15 shows performance levels on structure's capacity curve.

Target displacement calculated from FEMA356 coefficient method is 9.17 mm; at this top displacement structure is in yielding stage with roof drift ratio of 0.23%. Plastic hinges are resisting moments but has not changed their limit states to immediate occupancy level yet. Therefore expected performance level is within the acceptance criteria specified by 2007 Turkish Earthquake code (Aydinoglu, 2007). Structure is expected to have very slight damages and will remain safe to use.

Table 5.10: Limit states – Block D

Limit state	Start (mm)	End (mm)
Yield	3.50	-
IO	3.50	37.33
LS	37.33	67.33
CP	67.33	81.76
Collapse	81.76	83.22

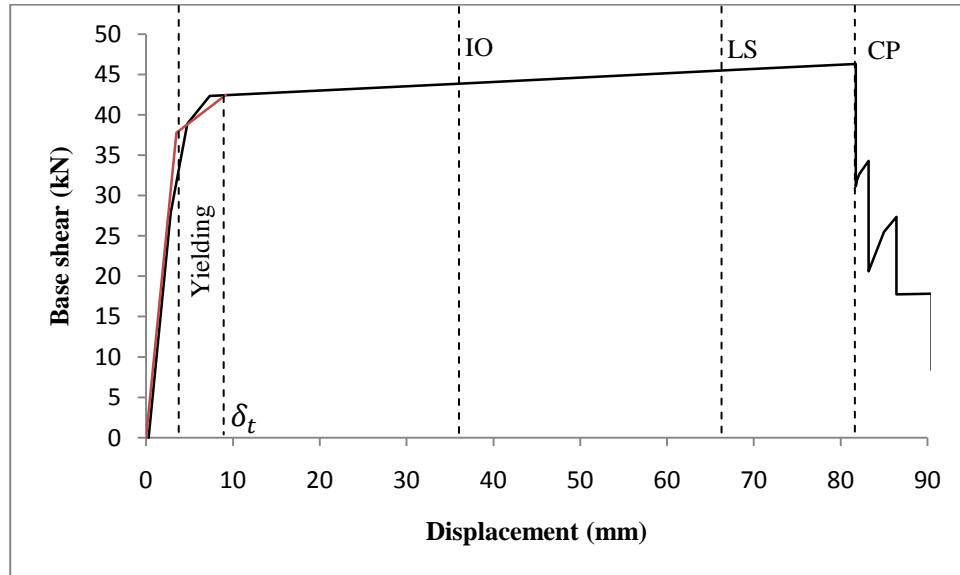


Figure 5.15: Structure performance limit states of frame model – Block D

5.1.3 Damage prediction

According to the pushover analysis obtained for each block and classification of reinforced concrete structures proposed by (Lang, 2002), point of generation of first plastic hinge is identified. This is the point where structure starts to lose its stiffness, cracks and moderate damage to structural members is expected, and is classified to damage grade 2 for reinforced concrete buildings. Damage grade 3 is representing a point in pushover process where last plastic section is identified and represents heavy damage on structure where there is risk of concrete cover falling and large cracks. Damage grade 4 is where structure is experiencing collapse of one or more members and

classified to be the first plastic hinge failure during pushover process. Finally collapse of ground columns or complete collapse of structure is specified as grade 5.

Damage grades of each building have been identified according to displacement of control node and are recorded in tables below. Relationship between displacement demand and top displacement of structure explained in chapter 2 is constructed and damage grades are shown in following figures for each building and displacement demands representing the expected damage grade for each structure are specified.

5.1.3.1 Block A

Displacement demand (Δ_{top}) is calculated for block A as 23.24 mm, this point is representing expected damage grade 3 for this building. According to classifications of damage grades by Lang (Lang, 2000), structure is expected to have moderate structural damage and heavy non-structural damages with large cracks in partition, infill walls and failure of wall panels. Table 5.11 shows the limit states of damages grades with respect to top displacement.

Table 5.11: Damage grade limits of Block A

Damage	Start (mm)	End (mm)
1	0	3.62
2	3.62	37.36
3	37.36	118.28
4	118.28	129.30
5	129.30	-

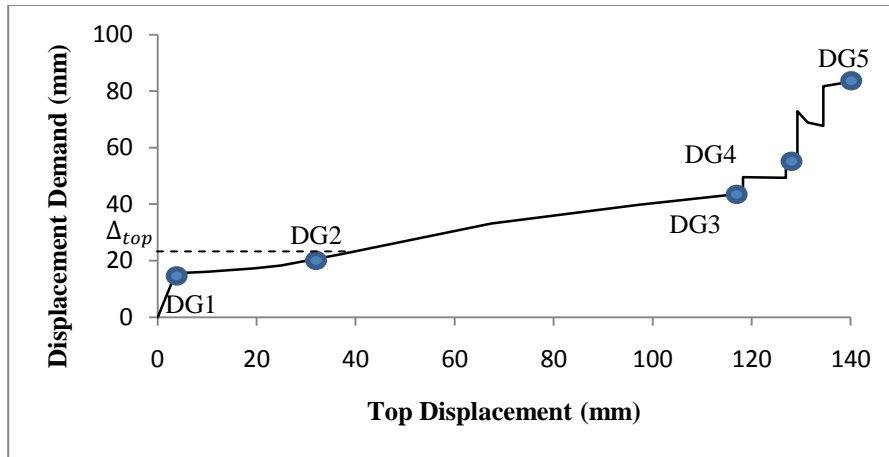


Figure 5.16: Damage grades of Block A

5.1.3.2 Block B1

Displacement demand (Δ_{top}) is calculated for block A as 9.91 mm, this point is representing expected damage grade 3 for this building. According to classifications of damage grades by Lang (Lang, 2002), structure is expected to have moderate structural damage and heavy non-structural damages with large cracks in partition, infill walls and failure of wall panels. Table 5.12 shows the limit states of damages grades with respect to top displacement.

Table 5.12: Damage grade limits of Block B1

Damage	Start (mm)	End (mm)
1	0	0.5
2	0.5	0.7
3	0.7	70.0
4	70.0	88.0
5	88.0	-

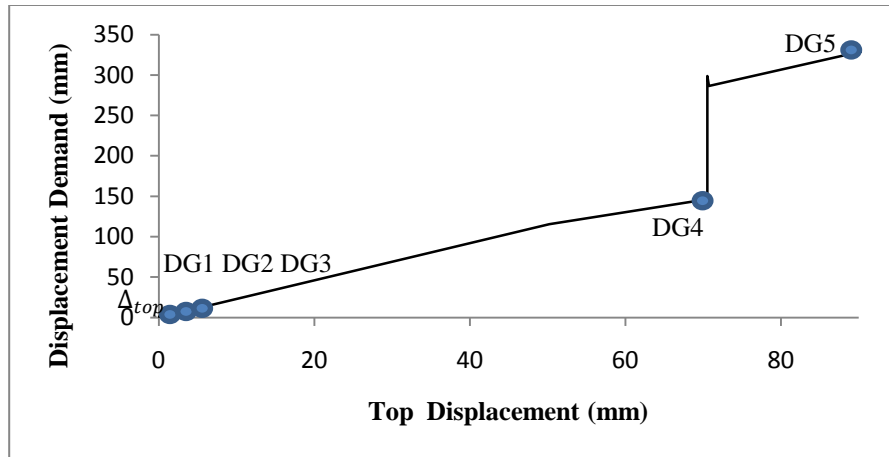


Figure 5.17: Damage grades of Block B1

5.1.3.3 Block B2

Displacement demand (Δ_{top}) is calculated for block A as 35.85 mm, this point is representing expected damage grade 3 for this building. According to classifications of damage grades by Lang (Lang, 2002), structure is expected to have moderate structural damage and heavy non-structural damages with large cracks in partition, infill walls and failure of wall panels. Table 5.13 shows the limit states of damages grades with respect to top displacement.

Table 5.13: Damage grade limits of Block B2

Damage	Start (mm)	End (mm)
1	0	0.40
2	0.40	0.64
3	0.64	69.70
4	69.70	99.70
5	99.70	-

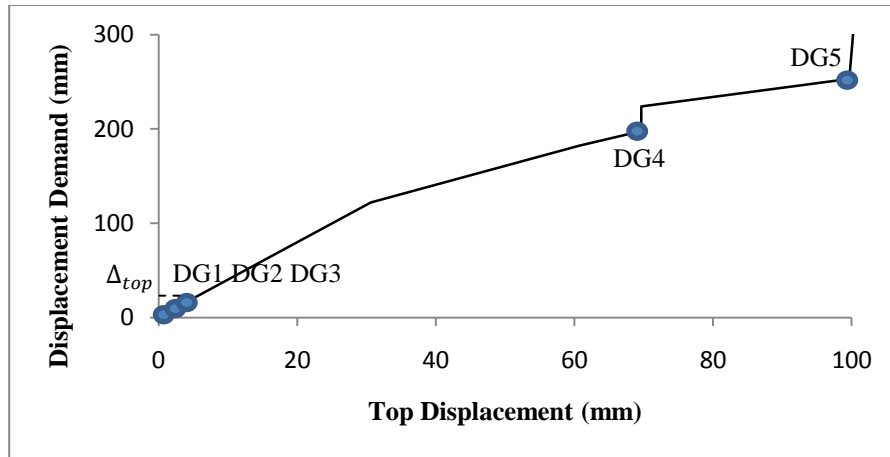


Figure 5.18: Damage grades of Block B2

5.1.3.4 Block C

Displacement demand (Δ_{top}) is calculated for block A as 130.2 mm, this point is representing expected damage grade 3 for this building. According to classifications of damage grades by Lang (Lang, 2002), structure is expected to have moderate structural damage and heavy non-structural damages with large cracks in partition, infill walls and failure of wall panels. Table 5.14 shows the limit states of damages grades with respect to top displacement.

Table 5.14: Damage grade limits of Block C

Damage	Start (mm)	End (mm)
1	0	18.48
2	18.48	40.31
3	40.31	131.17
4	131.17	154.24
5	154.24	-

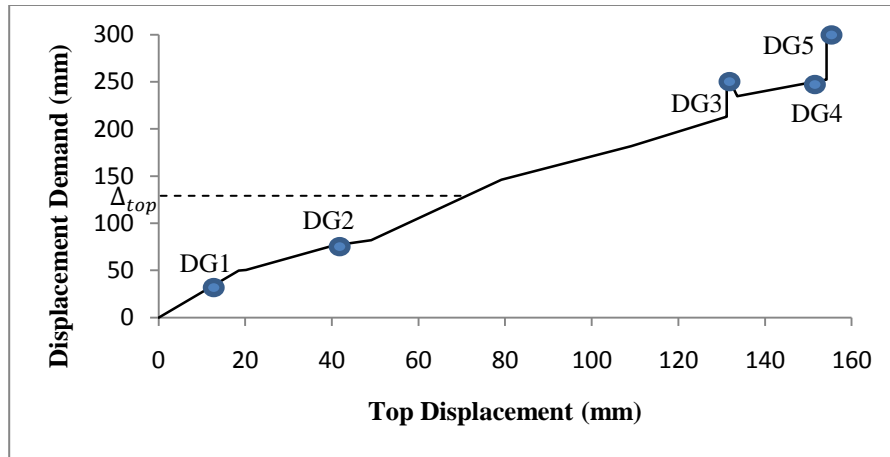


Figure 5.19: Damage grades of Block C

5.1.3.5 Block D

Displacement demand (Δ_{top}) is calculated for block A as 14.27 mm, this point is representing expected damage grade 3 for this building. According to classifications of damage grades by Lang (Lang, 2002), structure is expected to have moderate structural damage and heavy non-structural damages with large cracks in partition, infill walls and failure of wall panels. Table 5.14 shows the limit states of damages grades with respect to top displacement.

Table 5.15: Damage grade limits of Block D

Damage	Start (mm)	End (mm)
1	0	2.84
2	2.84	7.33
3	7.33	81.76
4	81.76	86.43
5	86.43	-

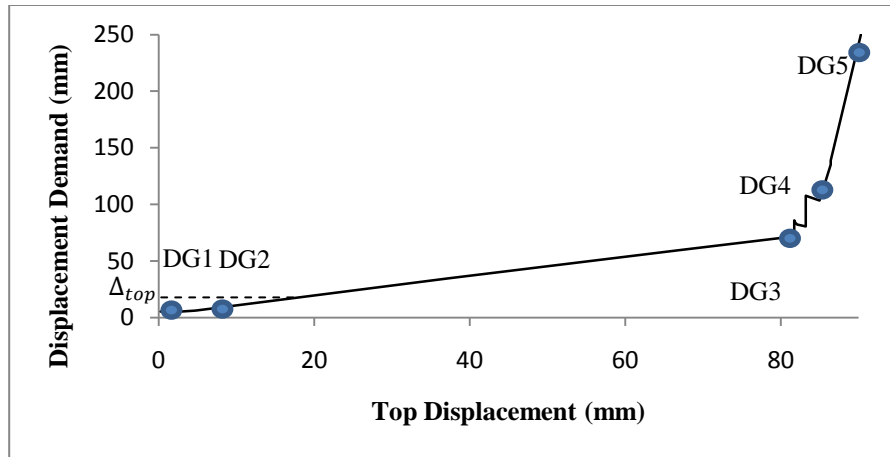


Figure 5.20: Damage grades of Block D

5.2 Time-History analysis

Each building's force-displacement relationship is obtained and displacement capacity due to lateral loading to reach different performance and damage levels are identified. Capacity of structure alone will not allow engineer to predict the vulnerability of structure, in order to investigate the response of structure in an event of earthquake with existing building member characteristics, it is required to apply ground motion accelerations as lateral loading to find out its behavior and vulnerability relationship to be able to comment on present condition of building in case of an earthquake. To achieve a better understanding of building's behavior, nonlinear time history analysis was chosen.

Nonlinear time history analysis has been performed on buildings located on "Bekir Pasa High School". Twenty earthquake records were selected and scaled according to specifications explained in chapter 3 and analysis performed as explained in methodology, results obtained for each building is discussed in sections below.

Maximum top displacement during application of each earthquake ground motion to structure are identified and shown in following tables. Furthermore maximum top displacement is checked through limit states calculated for each building to find out the structure's performance level in that displacement. Spectral acceleration and spectral displacement of control node is constructed is following figures for each time history analysis, this figure shows the vibration of control node during time history analysis. Time histories causing structure to be in same performance level are grouped together, percentage of structure being in different performance levels; Immediate Occupancy, Life Safety and Collapse, according to twenty selected time histories are calculated and probability of structure to be in those performance levels are plotted in figures below. This will show the vulnerability of structure in accordance with its roof displacement caused by selected earthquake ground motions.

5.2.1 Block A

Maximum displacement due to applied time histories for block A is shown in Table 5.16. Figure 5.21 is showing behavior of control node in terms of (S_a-S_d) where structure is responding elastically to the applied time series.

Table 5.16: Maximum spectral displacement & corresponding spectral acceleration – block A

GM	S_a (g)	Max S_d (mm)
TH1	0.15	14.59
TH2	0.96	599.42
TH3	0.41	256.16
TH4	0.38	59.91
TH5	0.43	111.35
TH6	0.05	7.89
TH7	0.12	70.70
TH8	21.57	42.61
TH9	0.22	34.09
TH10	0.59	59.52
TH11	9.45	18.48
TH12	0.38	238.71
TH13	0.28	157.15
TH14	1.08	668.43
TH15	0.02	12.21
TH16	0.15	84.35
TH17	25.50	45.43
TH18	0.01	3.70
TH19	0.01	1.10
TH20	0.62	0.97

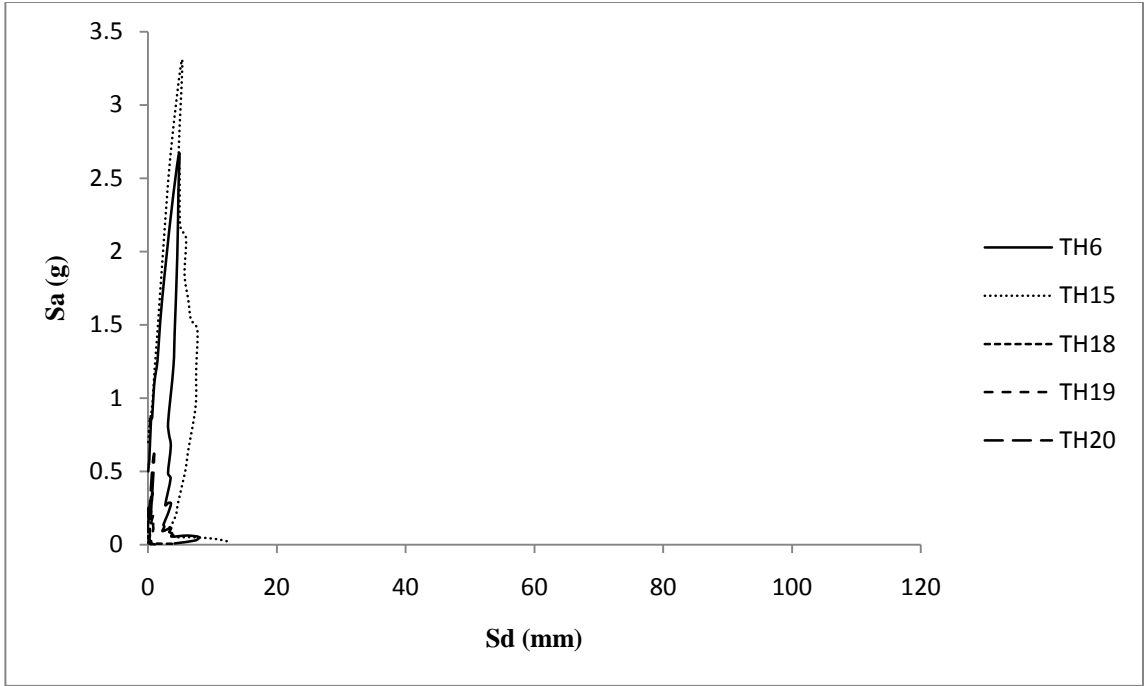


Figure 5.21: S_a - S_d showing group of time histories causing elastic behavior for block A

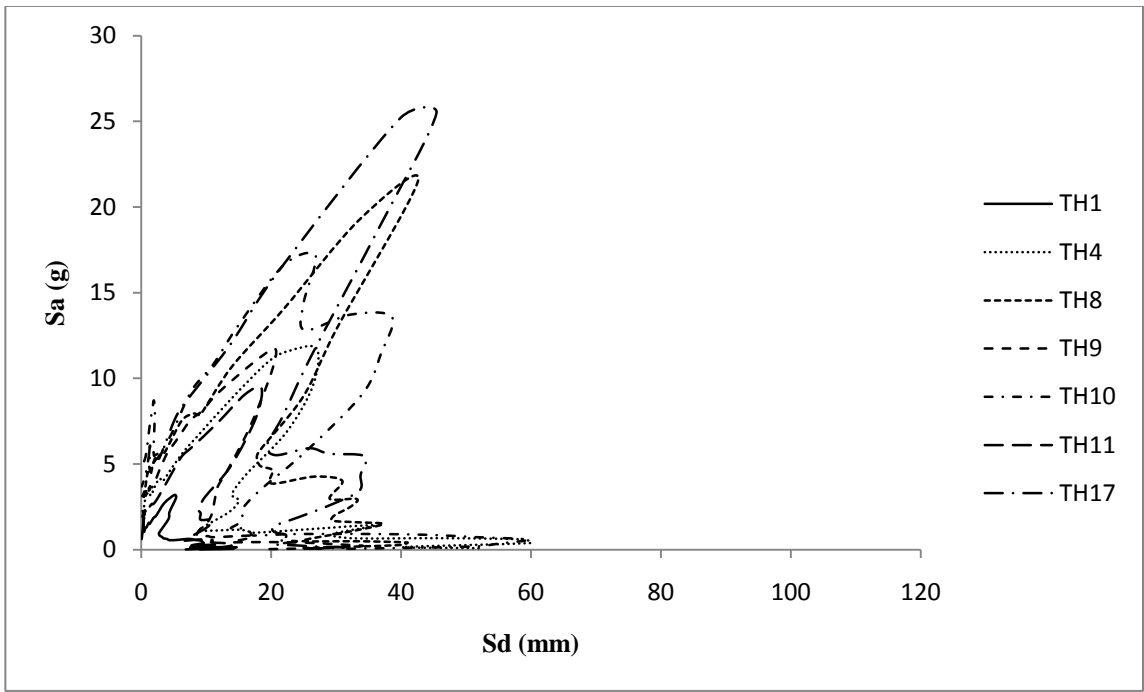


Figure 5.22: S_a - S_d showing group of time histories causing IO performance level for block A

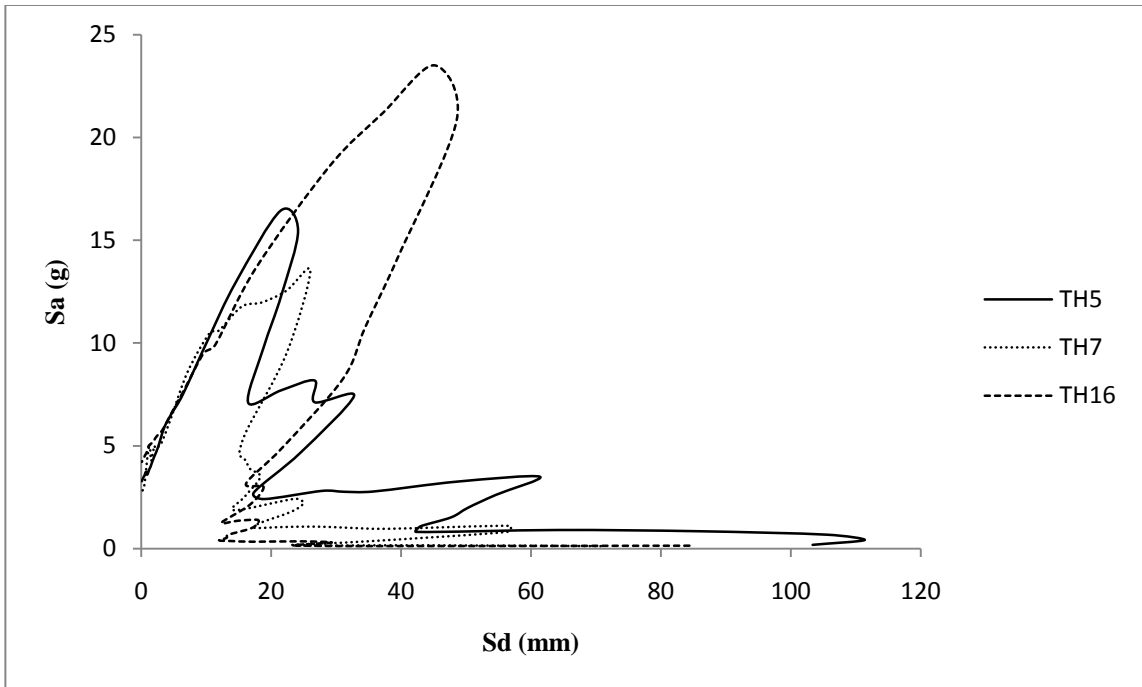


Figure 5.23: S_a - S_d showing group of time histories causing LS performance level for block A

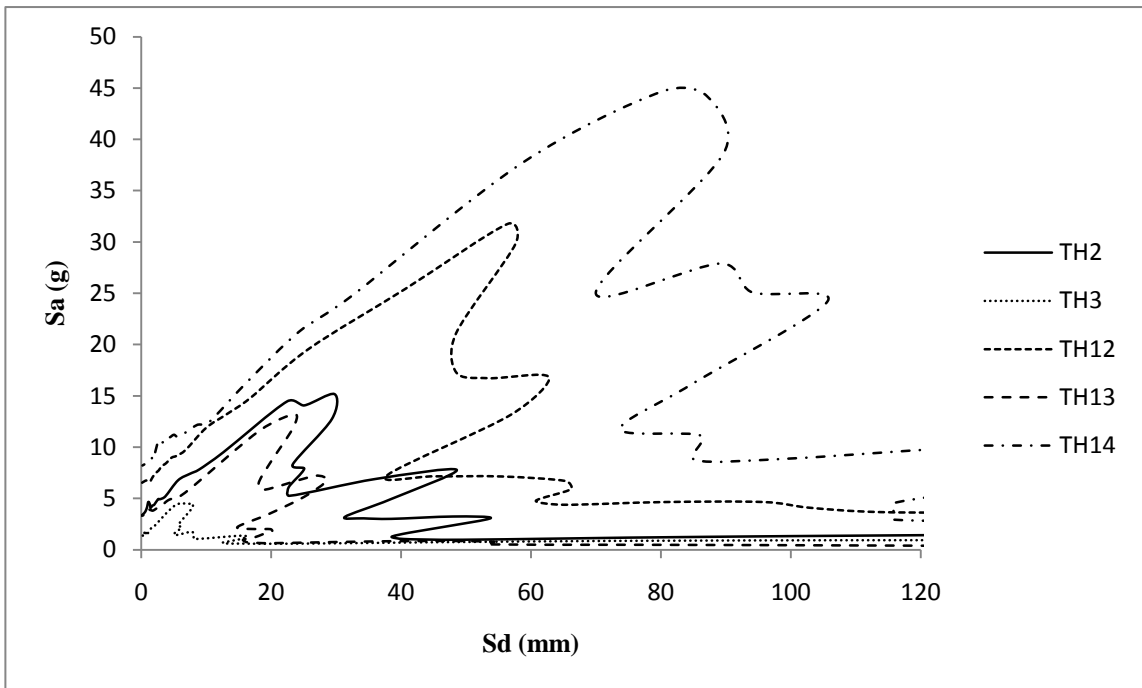


Figure 5.24: S_a - S_d showing group of time histories causing collapse performance level for block A

According to the results obtained for Block A from application of selected earthquakes; this structure responded 25% elastically, 35% in Immediate Occupancy level, 15% in

Life Safety level and 25% of time building Collapses. Implicating that this structure is 60% in accepted criteria and 40% will be unstable. Figure 5.25 shows an exponential increase in probability of Block A to be in performance levels defined by FEMA356 specifications due to increase in top displacement caused by selected time histories applied to structure. Target displacement calculated for this block is 27 mm shown in Figure 5.25. At this displacement structure has probability of 62% to be in IO level, 50% to be in LS and 37% probability of collapse according to Time History analysis results.

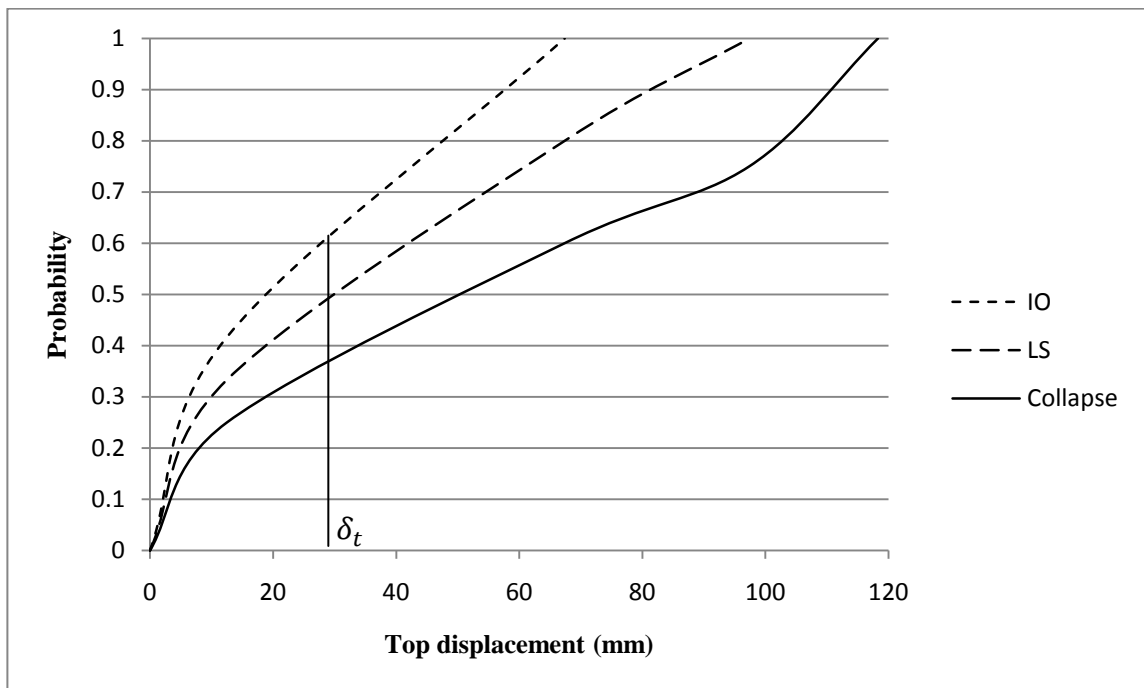


Figure 5.25: Probability of structure performing in different levels – block A

Structure at target displacement according to its capacity obtained from push over analysis will be in Immediate Occupancy level that defines it will be safe to use with slight damages after earthquake, but time history shows considerable probability of risk

of life safety and collapse. Therefore this has to be taken into consideration that this building's critical points has to be identified and strengthened to decrease the risk of life safety and collapse to be secure to occupy after earthquake.

5.2.2 Block B1

Maximum displacement due to applied time histories for block B1 is shown in Table 5.17. Figure 5.26 is showing behavior of control node in terms of (S_a-S_d) where structure is responding elastically to the applied time series.

Table 5.17: Maximum spectral displacement & corresponding spectral acceleration – block B1

GM	S_a (g)	Max S_d (mm)
TH1	0.15	14.61
TH2	0.95	596.99
TH3	0.41	255.15
TH4	0.37	58.39
TH5	0.42	109.44
TH6	0.03	7.65
TH7	0.12	71.37
TH8	0.4	40.05
TH9	0.21	33.05
TH10	0.57	57.22
TH11	0.29	11.54
TH12	0.38	235.71
TH13	0.26	156.55
TH14	1.05	659.16
TH15	0.02	11.09
TH16	0.14	85.58
TH17	0.10	26.08
TH18	0.01	3.69
TH19	0.01	0.97
TH20	0.01	0.40

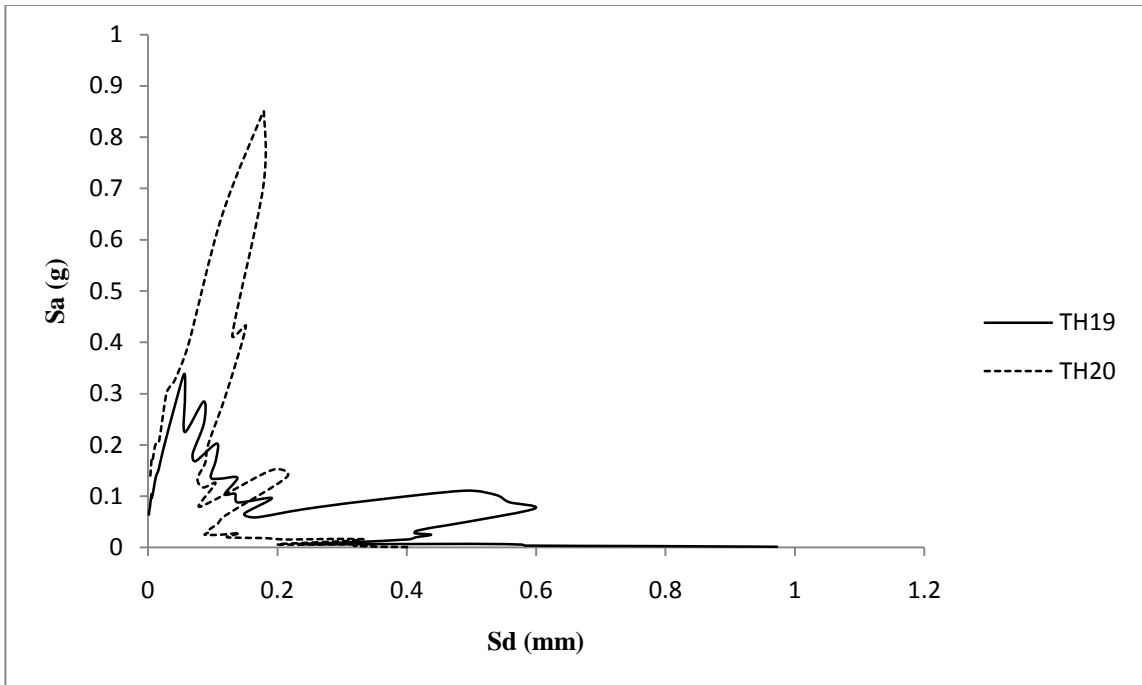


Figure 5.26: S_a - S_d showing group of time histories causing elastic behavior for block B1

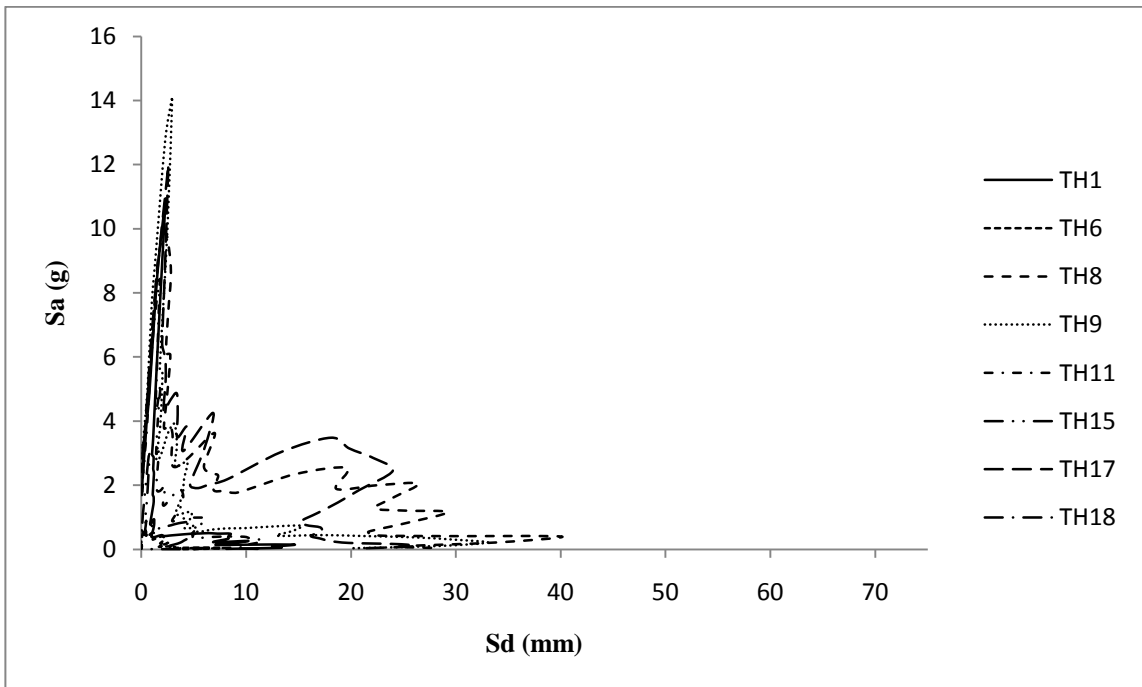


Figure 5.27: S_a - S_d showing group of time histories causing IO performance level for block B1

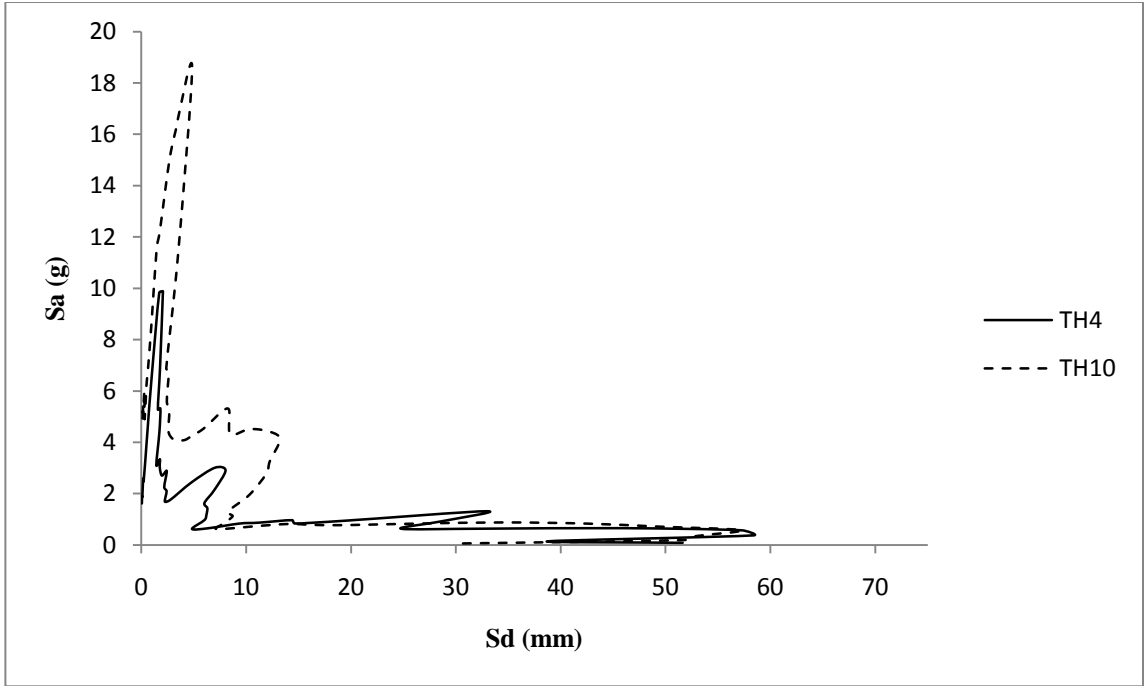


Figure 5.28: S_a - S_d showing group of time histories causing LS performance level for block B1

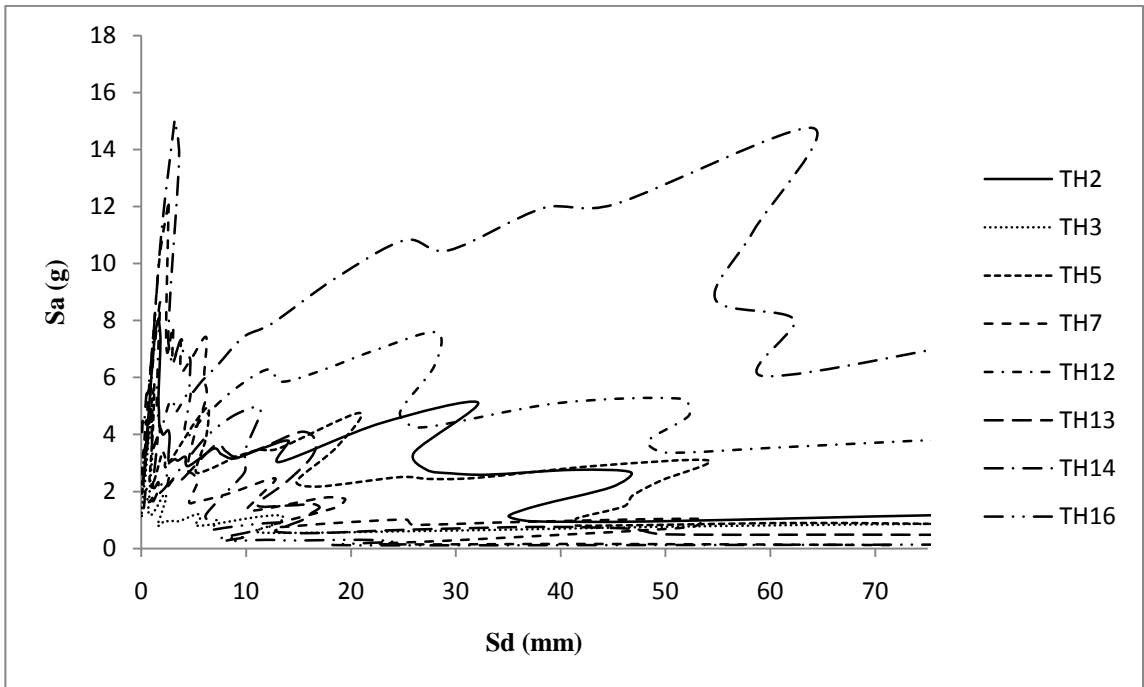


Figure 5.29: S_a - S_d showing group of time histories causing collapse performance level for block B1

According to the results obtained for Block A from application of selected earthquakes; this structure responded 10% elastically, 40% in Immediate Occupancy level, 10% in Life Safety level and 40% of time building Collapses. Implicating that this structure is 50% in accepted criteria and 50% will be unstable. Figure 5.30 shows an exponential increase in probability of Block A to be in performance levels defined by FEMA356 specifications due to increase in top displacement caused by selected time histories applied to structure. Target displacement calculated for this block is 2.7 mm shown in Figure 5.30. At this displacement structure has probability of 24% to be in IO level, 20% to be in LS and 12% probability of collapse according to Time History analysis results.

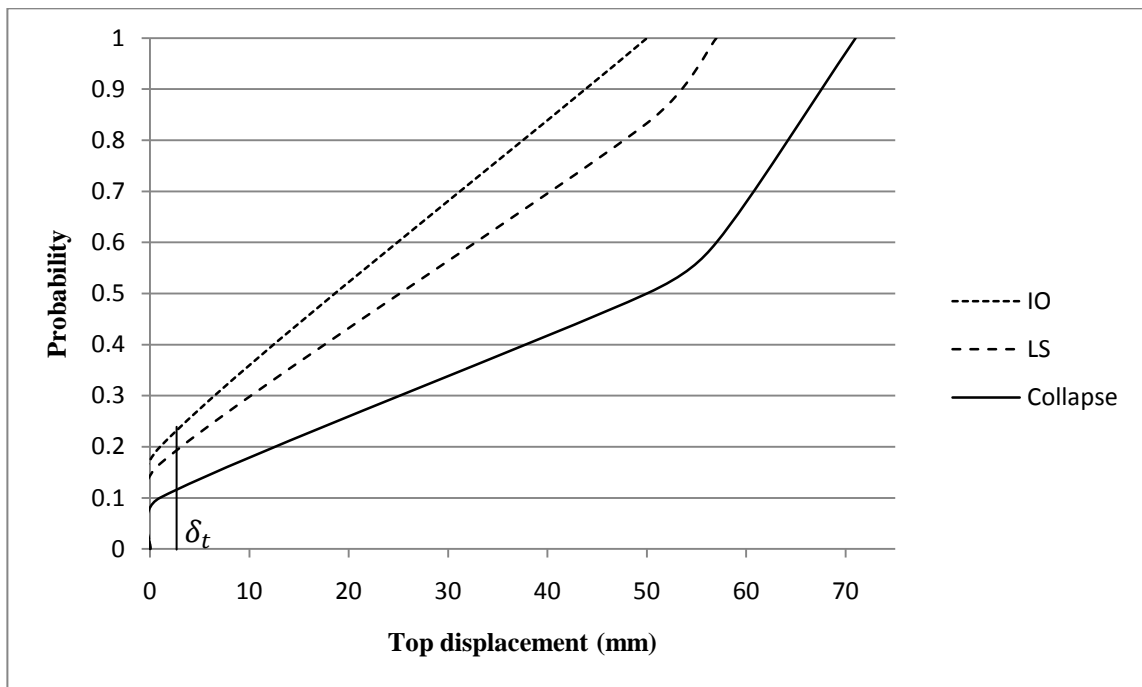


Figure 5.30: Probability of structure performing in different levels – block B1

Structure at target displacement according to its capacity obtained from push over analysis will be in Immediate Occupancy level that defines it will be safe to use with slight damages after earthquake, but time history shows considerable probability of risk of life safety and collapse. Therefore this has to be taken into consideration that this

building's critical points has to be identified and strengthened to decrease the risk of life safety and collapse to be secure to occupy after earthquake.

5.2.3 Block B2

Maximum displacement due to applied time histories for block B2 is shown in Table 5.18. Figure 5.31 is showing behavior of control node in terms of (S_a - S_d) where structure is responding elastically to the applied time series.

Table 5.18: Maximum spectral displacement & corresponding spectral acceleration – block B2

GM	Sa (g)	Max Sd (mm)
TH1	0.14	14.60
TH2	0.96	597.75
TH3	0.41	255.38
TH4	0.06	58.65
TH5	0.42	109.71
TH6	0.03	7.67
TH7	0.12	71.23
TH8	0.41	40.48
TH9	0.21	33.33
TH10	0.58	57.66
TH11	0.30	11.61
TH12	0.38	236.07
TH13	0.26	157.05
TH14	1.05	659.42
TH15	0.02	11.25
TH16	0.14	85.73
TH17	0.1	26.66
TH18	0.01	3.69
TH19	0.01	0.99
TH20	0.01	0.41

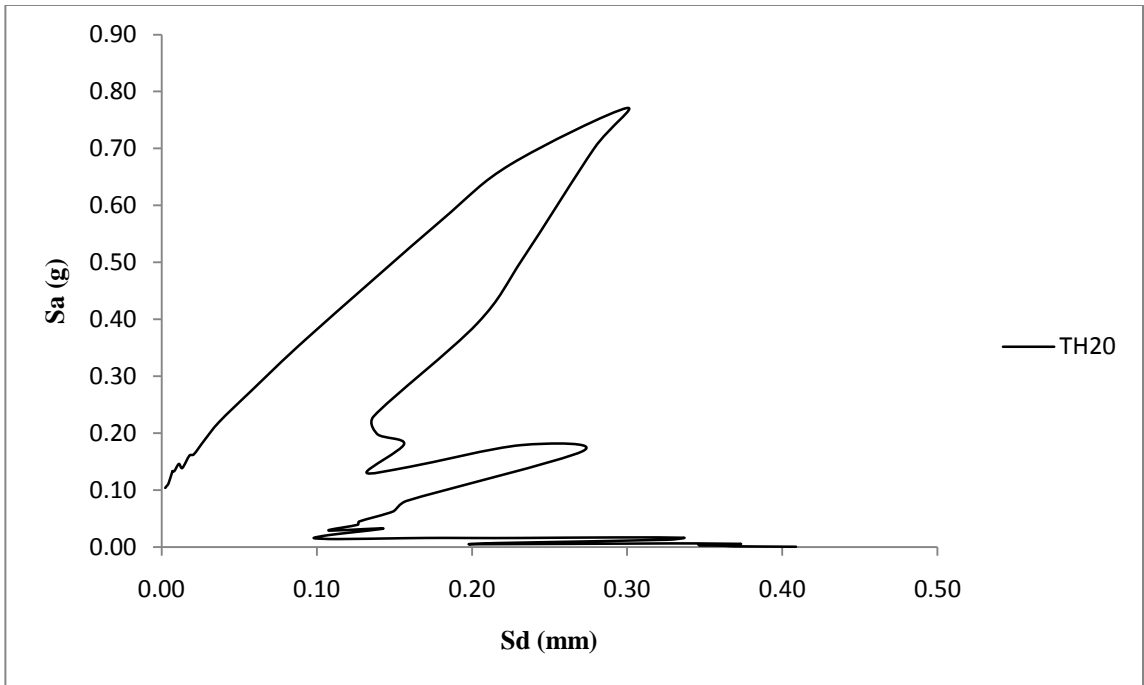


Figure 5.31: S_a - S_d showing group of time histories causing elastic behavior for block B2

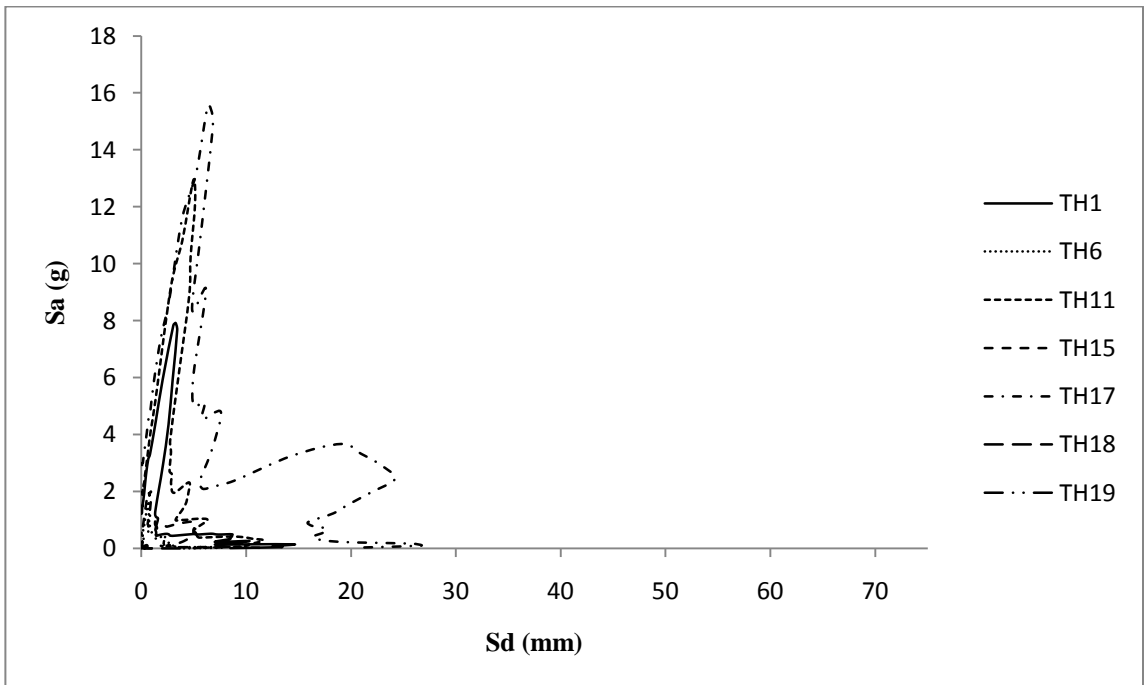


Figure 5.32: S_a - S_d showing group of time histories causing IO performance level for block B2

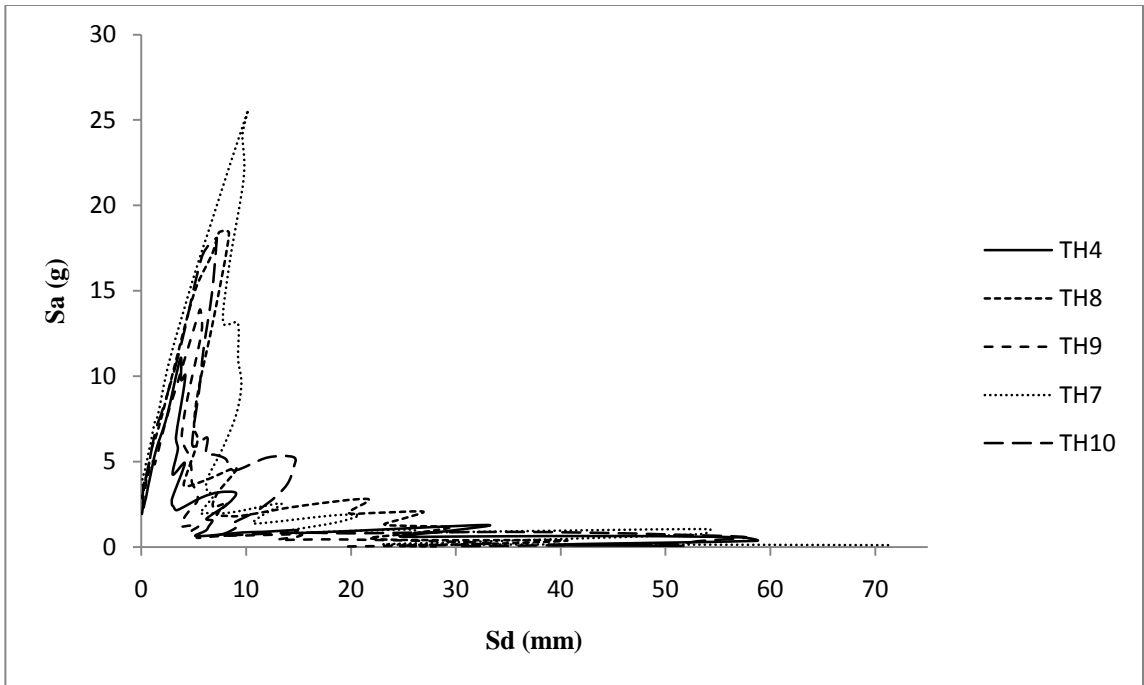


Figure 5.33: S_a - S_d showing group of time histories causing LS performance level for block B2

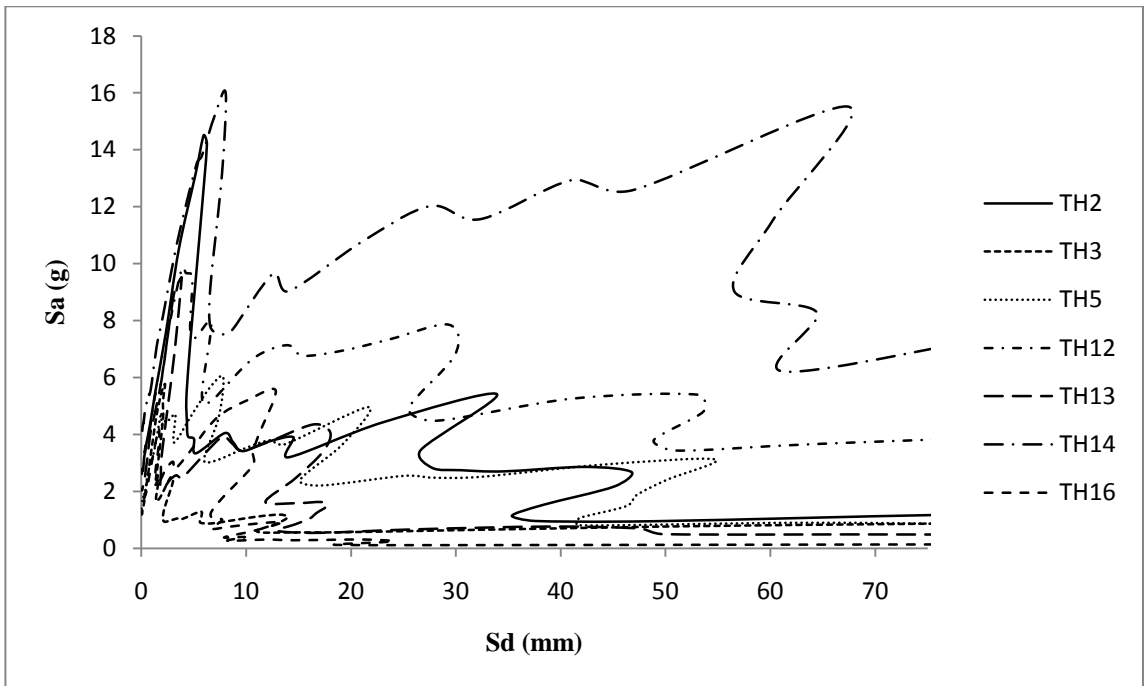


Figure 5.34: S_a - S_d showing group of time histories causing collapse performance level for block B2

According to the results obtained for Block A from application of selected earthquakes; this structure responded 5% elastically, 35% in Immediate Occupancy level, 25% in Life Safety level and 35% of time building Collapses. Implicating that this structure is 40% in accepted criteria and 60% will be unstable. Figure 5.35 shows an exponential increase in probability of Block A to be in performance levels defined by FEMA356 specifications due to increase in top displacement caused by selected time histories applied to structure. Target displacement calculated for this block is 6.33 mm shown in Figure 5.35. At this displacement structure has probability of 28% to be in IO level, 18% to be in LS and 12% probability of collapse according to Time History analysis results.

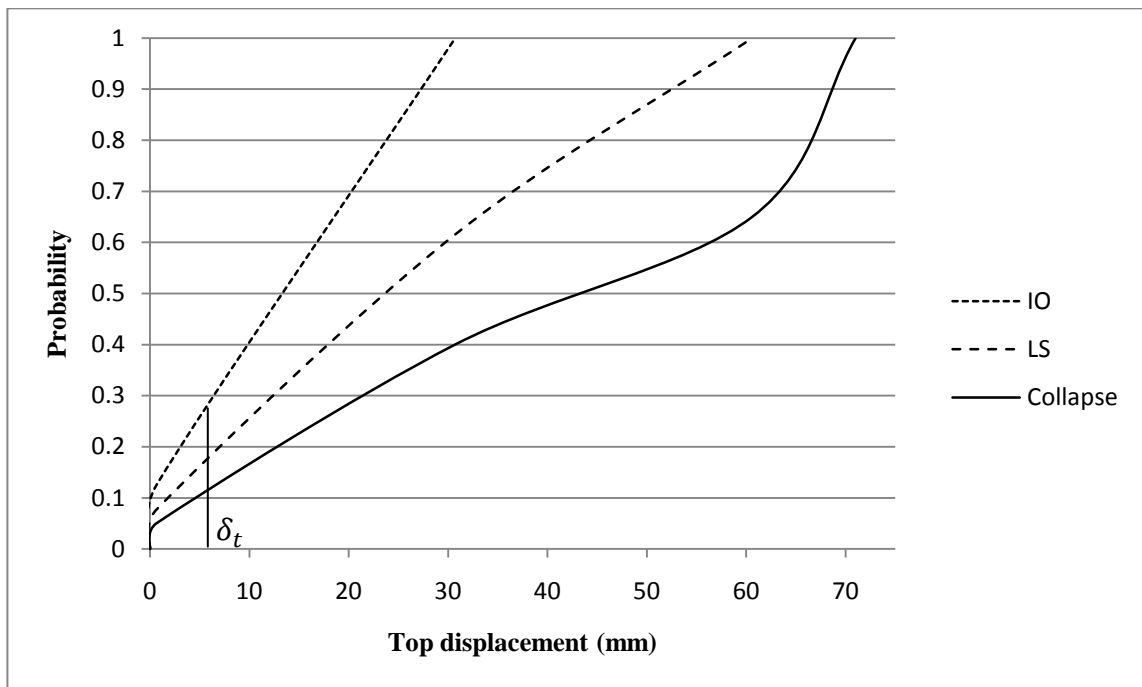


Figure 5.35: Probability of structure performing in different levels – block B2

Structure at target displacement according to its capacity obtained from push over analysis will be in Immediate Occupancy level that defines it will be safe to use with slight damages after earthquake, but time history shows considerable probability of risk

of life safety and collapse. Therefore this has to be taken into consideration that this building's critical points has to be identified and strengthened to decrease the risk of life safety and collapse to be secure to occupy after earthquake.

5.2.4 Block C

Maximum displacement due to applied time histories for block C is shown in Table 5.19. Figure 5.36 is showing behavior of control node in terms of (S_a-S_d) where structure is responding elastically to the applied time series.

Table 5.19: Maximum spectral displacement & corresponding spectral acceleration – block C

GM	Sa (g)	Max Sd (mm)
TH1	0.16	15.6
TH2	0.97	604.34
TH3	0.41	257.56
TH4	0.39	60.85
TH5	0.43	112.59
TH6	2.80	8.74
TH7	0.11	68.56
TH8	0.40	47.81
TH9	0.22	33.59
TH10	30.79	99.95
TH11	6.09	19.04
TH12	0.42	245.1
TH13	0.27	149.25
TH14	1.08	669.18
TH15	2.58	13.39
TH16	0.14	84.48
TH17	6.0	46.31
TH18	0.01	3.71
TH19	0.35	1.54
TH20	0.02	0.4

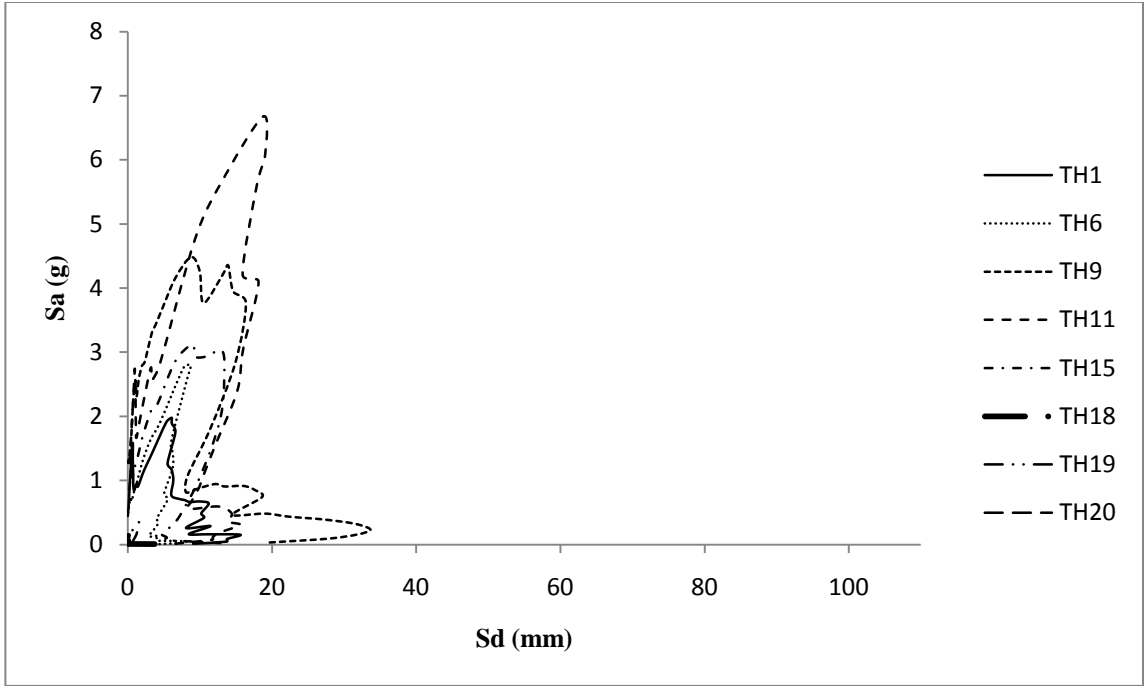


Figure 5.36: S_a - S_d showing group of time histories causing elastic behavior for block C

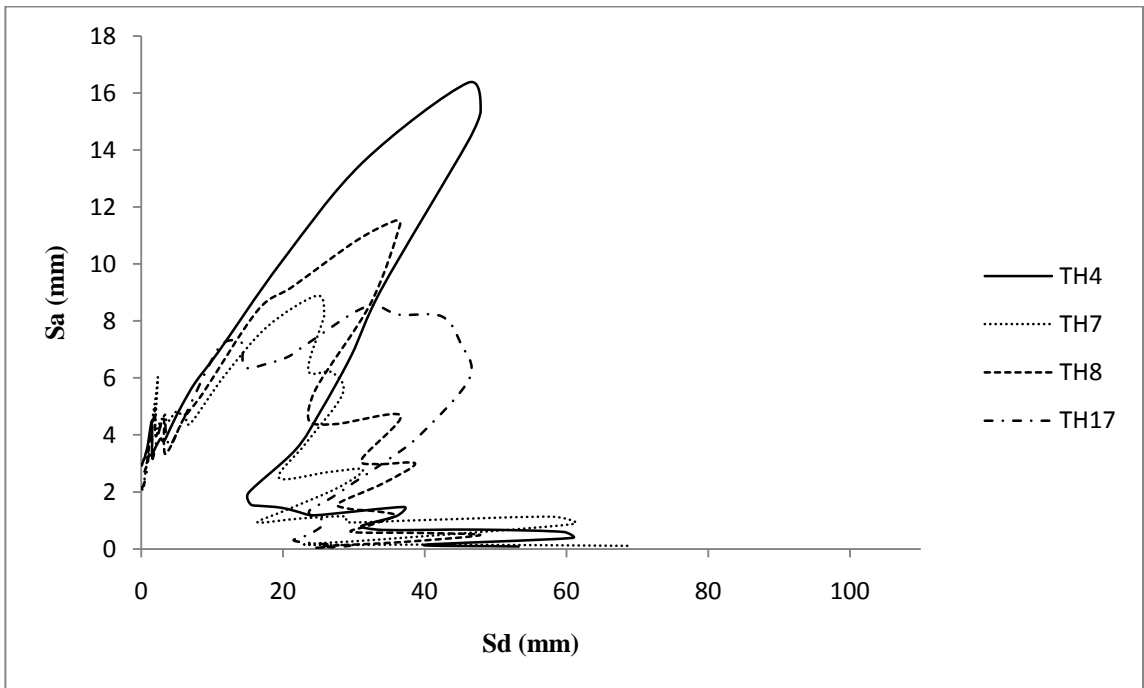


Figure 5.37: S_a - S_d showing group of time histories causing IO performance level for block C

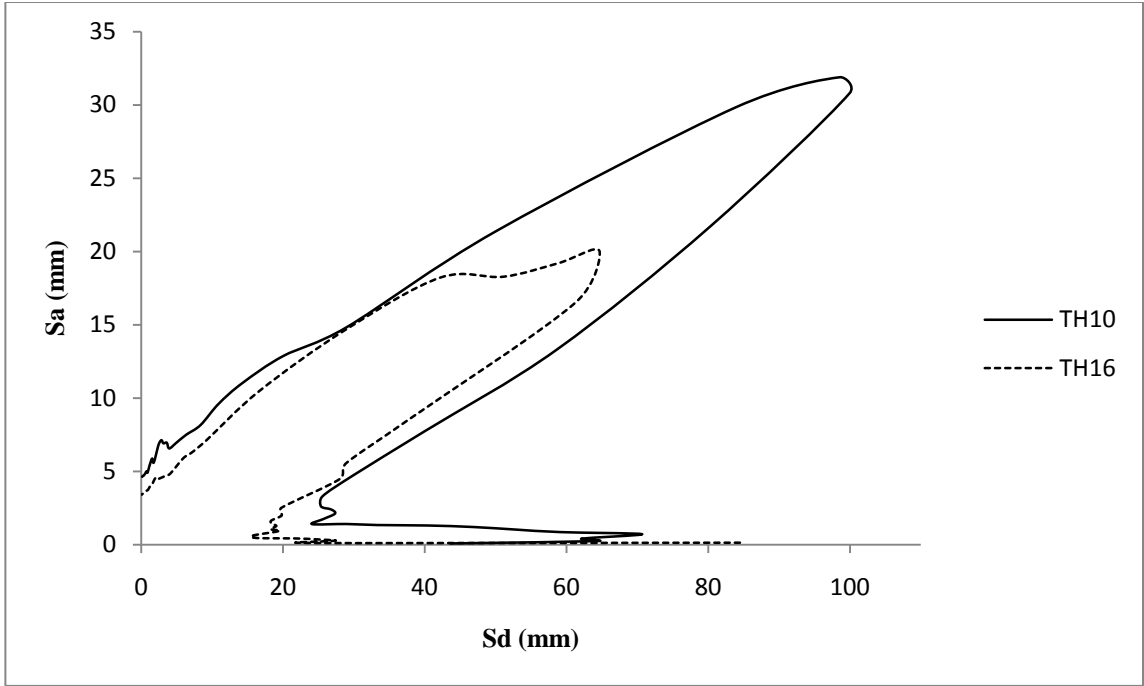


Figure 5.38: S_a - S_d showing group of time histories causing LS performance level for block C

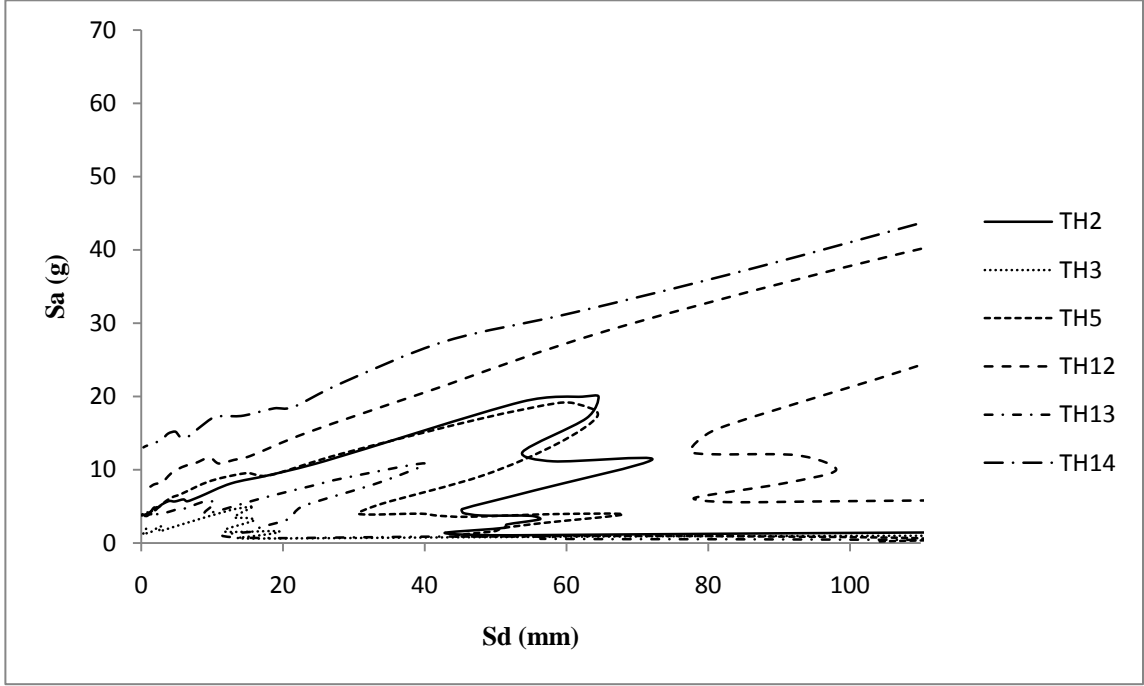


Figure 5.39: S_a - S_d showing group of time histories causing collapse performance level for block C

According to the results obtained for Block A from application of selected earthquakes; this structure responded 40% elastically, 20% in Immediate Occupancy level, 10% in Life Safety level and 30% of time building Collapses. Implicating that this structure is 60% in accepted criteria and 40% will be unstable. Figure 5.40 shows an exponential increase in probability of Block A to be in performance levels defined by FEMA356 specifications due to increase in top displacement caused by selected time histories applied to structure. Target displacement calculated for this block is 62 mm shown in Figure 5.40. At this displacement structure has probability of 88% to be in IO level, 76% to be in LS and 53% probability of collapse according to Time History analysis results.

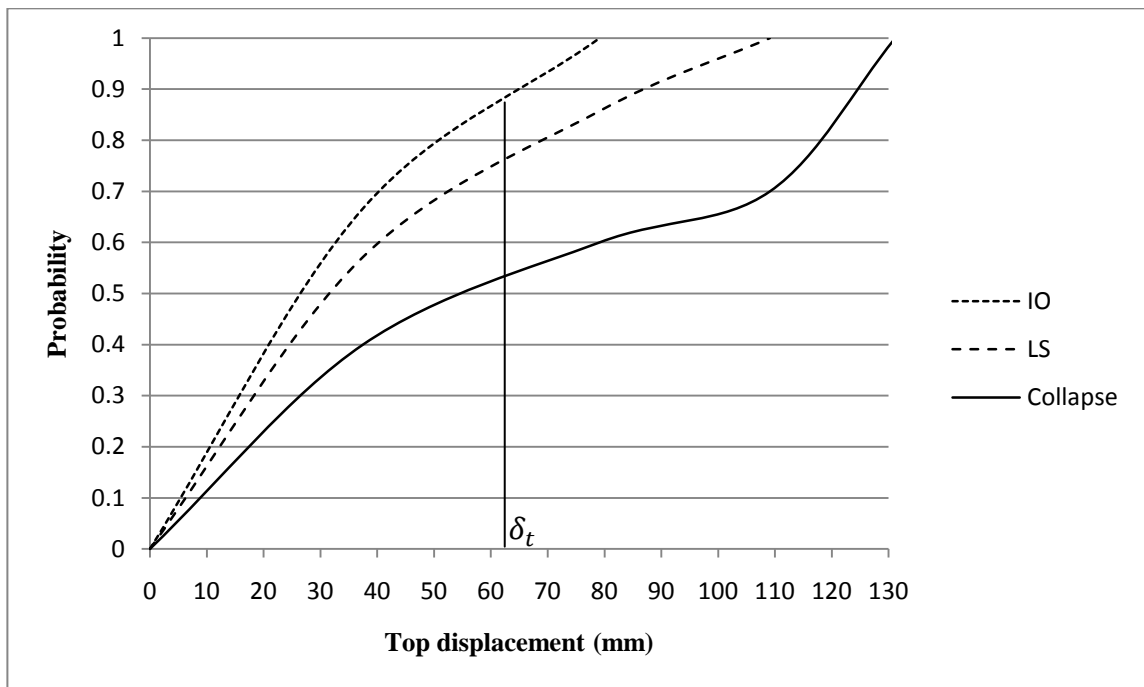


Figure 5.40: Probability of structure performing in different levels – block C

Structure at target displacement according to its capacity obtained from push over analysis will be in Immediate Occupancy level that defines it will be safe to use with slight damages after earthquake, but time history shows considerable probability of risk

of life safety and collapse. Therefore this has to be taken into consideration that this building's critical points has to be identified and strengthened to decrease the risk of life safety and collapse to be secure to occupy after earthquake.

5.2.5 Block D

Maximum displacement due to applied time histories for block D is shown in Table 5.20. Figure 5.41 is showing behavior of control node in terms of (S_a-S_d) where structure is responding elastically to the applied time series.

Table 5.20: Maximum spectral displacement & corresponding spectral acceleration – block D

GM	Sa (g)	Max Sd (mm)
TH1	0.15	14.80
TH2	0.96	598.61
TH3	0.41	255.51
TH4	0.37	58.81
TH5	0.42	109.81
TH6	0.05	7.72
TH7	0.12	72.23
TH8	0.41	41.09
TH9	0.21	33.31
TH10	0.58	57.47
TH11	0.31	11.94
TH12	0.38	236.71
TH13	0.27	157.37
TH14	1.05	658.55
TH15	0.02	11.39
TH16	0.14	85.91
TH17	2.72	26.85
TH18	0.01	3.69
TH19	0.00	0.99
TH20	0.00	0.37

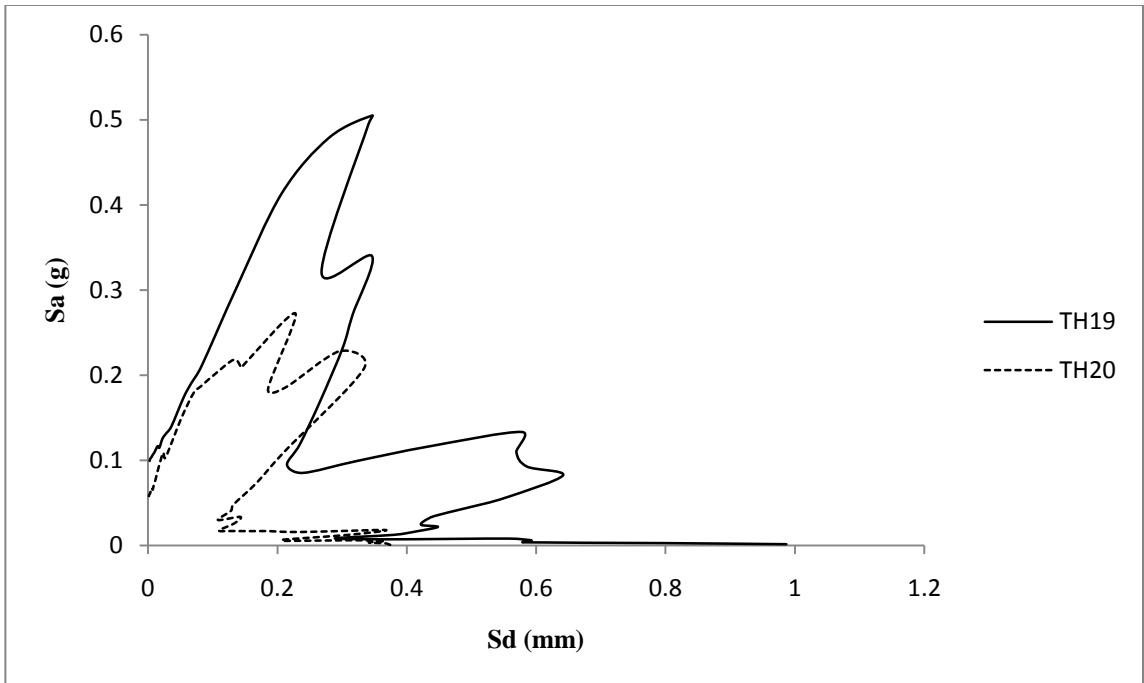


Figure 5.41: S_a - S_d showing group of time histories causing elastic behavior for block D

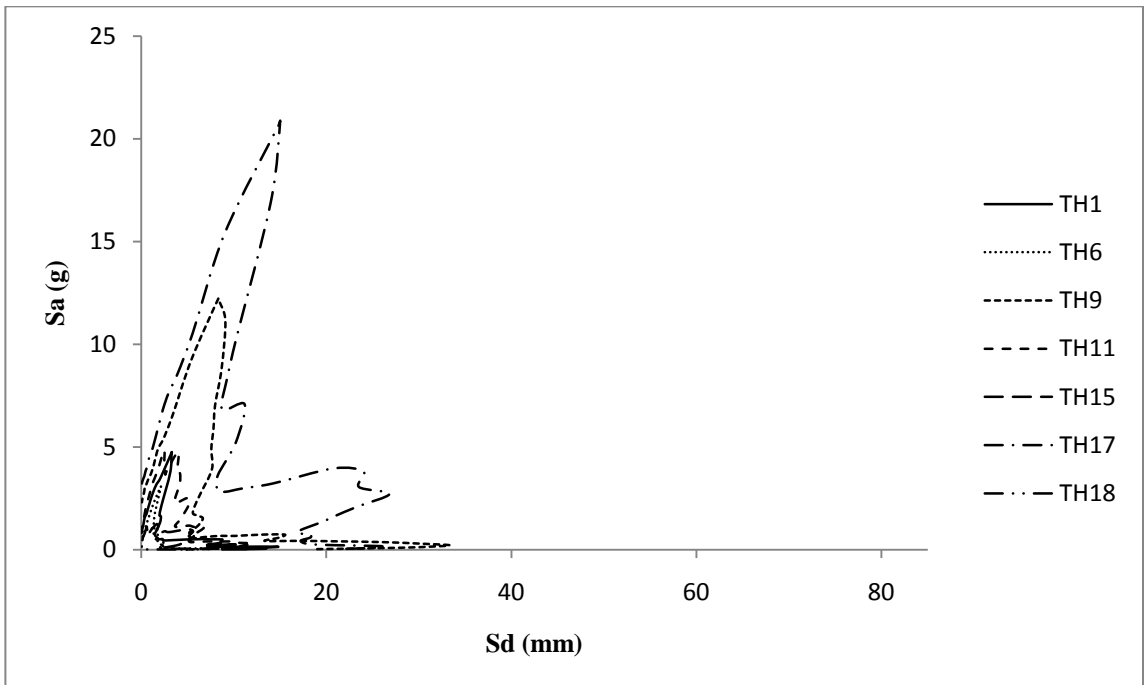


Figure 5.42: S_a - S_d showing group of Time Histories causing IO performance level for block D

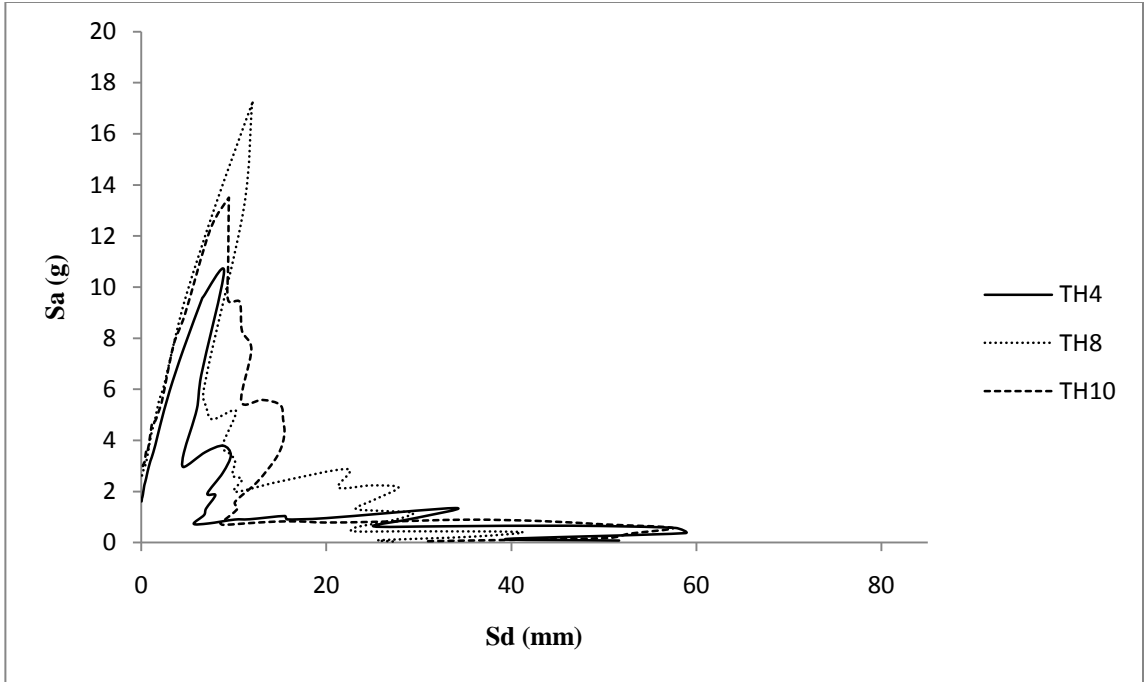


Figure 5.43: S_a - S_d showing group of time histories causing LS performance level for block D

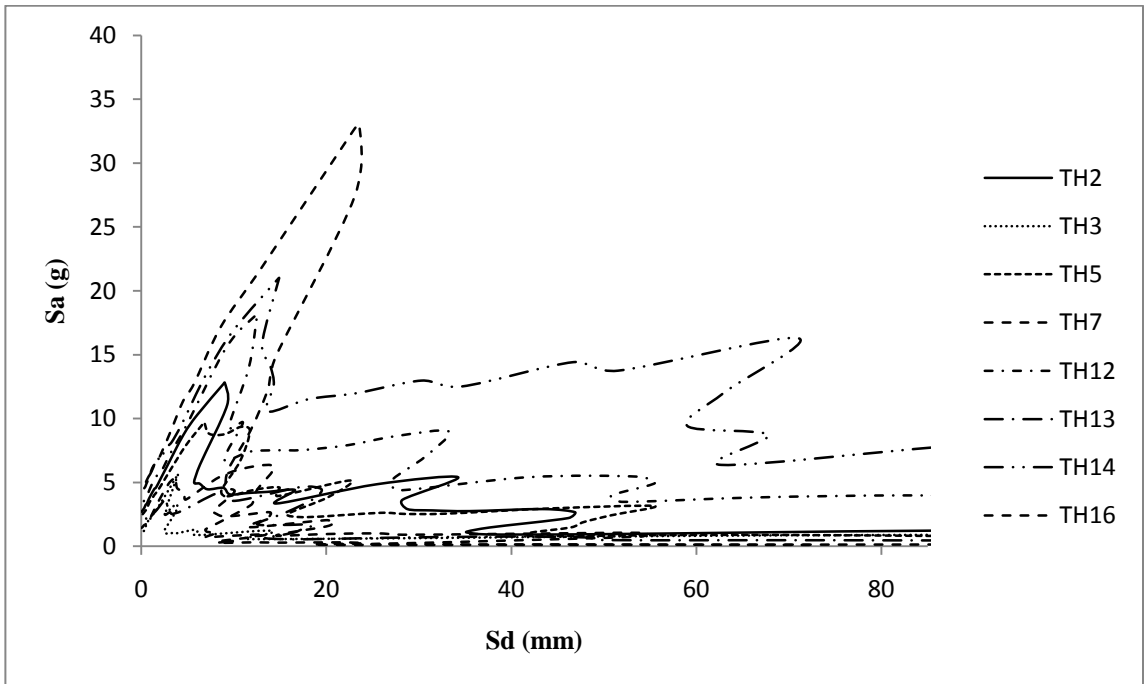


Figure 5.44: S_a - S_d showing group of time histories causing collapse performance level for block D

According to the results obtained for Block A from application of selected earthquakes; this structure responded 10% elastically, 35% in Immediate Occupancy level, 15% in

Life Safety level and 40% of time building Collapses. Implicating that this structure is 45% in accepted criteria and 55% will be unstable. Figure 5.45 shows an exponential increase in probability of Block A to be in performance levels defined by FEMA356 specifications due to increase in top displacement caused by selected time histories applied to structure. Target displacement calculated for this block is 9.17 mm shown in Figure 5.45. At this displacement structure has probability of 37% to be in IO level, 28% to be in LS and 17% probability of collapse according to Time History analysis results.

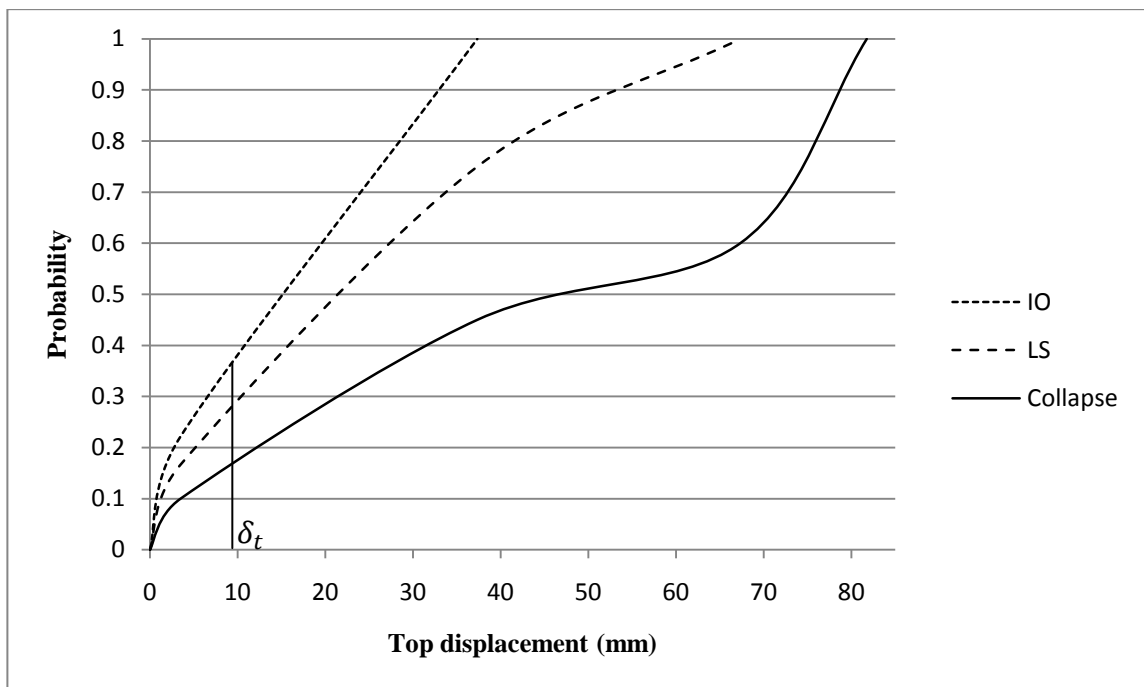


Figure 5.45: Probability of structure performing in different levels – block D

Structure at target displacement according to its capacity obtained from push over analysis will be in Immediate Occupancy level that defines it will be safe to use with slight damages after earthquake, but time history shows considerable probability of risk of life safety and collapse. Therefore this has to be taken into consideration that this

building's critical points has to be identified and strengthened to decrease the risk of life safety and collapse to be secure to occupy after earthquake.

Results obtained from time history analysis are showing more accurate outcome comparing to push over analysis results. Therefore it can be stated that nonlinear static analysis is a good tool to find the capacity of structure to lateral loading but at the same time it can only predict an approximate performance level. Using push over together with time history analysis will bring engineer to a better understanding to be able to predict a more realistic performance of structure in case of an earthquake. Structures studied here according to static analysis are all in accepted criteria defined by Turkish Earthquake code but comparing it to the dynamic analysis performed it can be observed that there is a considerable probability for all structures to show unstable performances which are having high risk of life safety and collapse subjected to lateral loading representing earthquake loads.

Chapter 6

CONCLUSIONS

6.1 Summary of works done

This studies framework is to assess buildings located in “Bekir Paşa High School” site and investigate their performance in event of an earthquake. All buildings are constructed as low rise reinforced concrete frame structures and are aged more than 35 years. Methodology for assessing these buildings and demonstrating their seismic performances is divided to two parts; first finding structural member section properties and geometry of buildings to simulate a computer model of them, second running analysis on models to find out their capacity and behavior.

In order to simulate models, buildings were measured; concrete core samples were taken from columns, prepared and tested for actual compressive strength in laboratory. Details of existing structural members were identified after detecting reinforcement bars locations and concrete covers of members. Structures then were modeled as moment resisting frames with gravity loads acting uniformly distributed on members.

Two methods of nonlinear analysis were performed to investigate building’s behavior; nonlinear pushover analysis was performed to measure frame structure’s first yield and plastic mechanism development capacity till collapse. Nonlinear time history analysis were performed using twenty past earthquakes recorded data, scaled to design response

spectrum provided for Cyprus to find out top floor displacement of structures in each of those events, hence comparison between results obtained were made with displacement capacity to find out the possible performance levels (FEMA356; Immediate Occupancy, Life Safety and Collapse Prevention) and damage levels (Lang's procedure; DG1, DG2, DG3, DG4, DG5) of all frame structures.

6.2 Low rise RC frame structures

Buildings assessed in this study are considered as low rise reinforced concrete structures, none of the buildings were constructed with more than two stories. This type of frame structures constructed in regions with low or moderate risk of seismic activity like Cyprus was usually designed considering only gravity loads. When structure is only designed to carry gravity loads and lateral loadings are not considered, leads frame members specially columns to have no special reinforcing details, therefore will be having lower beam-column moment capacity and confinement strength comparing to structures designed with consideration of lateral loading. This lack of required strength in columns will cause soft storey failure. In other words structure will experience column hinging under lateral loading and starts to develop storey mechanism; hence the building's resistance is only provided by the post yield strength of column ends. On the other hand materials of structural members slightly lose their strength during years after construction; this loss is dependant to environment conditions. Moreover throughout an earthquake this insufficient column strength and section details for ductility, causes structure to act brittle and failure mechanisms can be developed.

Response to lateral loading obtained from nonlinear pushover and time history analysis shows that all buildings of Bekir Paşa High School do not have sufficient column

reinforcement detailing and has been designed to carry gravity loads. Buildings have been constructed on 1974 that makes them over 30 years aged reinforced concrete structures. During visual investigation of building's cracks have been spotted on walls and members, at the same time reinforcement bars observed through removed concrete covers were rusty which is caused by corrosion. For the purpose of this study effect of corrosion has not been taken into consideration during analysis, but the existing characteristics of structural members have shown that buildings are not designed to resist lateral loading. Since these building are still in use by academic staff and students care has to be taken to consideration that they will be risk of life safety during possible ground motions. Regardless of cost, buildings have to be strengthened to act more ductile during possible ground motions.

Earthquake itself is no harm to human being unless they are inside a building; hence strengthening methods shall be chosen to bring more ductile response to possible ground motions. Shear capacity, beam-column moment capacity and most importantly confinement strengthening strategies can be designed and applied to the investigated weak frames of each building to assure that risk of life safety decreases to its minimum for higher ground motion acceleration than are expected to occur in the area.

6.3 Concluding findings for buildings

In this section weak columns detected from analysis are shown and summary of findings and their seismic performance are concluded.

Table 6.1: Seismic performance of buildings

Block	Push over analysis		Time history analysis	
	δ_t (FEMA356)	DG (Lang)	Accepted	Unstable
A	IO	3	60%	40%
B1	IO	3	50%	50%
B2	IO	3	40%	60%
C	IO	3	60%	40%
D	IO	3	45%	55%

Accepted criteria: Immediate Occupancy, Unstable: Life safety and Collapse

6.3.1 Block A

Block A is a two storey reinforced concrete frame structure that has two types of column sections were C45x30 is designed to hold the main building and C30x30 are constructed to hold balcony. Building has total height of 7.79 m to the roof and area of 39.5 x 9.7 m². The whole structural members including slabs weights 2404 kN and mass of the frames in width of building are 130 kN.

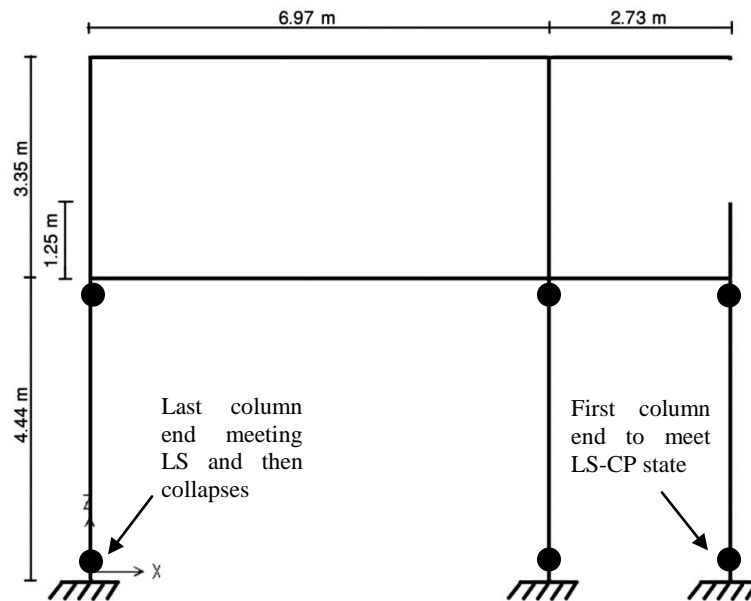


Figure 6.1: Critical frame – Block A

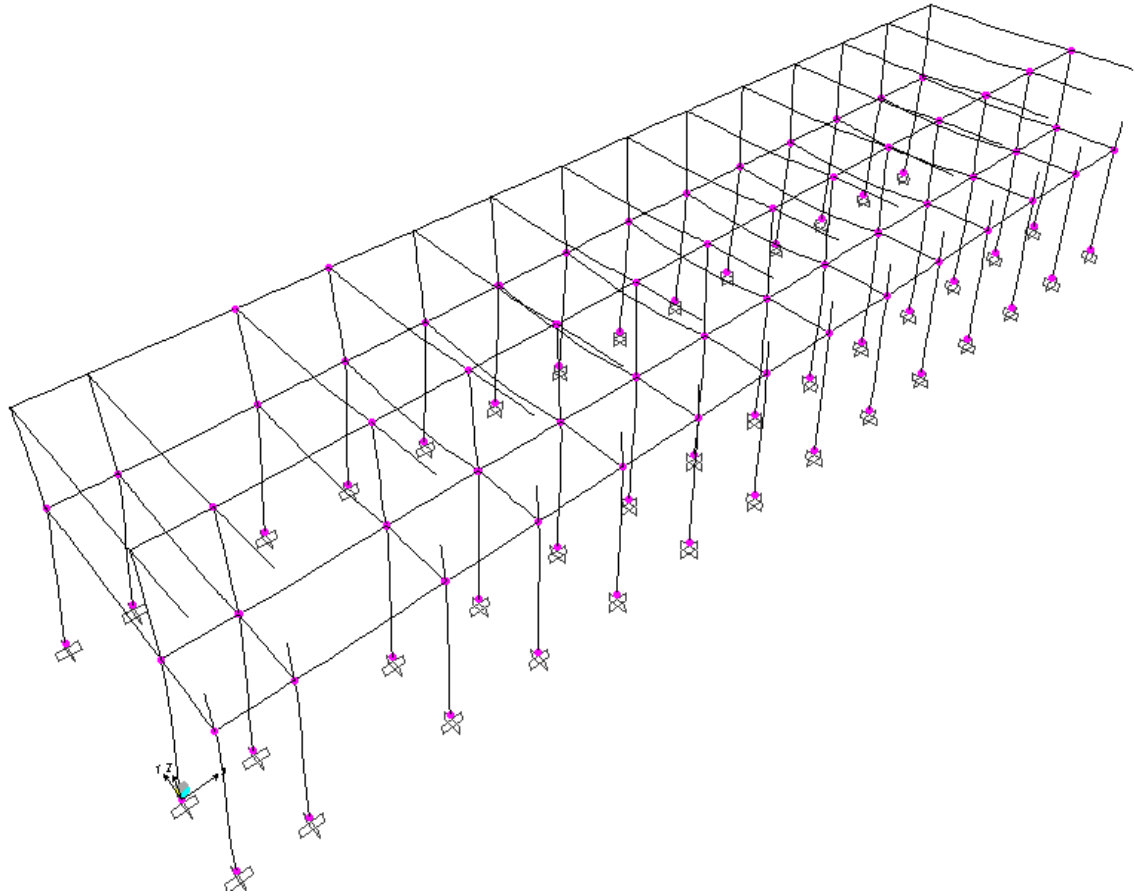


Figure 6.2: Deformed shape and generation of plastic hinges on 3D model of block A

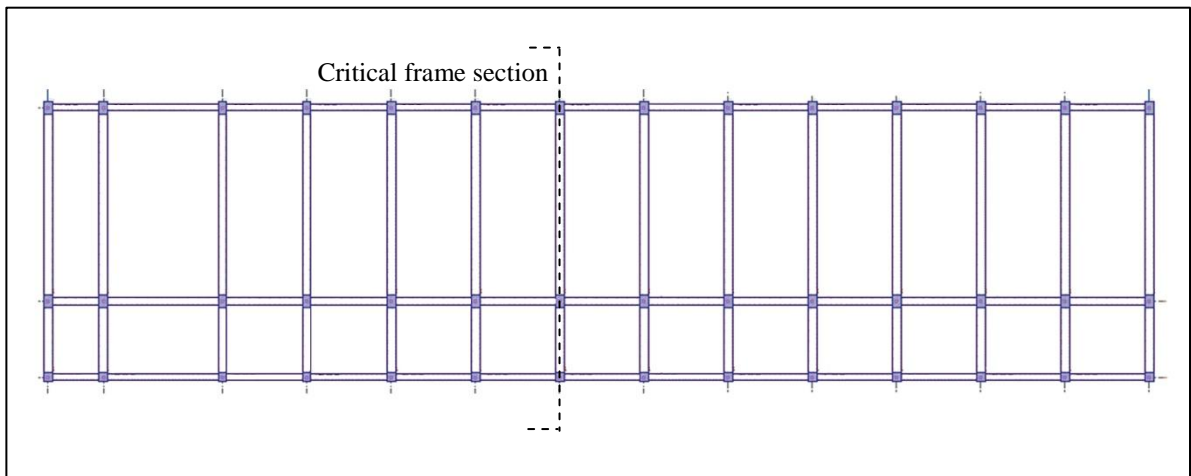


Figure 6.1 shows the critical frame of this building; lateral loading during pushover analysis has shown that structure starts to yield when base shear reaches 40 percent of structure's weight (base shear to mass ratio = 0.4). From this point on frame is in its

plastic stage and resistance to applied lateral loading is only provided by column end hinges capacity. First hinge that fails is from the columns that are holding the balcony and shortly after main building's ground columns are failed. Although structure has shown good resistance while yielding till collapse of column ends but it has not shown good elastic resistance to loading. Target displacement obtained for this frame is 27 mm, choosing adequate strengthening methods for selected columns will cause shifting of first yield to occur after displacement equal or greater than target displacement. This will fulfill the lack of column strength and help structure to improve its ductility during an earthquake and definitely will improve its resistance to ground motions to have lower risk of life safety, after choosing strengthening strategy structure shall be re evaluated to check whether the methods chosen are changing building's behavior to accepted performance or not.

6.3.2 Block B1

This building is a two storey reinforced concrete frame structure with total height of 6.61 m to the roof and area of 17.75 x 11.74 m². Structural members including slab weights 2641.5 kN and critical frame chosen from building has weight of 506 kN. All column sections constructed for this building are C30x30 sections.

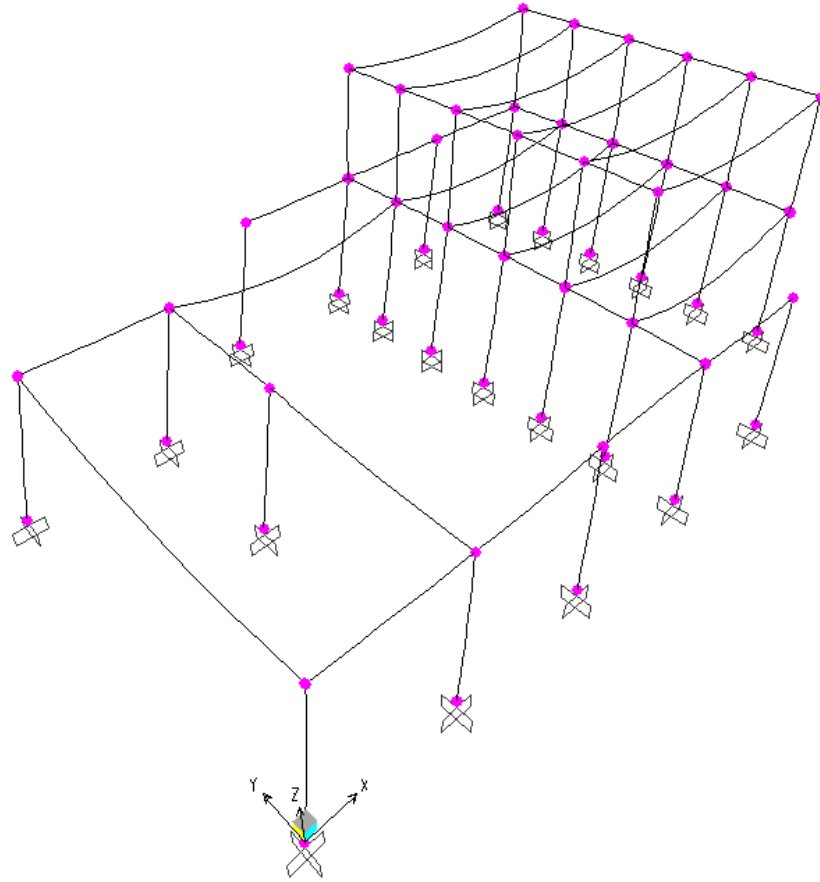


Figure 6.3: Deformed shape and generation of plastic hinges on 3D model of block B1

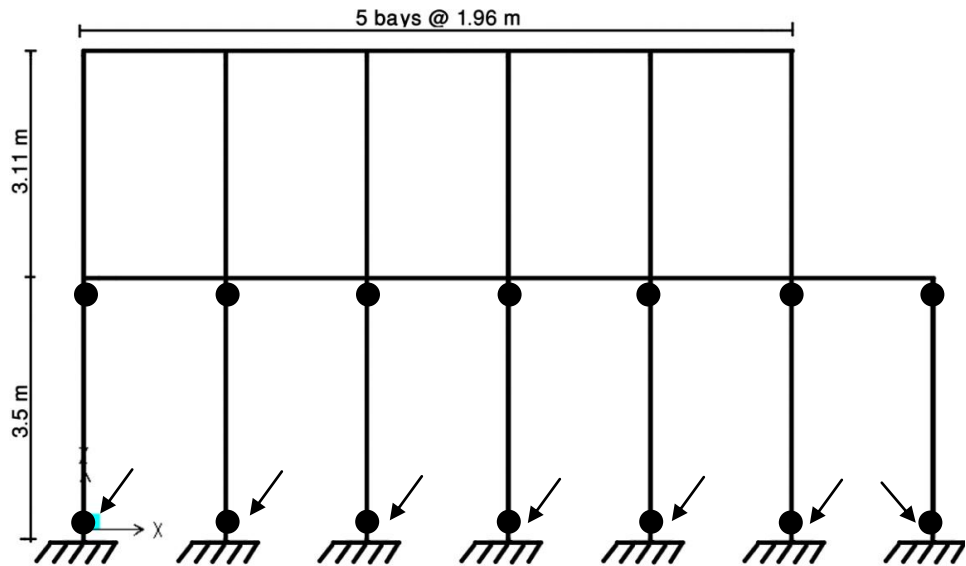
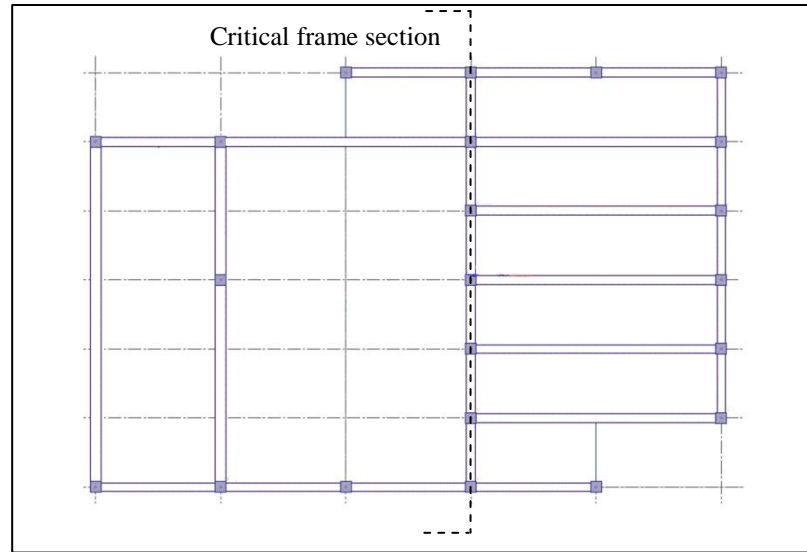


Figure 6.4: Critical frame – Block B1



Hinges shown in figure 6.2 are all changing their performance state to life safety level and very shortly after that all ground column ends collapse together. First yield happens when base shear applied along the height of building reaches 20 percent of its weight (base shear to mass ratio = 0.21). This shows that this building has a very small resistance to lateral loading since it reaches to plastic stage within a very small application of horizontal loads. Although this frame structure shows good yielding but it collapses at a certain point when lateral loading increases to 25 percent of its weight, therefore displacement while yielding happens very fast and definitely design of existing building is not adequate for resisting ground motions. Hence this building has high risk of life safety in event of an earthquake and strengthening strategies shall be considered for frames change its brittleness to become more ductile.

6.3.3 Block B2

Block B2 is a two storey reinforced concrete frame structure with total height of 6.57 to the roof and area of 17.75 x 9.78 m². Total weight of frame structure including slabs is

3423 kN and critical frame has weight of 543 kN. column sections constructed for this building are C30x30 except two columns that have section of C60x30.

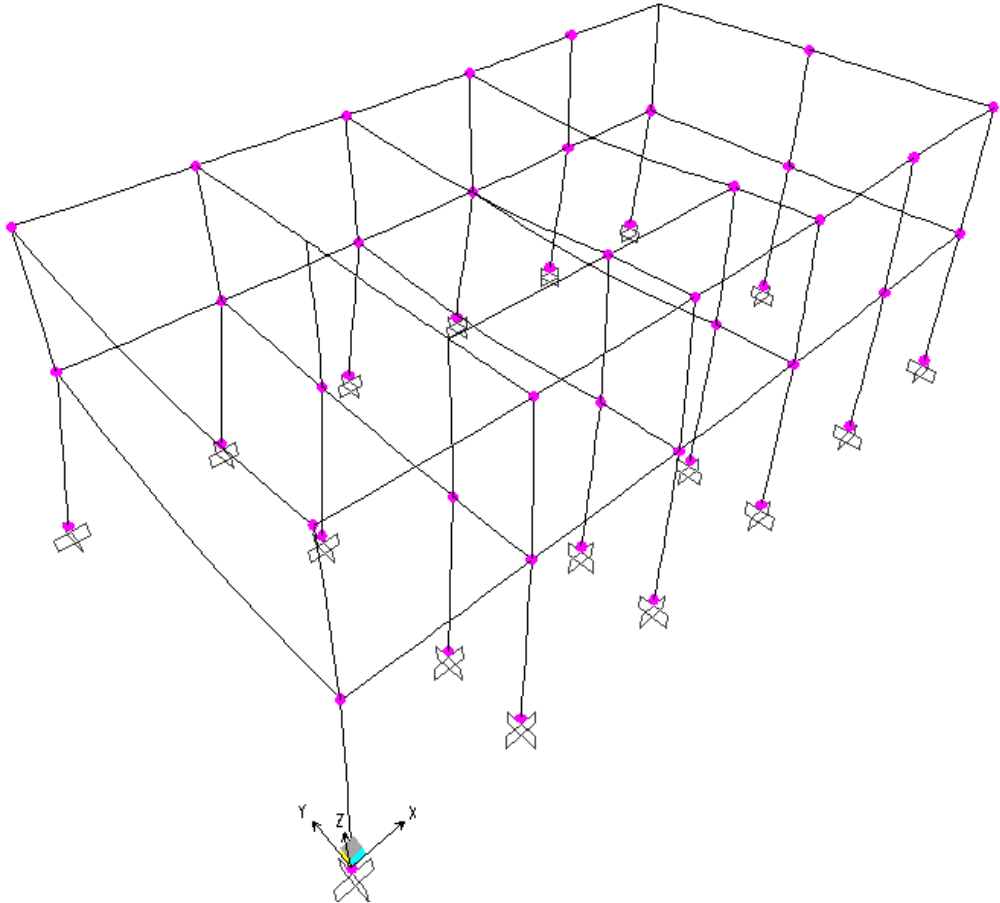


Figure 6.5: Deformed shape and generation of plastic hinges on 3D model of block B2

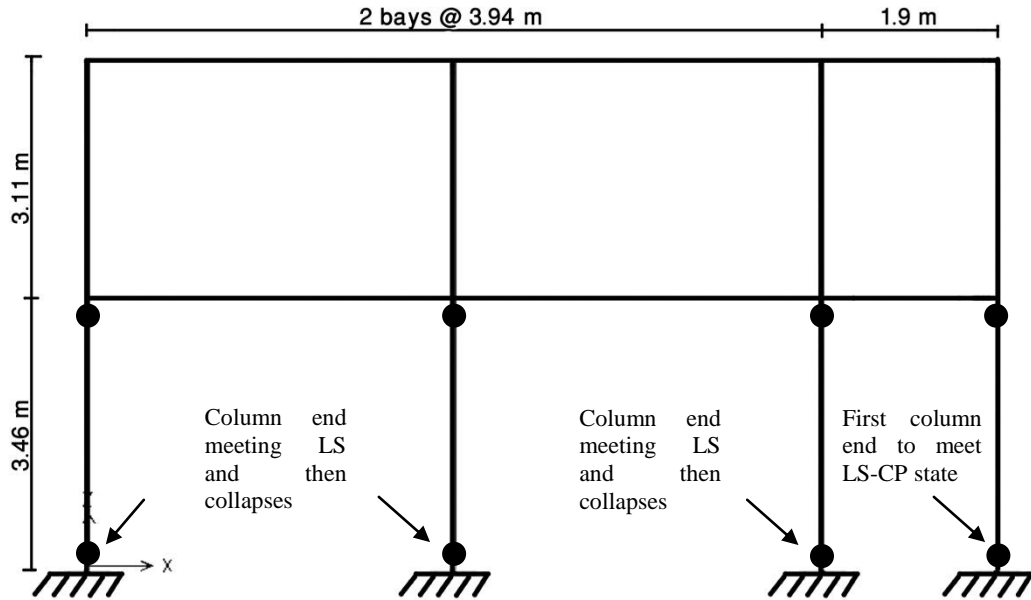


Figure 6.6: Critical frame – Block B2

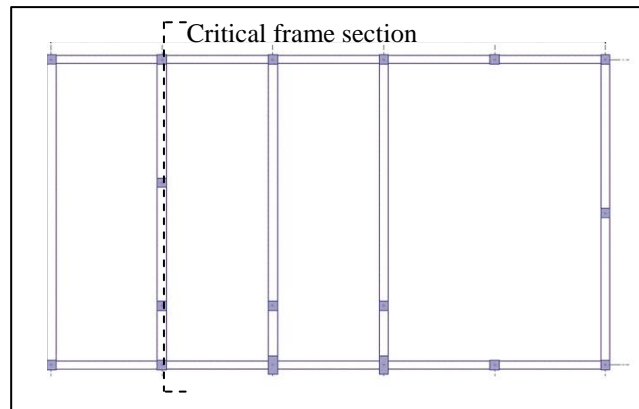


Figure 6.3 shows the critical frame of building that has been analyzed for its performance during lateral loading. Columns that are holding the balcony are the first where end hinges collapse and other columns holding the main building will collapse shortly after. First yield of building happens when lateral loading reaches 10 percent of frames weight and collapses when it exceeds 12 percent of its weight (base shear to mass ratio = 0.12). This building shows no elastic behavior to lateral loading and

application of very small ground acceleration will cause frames to yield. Existing columns of building has not enough reinforcement detailing to resist when it is in post yield stage and ground columns collapse after 70 mm displacement of top center of mass. All ground columns of this building shall be strengthened for beam-column moment capacity and confinement strength to be able to increase its elastic behavior and post yield strength to observe better ductility during an earthquake.

6.3.4 Block C

Block C is a two storey reinforced concrete frame structure with total height of 8.3 m to the roof and area of $36.31 \times 9.7 \text{ m}^2$. Total weight of 3D structure including slabs is equal to 1777 kN and critical frame chosen has weight of 104 kN. Columns constructed for building are all having section of C45x30 located symmetrically with respect to center of mass.

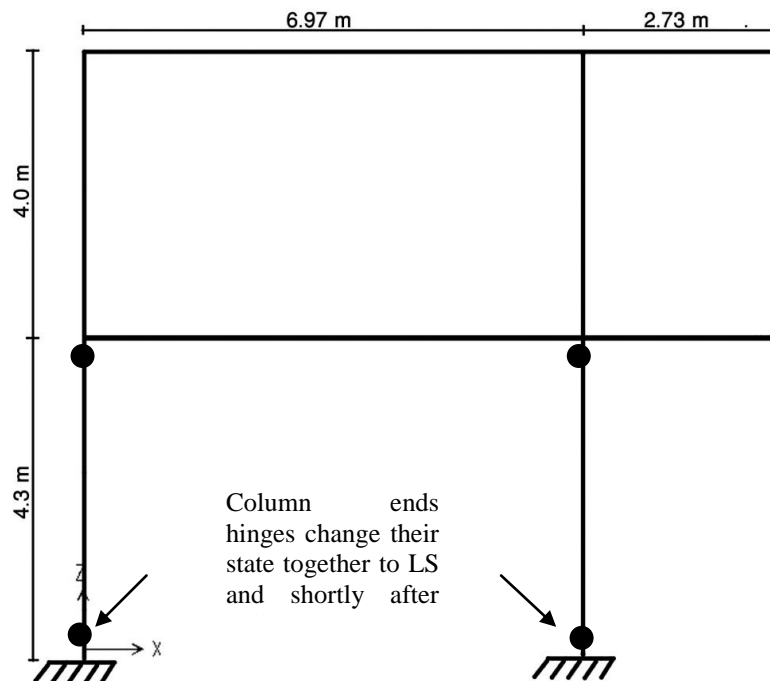


Figure 6.7: critical frame – Block C

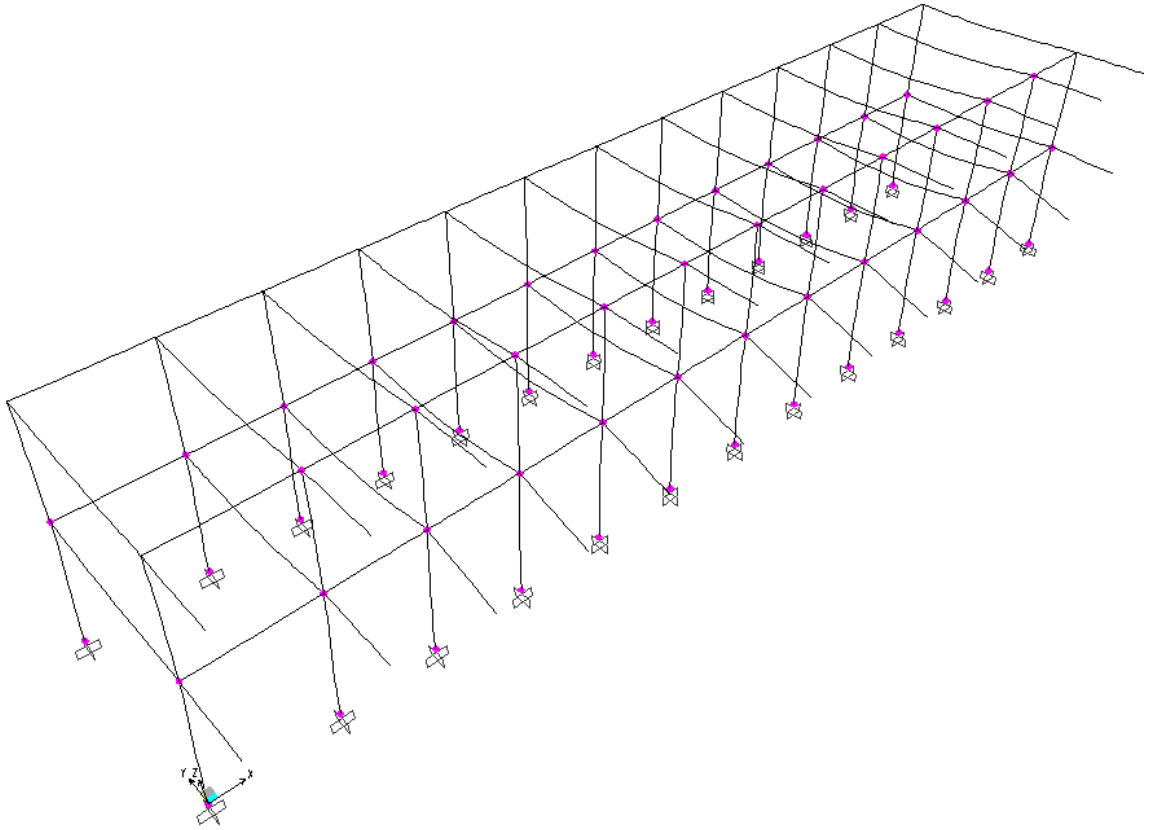
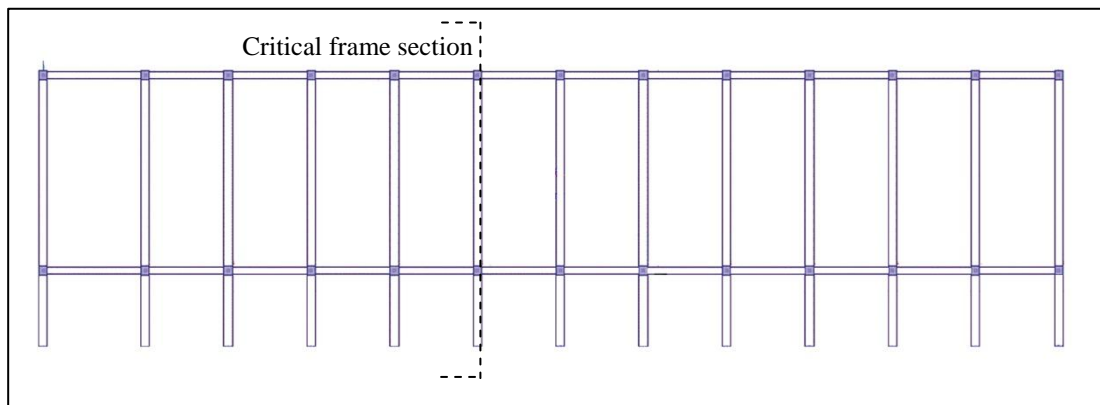


Figure 6.8: Deformed shape and generation of plastic hinges on 3D model of block C

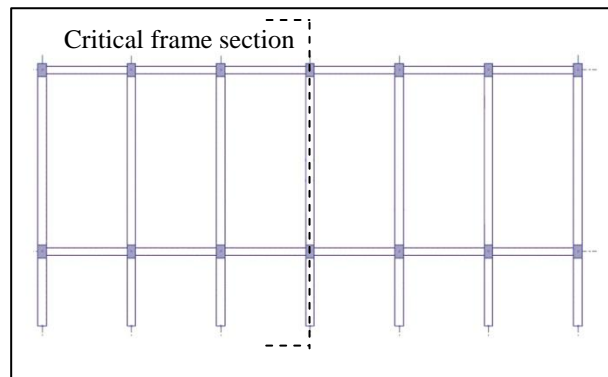


Critical frame of block C shown in figure 6.4 has shown better elastic behavior comparing to other buildings, although existing concrete class of this building is detected to be C16 but having columns located symmetrically with respect to center of mass helps improving in ductility. First yield happens when lateral loading reaches 20

percent of frames weight, but since it is not designed considering the lateral loading along the height of building, post yield resistance that is provided by column ends hinges does not have enough capacity to hold and yield more till collapse where occurs with application of horizontal forces equal to 25 percent of structure's weight. This building is being used as classrooms and students will be in risk of life safety during earthquake. Column confinement strength, shear capacity and beam-column moment capacity has to be improved by strengthening strategies to improve its elastic behavior and its post yield resistance capacity to higher level so structure can respond more ductile during an earthquake and risk of life safety will be decreased to an acceptable criteria.

6.3.5 Block D

Block D is the only single storey reinforced concrete frame structure that is located in site. Building has total height of 3.96 m to the roof and area of $18.42 \times 8.75 \text{ m}^2$. All column section is constructed as C45x30 sections located symmetrically with respect to center of mass.



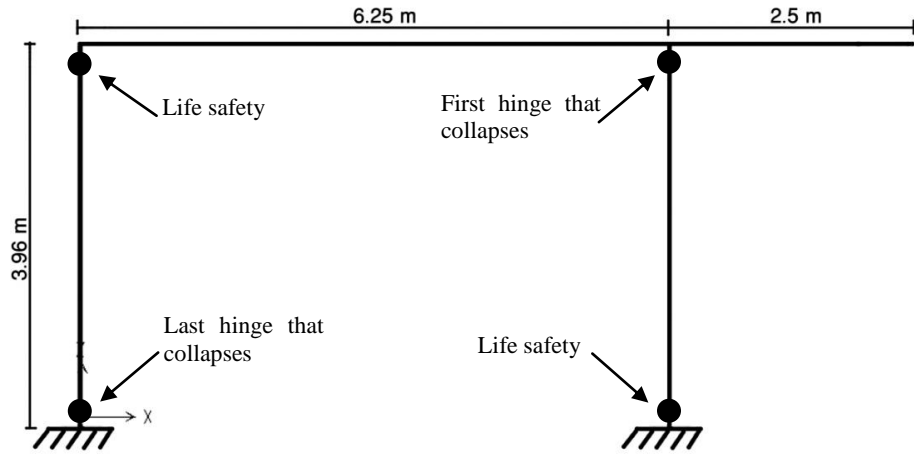


Figure 6.9: Critical frame – Block D

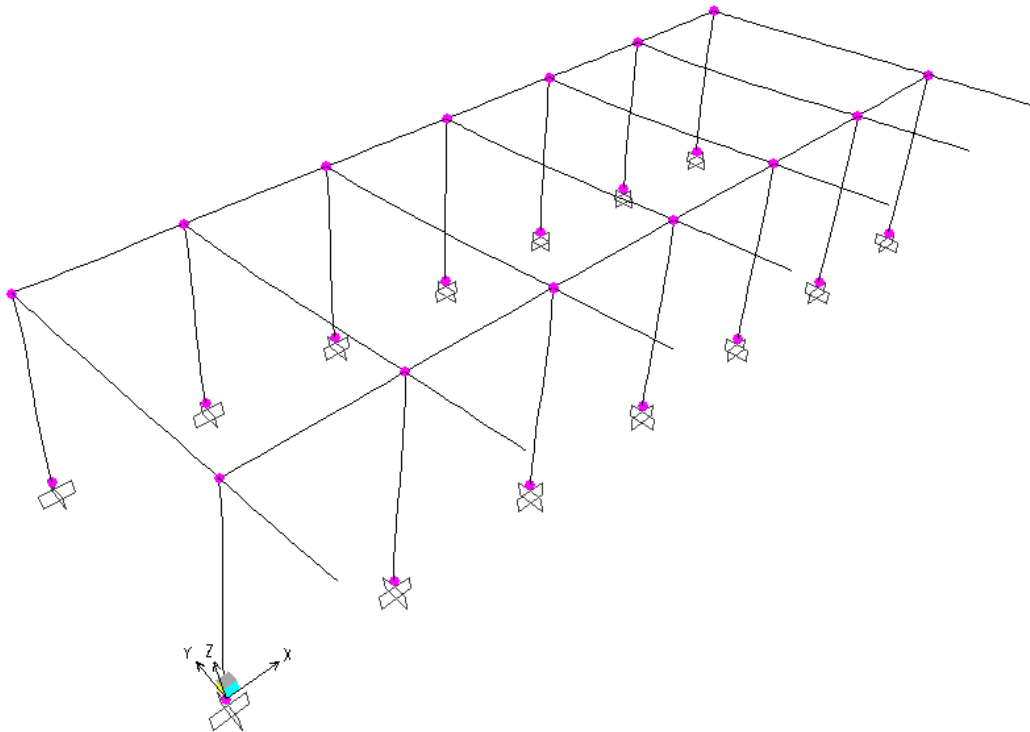


Figure 6.10: Deformed shape and generation of plastic hinges on 3D model of block D

Block D has been forbidden to use when team visited the site for the first time, it was suspicious for life safety. Assessment of this building shows that building is not designed for resisting lateral loadings because it yields within a short displacement of top center of mass. On the other hand first yield happens when horizontal loads reach 50 percent of structure weight; this is due to columns application where they are all symmetrically located with respect to center of mass and also section area of columns are adequate (C45x30), therefore automatically with beams (B30x80) they have higher moment capacity. At the same time it is a single storey building so this will also help to increase resistance to lateral loads.

Although lateral loadings equal to half of structure weight cause it to yield and section areas are adequate, but it has to be taken into consideration that no reinforcement details in columns are designed to resist lateral loads, therefore in post yield stage after horizontal loads reach 60 percent of structure weight building will collapse. Definitely this building is very weak in confinement strength of columns and at the same time it is very weak in its elastic stage, so strategies shall be evaluated to increase frames shear capacity and confinement strength to improve its ductility to a certain point that will have a low risk of life safety during an earthquake.

6.4 Conclusions

The methods used to assess buildings of Bekir Paşa High School site is based on their top displacement due to lateral loading obtained from nonlinear static and dynamic analysis. This performance assessment is sensitive to the existing structural members material and section design characteristic which were detected and modeled using CSI SAP2000 analysis program for structures. According to results obtained for each

building it is obvious that buildings were only designed to carry gravity loads and since they have been constructed and used for over 30 years, material have also slightly lost their strength due to climate conditions.

Building behavior under lateral loadings in nonlinear static analysis brings engineer to understand the existing capacity of structure to lateral loading and thereafter during nonlinear dynamic analysis structure's possible behavior to earthquake is reviewed. Comparing capacity and behavior of building allows engineer to realize vulnerability of buildings and their weak points that makes it to behave brittle. In framework of this study seismic performance of reinforced concrete frame structures located in Bekir Paşa High School have been assessed and results are discussed. According to structural behavior and critical frames detected some strengthening strategies are suggested, these strategies shall be designed and re evaluated to investigate the new performance of buildings due to lateral loading. On the other hand a cost analysis shall be done to find out whether it is economically to owners benefit to strengthen and repair existing buildings or it is beneficial to demolish and reconstruct new buildings with respect to expected life time usage of buildings.

The proposed methodology is an efficient tool to investigate the seismic performance of reinforced concrete frame structures. It will allow engineer to obtain the possible behavior of structure during an earthquake and find out building's life safety and collapse risk in that matter, hence decisions can be made to bring structures to better resistance and decrease the life safety risk of buildings. This methodology can also be applied to other reinforced concrete frame structures.

REFERENCES

Algermissen T. and Rogers A. (2004). Seismic Hazard Risk Assessment of the Greater Nicosia Area.

A. S. C. E. (2000). Prestandard and Commentary for the Seismic Rehabilitation of Buildings. *Reston: Federal Emergency Management & American Society of Civil Engineers.*

Aydinoglu M. N. (2007). Specifications for Structures to be Built in Disaster Areas. *Earthquake Engineering. Istanbul: Ministry of public works and settlement government of republic of Turkey, p. 84.*

Bungey J. H. (2006). Testing of Concrete in Structures. 4. *New York: Taylor & Francis, p. 353.*

Cagnan Z. and Tanircan G. B. (2009). Seismic Hazard Assessment for Cyprus. *Journal of Springer Science + Business Media, p. 22.*

Chopra A. K. and Goel R. K. (2003). A Modal Pushover Analysis Procedure to Estimate Seismic Demands for Unsymmetric Plan Buildings. *Journal of Earthquake Engineering and Structural Dynamics, p.25.*

Concrete society (1987). Concrete Core Testing for Strength. *Camberely: Technical report 11. P. 43.*

- Emmons P. H. (1993). Concrete Repair and Maintenance Illustrated. *Kingstone: Construction Publishers & Consultants*, p. 295.
- Elnashai A. S. and Di Sarno L. (2008). Fundamental of Earthquake Engineering. *1. John Wiley & Sons Ltd*, 2008, p. 374.
- Goel R. K. (2011). Variability and Accuracy of Target Displacement from Nonlinear static Procedures. *International Scholarly Research Network*, p. 16.
- Kirc M. S. and Polat. Z. (2006). Fragility Analysis of Mid-Rise R/C Frame Buildings. *Istanbul: Elsevier Ltd, Journal of Engineering Structures*, p. 11.
- Lang K. (2002). Seismic Vulnerability of Existing Buildings. *Zurich: Swiss Federal Institute of Technology, for the degree of Doctor of Technical Sciences*, p. 160.
- P. E. E. R. (2010). Technical Report for the Ground Motion Database Web Application. *California: Pacific Earthquake Engineering Research Center*, p. 41.
- Pinho R. (2007). Advanced Earthquake Engineering Analysis. [ed.] Pecker A. *Pavia: CISM*, p. 218. Vols. *Courses and Lectures No-494*.
- Shinozuka M., Feng. M. Q., Uzawa. T. and Ueda T. (2001). Statistical Analysis of Fragility Curves. *Los Angeles: University of Sothern California, Department of Civil Engineering and Environmental Engineering, Technical Report*, p. 160.
- Wen Y. K., Elligwood B. R. and Bracci J. (2004). Vulnerability Function Framework for Consequence based Engineering. *1, MAE Center*, p. 101.

APPENDICES

Appendix A: FEMA356 parameters to calculate target displacement

Table A.1: FEMA356 parameters for 3D model – Block A

Item	Value
C_0	1.34
C_1	1.30
C_2	1.00
C_3	1.00
S_a	1.10
T_e	0.30
T_i	0.29
K_i	163732
K_e	150137
α	0.03
R	1.48
V_y	1784.88
Weight	2404.16
C_m	1.00

Table A.2: FEMA356 parameters for frame model Block A

Item	Value
C_0	1.20
C_1	1.35
C_2	1.00
C_3	1.00
S_a	1.10
T_e	0.25
T_i	0.25
K_i	3950.55
K_e	4017.62
α	0.32
R	2.91
V_y	49.24
Weight	130.20
C_m	1.00

Table A.3: FEMA356 parameters for 3D model - Block B1

Item	Value
C_0	1.1523
C_1	1.3591
C_2	1
C_3	1
S_a	1.1
T_e	0.2358
T_i	0.1501
K_i	1292546
K_e	524115
α	1.65E-03
R	5.3772
V_y	540.369
Weight	2641.53
C_m	1

Table A.4: FEMA356 parameters for frame model – Block B1

Item	Value
C_0	1.1423
C_1	1.5
C_2	1
C_3	1
S_a	0.9041
T_e	0.0818
T_i	0.0818
K_i	209107
K_e	209107
α	1.13E-03
R	4.2366
V_y	107.984
Weight	506.012
C_m	1

Table A.5: FEMA356 parameters for 3D model – Block B2

Item	Value
C ₀	1.22
C ₁	1.40
C ₂	1.00
C ₃	1.00
S _a	1.10
T _e	0.20
T _i	0.17
K _i	760988.20
K _e	536069.30
α	0.00
R	8.33
V _y	452.14
Weight	3422.92
Cm	1.00

Table A.6: FEMA356 parameters for frame model – Block B2

Item	Value
C ₀	1.09
C ₁	1.48
C ₂	1.00
C ₃	1.00
S _a	1.10
T _e	0.12
T _i	0.12
K _i	120357.26
K _e	120357.26
α	0.00
R	10.46
V _y	57.14
Weight	543.40
Cm	1.00

Table A.7: FEMA356 parameters for 3D model – Block C

Item	Value
C ₀	1.13
C ₁	1.19
C ₂	1.00
C ₃	1.00
S _a	1.10
T _e	0.40
T _i	0.40
K _i	76606.30
K _e	76606.30
α	0.01
R	3.93
V _y	496.85
Weight	1776.82
Cm	1.00

Table A.8: FEMA356 parameters for frame model – Block C

Item	Value
C ₀	1.13
C ₁	1.18
C ₂	1.00
C ₃	1.00
S _a	1.10
T _e	0.41
T _i	0.44
K _i	466.87
K _e	524.52
α	0.21
R	5.51
V _y	20.72
Weight	103.77
Cm	1.00

Table A.9: FEMA356 parameters for 3D model – Block D

Item	Value
C ₀	1.27
C ₁	1.43
C ₂	1.00
C ₃	1.00
S _a	1.10
T _e	0.17
T _i	0.17
K _i	106674.13
K _e	106674.13
α	0.03
R	1.53
V _y	455.56
Weight	634.56
Cm	1.00

Table A.10: FEMA356 parameters for 3D model – Block D

Item	Value
C ₀	1.00
C ₁	1.45
C ₂	1.00
C ₃	1.00
S _a	1.10
T _e	0.15
T _i	0.15
K _i	9791.36
K _e	9791.36
α	0.09
R	2.19
V _y	37.77
Weight	75.10
Cm	1.00

Appendix B: Rebound hammer readings from columns of buildings

Table B.1: Rebound hammer readings – Block A

Block A	1	2	3	4	5	6	7	8	9	10	σ (MPa)	S_d	Avg
Column1-A1	32.80	29.20	36.70	31.10	33.60	29.10	26.00	30.30	31.80	31.20	28.5	2.7	31.20
Column2-A2	33.90	39.70	40.30	35.20	37.20	28.30	24.00	40.50	42.90	37.10	34.9	6.0	36.80
Column3	35.50	30.30	36.90	30.70	34.00	38.10	36.90	26.30	41.00	36.20	31.1	4.1	34.60
Column4	34.70	35.70	43.30	38.20	37.60	36.20	44.70	34.00	42.30	45.80	44.0	6.0	41.90
Column5	17.90	20.50	25.60	22.60	23.50	27.30	23.20	26.60	23.20	19.30	13.6	2.9	23.00
Column6-A3	28.50	33.20	31.80	30.00	32.10	29.60	30.00	31.00	34.10	32.90	25.7	1.7	31.30

Table B.2: Rebound hammer readings – Block B1

Block B1	1	2	3	4	5	6	7	8	9	10	σ (MPa)	S_d	Avg
Column1-B11	30.40	34.40	32.70	29.30	32.50	28.40	33.00	21.20	32.90	33.50	24.2	3.4	30.30
Column2	24.60	25.20	31.50	32.50	28.30	29.50	31.60	31.30	23.10	30.30	22.7	2.7	29.40

Table B.3: Rebound hammer readings – Block B2

Block B2	1	2	3	4	5	6	7	8	9	10	σ (MPa)	S_d	Avg
Column1-B21	30.10	36.30	34.80	31.70	28.30	29.50	32.30	38.20	25.20	38.00	27.5	4.1	32.50
Column2-B22	29.90	28.90	25.30	27.70	33.40	28.20	25.80	28.10	27.50	31.50	21.5	2.3	28.60
Column3	28.90	23.40	26.50	28.50	28.60	27.90	35.70	26.10	27.70	26.30	20.6	2.9	28.00

Table B.4: Rebound hammer readings – Block C

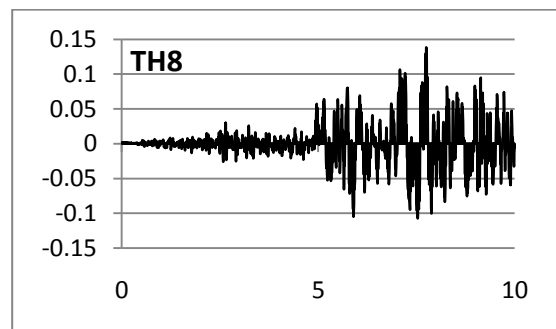
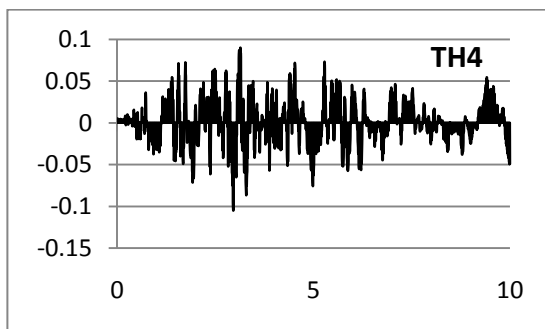
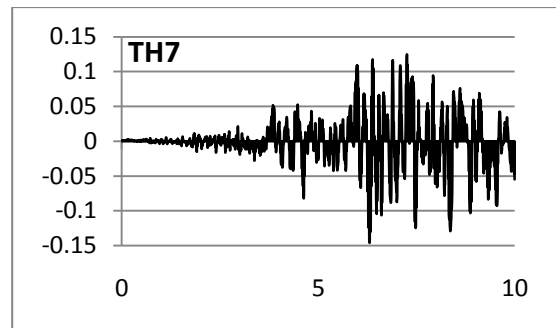
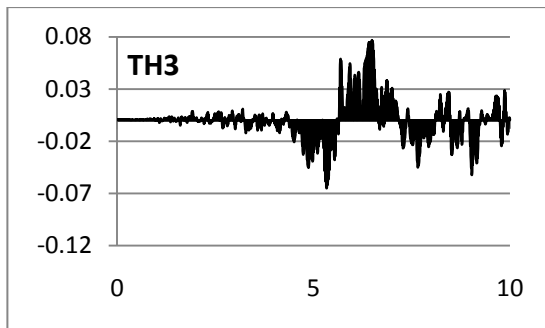
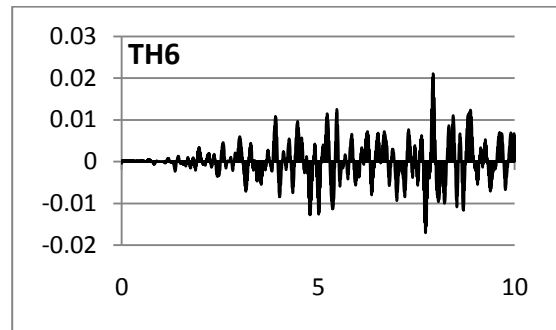
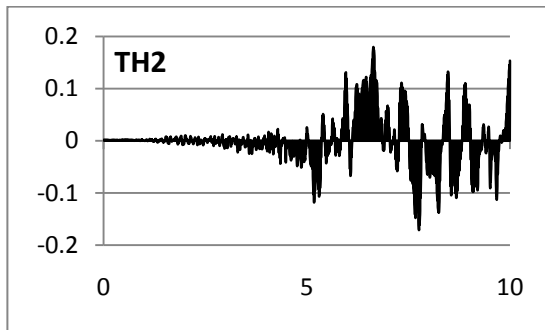
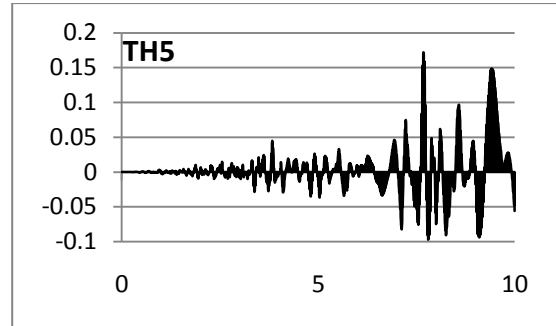
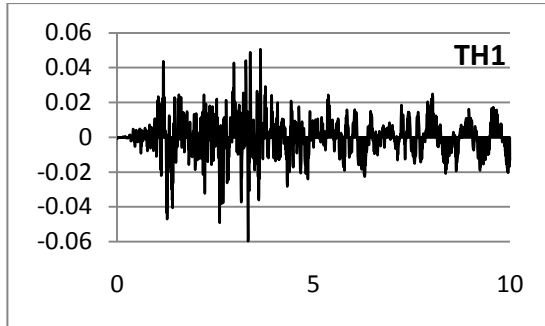
Block C	1	2	3	4	5	6	7	8	9	10	σ (MPa)	S_d	Avg
Column1-C1	39.50	36.30	35.50	39.40	34.30	43.40	35.40	34.40	33.70	36.60	34.9	2.9	36.90
Column2	40.20	40.00	38.50	39.50	36.10	43.60	41.00	38.50	39.50	39.50	39.7	4.5	39.50
Column3	27.90	31.30	31.90	36.50	38.70	31.10	30.70	27.90	36.90	30.60	27.4	3.6	32.40
Column4	26.90	31.10	33.30	32.40	34.10	40.10	34.00	25.80	32.60	34.30	28.1	3.9	32.80
Column5-C2	30.10	30.30	37.40	32.70	32.00	37.10	35.00	39.10	43.10	33.10	30.4	4.6	34.20
Column6-C3	25.70	25.30	32.50	19.60	26.90	27.90	27.20	24.80	26.20	23.70	17.4	3.1	25.80

Table B.5: Rebound hammer readings – Block D

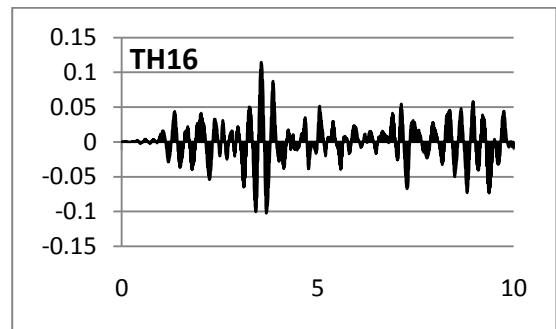
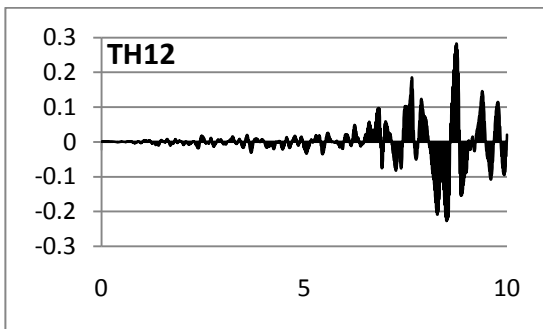
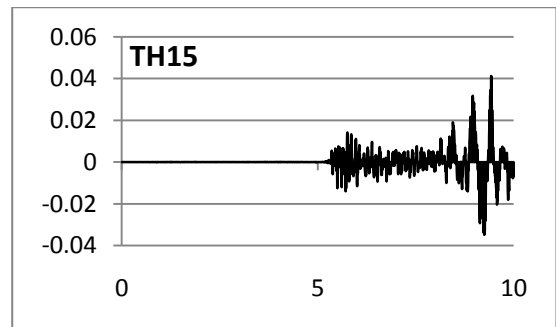
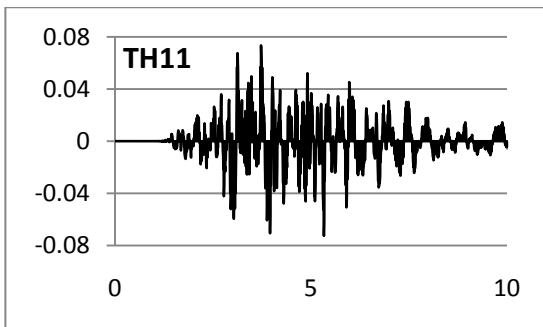
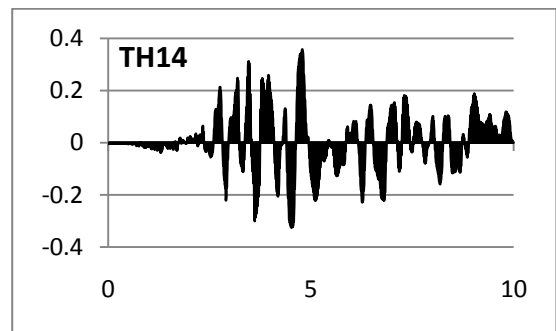
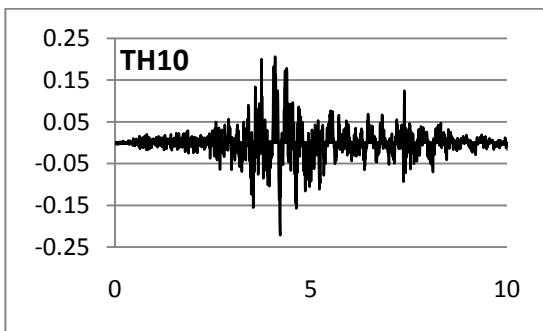
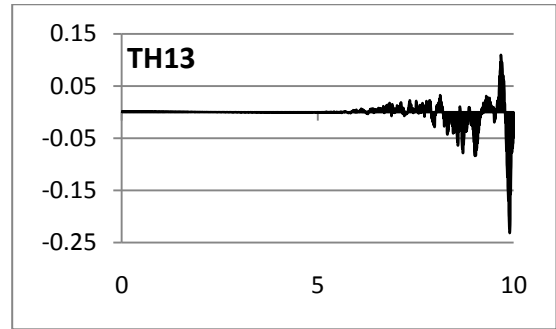
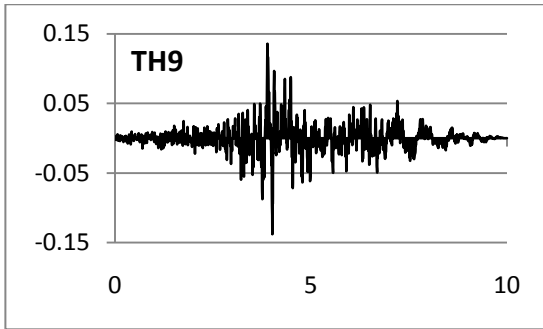
Block D	1	2	3	4	5	6	7	8	9	10	σ (MPa)	S_d	Avg
Column1	36.00	36.20	34.00	37.50	36.90	35.50	33.00	36.70	30.90	34.00	31.1	4.1	35.07
Column2	37.10	35.00	39.10	43.10	33.10	37.40	32.70	32.00	30.10	30.30	30.4	4.6	34.99

Appendix C: Time history functions of selected earthquakes

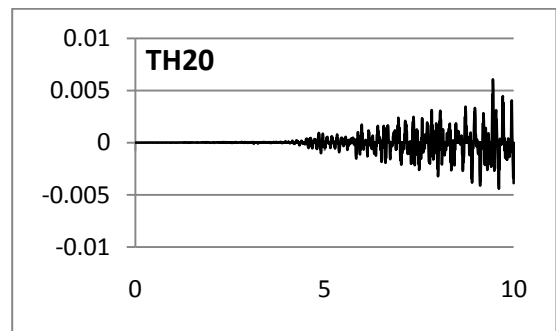
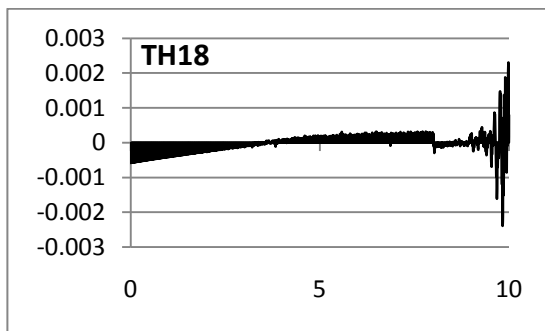
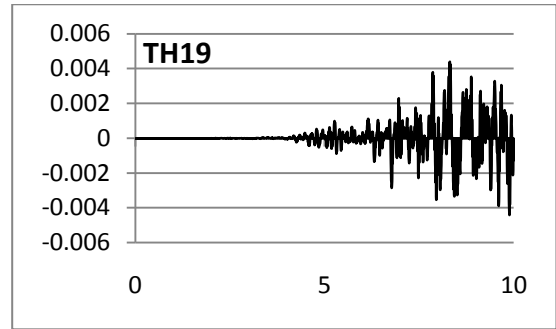
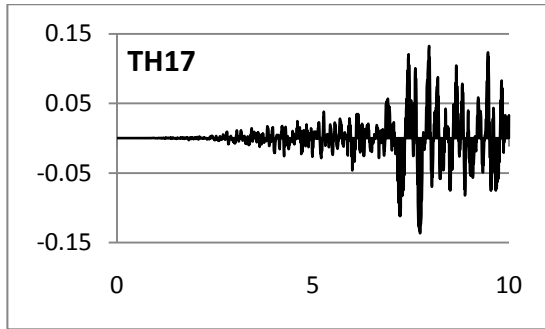
Horizontal axis presents time in seconds and vertical axis is spectral acceleration in g.



Horizontal axis presents time in seconds and vertical axis is spectral acceleration in g .



Horizontal axis presents time in seconds and vertical axis is spectral acceleration in g.



Name	MSE	Scale F	Event	Year	Magnitude	Mechanism	PGA (g)
TH1	0.3140	10.8413	Park field	1966	6.19	Strike-Slip	0.6470
TH2	0.0687	2.6382	Imperial Valley-06	1979	6.53	Strike-Slip	0.4741
TH3	0.0703	6.6741	Imperial Valley-06	1979	6.53	Strike-Slip	0.5122
TH4	0.1677	4.7040	Victoria- Mexico	1980	6.33	Strike-Slip	0.4950
TH5	0.0869	2.7845	Westmorland	1981	5.9	Strike-Slip	0.4788
TH6	0.3016	16.8445	Morgan Hill	1984	6.19	Strike-Slip	0.5485
TH7	0.1464	2.6054	Superstition Hills-02	1987	6.54	Strike-Slip	0.5476
TH8	0.1332	2.5265	Superstition Hills-02	1987	6.54	Strike-Slip	0.5226
TH9	0.0671	5.2387	Landers	1992	7.28	Strike-Slip	0.7231
TH10	0.0837	2.7455	Landers	1992	7.28	Strike-Slip	0.6087
TH11	0.1118	6.7796	Kobe- Japan	1995	6.9	Strike-Slip	0.4981
TH12	0.0892	1.7984	Kocaeli- Turkey	1999	7.51	Strike-Slip	0.5080
TH13	0.0403	1.8289	Kocaeli- Turkey	1999	7.51	Strike-Slip	0.5098
TH14	0.2194	3.2088	Kocaeli- Turkey	1999	7.51	Strike-Slip	0.4887
TH15	0.0700	16.3662	Duzce- Turkey	1999	7.14	Strike-Slip	0.6735
TH16	0.2197	7.6520	Duzce- Turkey	1999	7.14	Strike-Slip	0.8761
TH17	0.4343	4.8329	Hector Mine	1999	7.13	Strike-Slip	0.6601
TH18	0.0523	1.6906	Denali- Alaska	2002	7.9	Strike-Slip	0.5539
TH19	0.0403	8.8293	Chi-Chi- Taiwan-04	1999	6.2	Strike-Slip	0.4964
TH20	0.0564	12.0436	Chi-Chi- Taiwan-04	1999	6.2	Strike-Slip	0.5495

Appendix D: Calculation of actual compressive strength of concrete core samples

No	Vertical or Horizontal	F1	F2	Carrot name	L(mm)	D(mm)	$\lambda=L/D$	$1/\lambda$	Section area (cm ²)
1	H	2.5	3.25	A1	117.7	100	1.177	0.849	78.5398
2	H	2.5	3.25	A2	65.2	100	0.652	1.534	78.5398
3	H	2.5	3.25	A3	96.0	100	0.960	1.041	78.5398
4	H	2.5	3.25	B1	115.4	100	1.154	0.866	78.5398
5	H	2.5	3.25	B21	114.6	100	1.146	0.872	78.5398
6	H	2.5	3.25	B22	117.5	100	1.175	0.851	78.5398
7	H	2.5	3.25	C1	130.7	100	1.307	0.765	78.5398
8	H	2.5	3.25	C2	125.6	100	1.256	0.796	78.5398
9	H	2.5	3.25	C3	125.0	100	1.250	0.800	78.5398
10	H	2.5	3.25	D1	107.6	100	1.076	0.930	78.5398
11	H	2.5	3.25	D2	57.1	100	0.571	1.751	78.5398

No	Fracture load (kN)	Carrot compressive strength (kN)	Actual compressive strength (kN)
1	69.70	90.50	96.30
2	208.80	271.00	223.30
3	120.50	156.40	153.80
4	206.80	268.40	283.60
5	111.90	145.20	153.00
6	260.50	338.10	359.50
7	109.80	142.50	157.30
8	123.90	160.80	175.10
9	111.00	144.10	156.60
10	216.50	281.00	289.10
11	345.00	447.80	344.40

No	SF	Rebar	Diameter (mm)	Corrected actual strength (N/mm ²)
1	1.000	-	-	9.60
2	1.000	-	-	22.30
3	1.000	-	-	15.40
4	1.038	36.59	8	29.40
5	1.000	-	-	15.30
6	1.000	-	-	36.00
7	1.000	-	-	15.70
8	1.000	-	-	17.50
9	1.000	-	-	15.70
10	1.000	-	-	28.90
11	1.000	-	-	34.40

Building	Concrete Compressive Strength (MPa)
A	15.49
B	26.38
C	15.98
D	31.09